AUBURN

SAMUEL GINN
COLLEGE OF ENGINEERING

Evaluation of high-rate settling technology for sediment control in roadway construction sites

FINAL REPORT

Prepared by

Jose G. Vasconcelos
Michael Perez
Jue Wang
Wesley C. Zech
Xing Fang

Department of Civil Engineering
Auburn University

Submitted to

Alabama Department of Transportation
Montgomery, Alabama

AUGUST 2017

Highway Research Center
Harbert Engineering Center
Auburn, Alabama 36849

www.eng.auburn.edu/research/centers/hrc.html

TABLE OF CONTENTS

LIST OF TABLES

LIST OF FIGURES

1. Introduction

Construction sites are typically comprised of disturbed land areas lacking vegetative cover thereby exposing soils to runoff leading to stormwater induced erosion which may be a significant source of pollution. Construction sites have measured erosion rates of approximately 20 to 200 tons per acre per year (Pitt et al. 2007). Moreover, construction operations disturbing in-situ soil material increase sediment yields by as much as 10,000 times when compared to natural, undisturbed sites (Haan, 1994). Sediment-laden runoff flows are a concern to the environment as various natural biological processes may be impacted. Sediment loads in water bodies increase turbidity levels which affect habitats, water quality, temperature, pollutant transport, and can cause sedimentation in downstream receiving waters (EPA, 2009). One response has been the development of sediment control techniques employed on construction sites. The purpose of these techniques is to capture suspended sediment, thereby reducing turbidity levels in runoff, as well to control turbidity levels of effluent discharged from construction sites into natural water bodies. Such levels vary across the U.S. and the State of Alabama stipulates that "in no case shall turbidity exceed 50 nephelometric turbidity units (NTU) above background. Turbidity levels caused by natural runoff will be included in establishing background levels." (ADEM, 2013).

Figure 1.1: Example of a sediment plume resulting from road construction runoff (Clark et al., 2012)

Meeting such effluent discharge requirements can be challenging in roadway construction sites when the runoff turbidity can reach levels on the scale of thousands of NTU (Logan, 2012), especially if there are limited availability of areas to install sediment basins. At the same time, increased scrutiny by environmental groups provides additional motivation for developing improved sediment control techniques, particularly in sensitive watersheds. Figure 1.1 illustrates the significant impact sediment-laden discharge from a roadway construction site can have on nearby water bodies when sediment control practices are not deployed or functioning properly. Such impacts have provided the motivation for the proposed research, which proposes the use of high-rate settlers to enhance sediment basins ability to trap sediments, as is developed below.

1.1. Background

This background section is divided in two parts. The first part briefly presents and classifies the techniques currently used to perform sediment control. The second part focuses on sedimentation and on the fundamentals of high-rate settling.

1.1.1. Sediment control strategies

Various best management practices (BMPs) related to sediment control in construction sites are listed in the Environmental Protection Agencies (EPA's) National Pollutant Discharge Elimination System (NPDES) documents. Some sediment controls are located at down gradient

boundaries of the construction site and are commonly referred to as "perimeter controls". The Alabama Soil and Water Conservation Committee (ASWCC) (2009) and EPA (2012) provide examples of perimeter control BMPs, which include silt fences, brush barriers, compost filter berms/socks, and vegetated buffers, among other technologies. Another sediment control strategy involves retaining sediment-laden runoff, preventing these flows from leaving the construction site, or reducing their sediment content prior to discharge. Examples include sediment traps and sediment basins. Sediment traps consist of small impoundments that allow sediment to settle out of construction runoff, usually installed in drainageways or other points of discharge from disturbed areas (EPA, 2006). These traps have an effective lifespan around 24 months, and are applied for drainage areas smaller than 5 acres.

Sediment basins are applied in drainage areas larger than 5 acres, and are designed to create conditions to enhance sediment settling by slowing water velocity and creating favorable conditions for sedimentation to occur. The overarching idea is to generate quiescent conditions in which sediments would reach the bottom region of the basins and not be transported in the basin outflow. Logan (2012) has presented a comprehensive study on sediment basins. With regards to geometry, sediment basin lengths are usually 2 to 4 times larger than their width. Depth values range from 2 to 5 ft, with side slopes in the range of 3H:1V to 2H:1V. Over the years improvements have been added to these basins to increase their sediment removal effectiveness, as is shown in McLaughlin and Jarrett 2008; McLaughlin and McCaleb, 2010. Examples of such improvements include:

- Basins may be equipped with a forebay/sump at the upstream end to facilitate settling of coarser sediment;
- Internal baffles which are used to calm and create a more even flow distribution;
- Dewatering techniques based on skimmers, which will selectively discharge from the upper layers of the flow that theoretically contain water with the least amount of sediment;
- Use of flocculants such as polyacrylamide (PAM) to bind small particles together and enhance the capture of smaller soil particles (silt and clay).

An example of the sediment basin standard that is adopted by ALDOT and that contains all these improvements is presented in Figure 1.2.

1.1.2. Potential operational limitations associated with sediment basins

As field measurements presented by Logan (2012) indicate, inflows into sediment ponds had turbidity in excess of 1,000 NTU, and in some intense rain events reached levels above 25,000 NTU. Sediment removal was observed in such measurements, as these turbidity levels dropped in some cases to levels in the hundreds of NTU. However, as these numbers indicate, sediment basins may not be completely effective in bringing effluent standards into compliance levels. Difficulties associated with the operation of these basins are diverse, and according to Logan (2012) include:

- Insufficient storage volumes in sediment basins;
- Issues related to inadequate flocculant selection and application, with flows exceeding flow rate limit established by floc log manufacturer;
- Overtopping of baffles if water depth in the basin is excessive;
- Difficulty in ensure proper soil stabilization across construction slopes, which generates very large sediment loads in the inflows within basins.

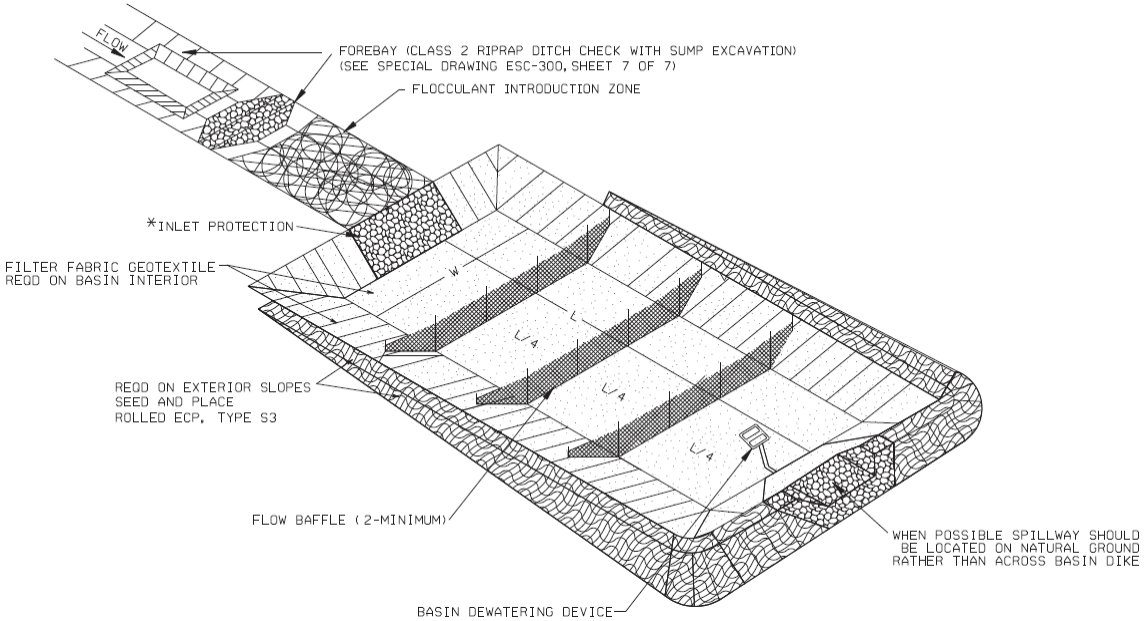

Figure 1.2: Design characteristics of a sediment basin as specified by ALDOT (2015).

As the main principle of enhancing water quality in sediment basins is based on the settling of particles, focus should be placed in developing means to improve settling mechanisms. One realizes that a certain range of sediment particles associated with high turbidity needs to reach the bottom of a sediment basin prior to the point where the basin outflow will draw it toward the discharge and into the receiving water body. There should be enough time for these particles in the runoff to settle. The smaller is the fraction of fine particles present in the runoff, the larger is the required settling time needed to drop outflow turbidity levels to an acceptable level. On the other hand, a decrease in the settling depth should facilitate sediment removal.

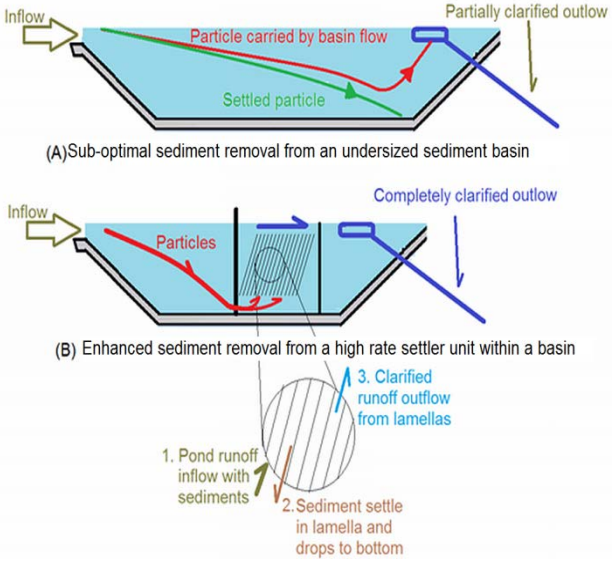

Figure 1.3: Schematic of a traditional settling mechanism used in a sediment basin and an alternative based on high-rate settlers

The principle of high-rate settling is to increase the available settling surfaces in a sedimentation process. These settling surfaces (i.e., plates) are deployed in a way to decrease the vertical distance a particle has to travel before it settles in a surface. By orienting the flow into these surfaces, the vertical distance is significantly reduced (from feet-scale into inch-scale), facilitating settling. Two other benefits from this approach are: 1) these added surfaces enhance flow orientation reducing short circuiting in the basin; and 2) flow between the surfaces is laminar, thus preventing turbulence and decreasing resuspension of settled particles. A common approach is to adopt planar surfaces, referred to as

lamellas, and position those surfaces in an angle with vertical (usually 60 degrees) to facilitate the sliding of these particles from the plate to the bottom of the basin. Figure 1.3 provides a comparative schematic of sediment particle trajectories in an undersized sediment basin and in a basin that has a high-rate settler deployed.

The technology of high rate settling was first proposed in the 1970's for application in industrial and residential wastewater treatment, and in water purification plants. However it has never been used to remove sediments in construction sites' runoffs. Different geometries have been proposed in this study for these settlers to be used to promote settling in basins on construction sites. As illustrated in Figure 1.4(A), one approach is to orient inflows parallel with the plates and have captured sediments settle at the plate underneath, with eventual settling at the settler bottom. Figure 1.4(B) presents another approach in which the flow is oriented upward over the plates, with sediment also being captured between plates and sliding to the bottom of the tank.

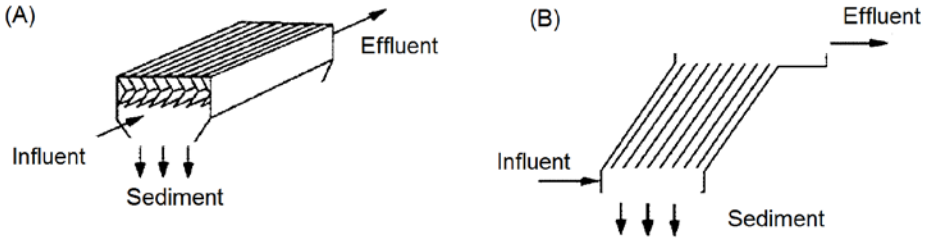

Figure 1.4: Geometry alternatives for high-rate settlers: (A) parallel flow orientation; (B) upward flow orientation

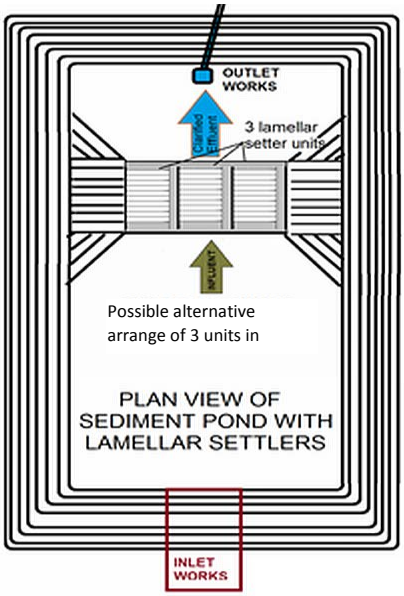

Figure 1.5: Arrangement of three high-rate lamella settlers in a sediment basin

As pointed out by Montgomery (1985), the level of effectiveness in sediment removal obtained with a traditional settler can be obtained from a lamella-based high-rate settler using up to 10 times less area. This can be a key factor for roadway construction sites with space constraints for sediment basins construction. The following example illustrates the much reduced areas that high-rate settlers require when compared to traditional sediment ponds. Assuming a deployment of 3 lamellar settlers in a sediment basin as presented in **Figure 1.5**. The use of 3 upward flow settler modules (dimensions of 6 x 8 x 10 ft^3), with boards 4.6 ft long, 6 ft wide, at an angle of 60^o and spaced every 2 inches could potentially remove particles/flocks 0.2 mm and larger from peak runoff inflows of 1.2 ft^3/s with required plan area of 180 ft^2. On identical conditions, a traditional sediment pond design would require an area of 1,450 ft^2 to settle the same sediments, demonstrating the potential advantage of high-rate settlers.

1.2. Previous related investigation results

1.2.1. Laboratory evaluation of lamella settlers to reduce turbidity

Recent work developed by the PI Vasconcelos in controlled laboratory conditions involved a direct comparison between a traditional settling approach and a high-rate settling approach. A 6 ft long tank with height of 4 ft was divided in two longitudinal segments (~6 in. wide each), one having an upward-flow lamella settler, and the other mimicking conditions of a traditional

sediment basin. A fixed flow rate of 9.5 gpm was maintained the apparatus, and sediment was added at the upstream end. Both traditional (referred here as control) and high-rate lamella settlers shared a forebay and the same sediment-laden inflow was uniformly introduced in both settlers. Figure 1.6(A) presents a lateral view of the experimental apparatus, while Figure 1.6(B) presents the apparatus outlet, showing both the high rate and the traditional settler.

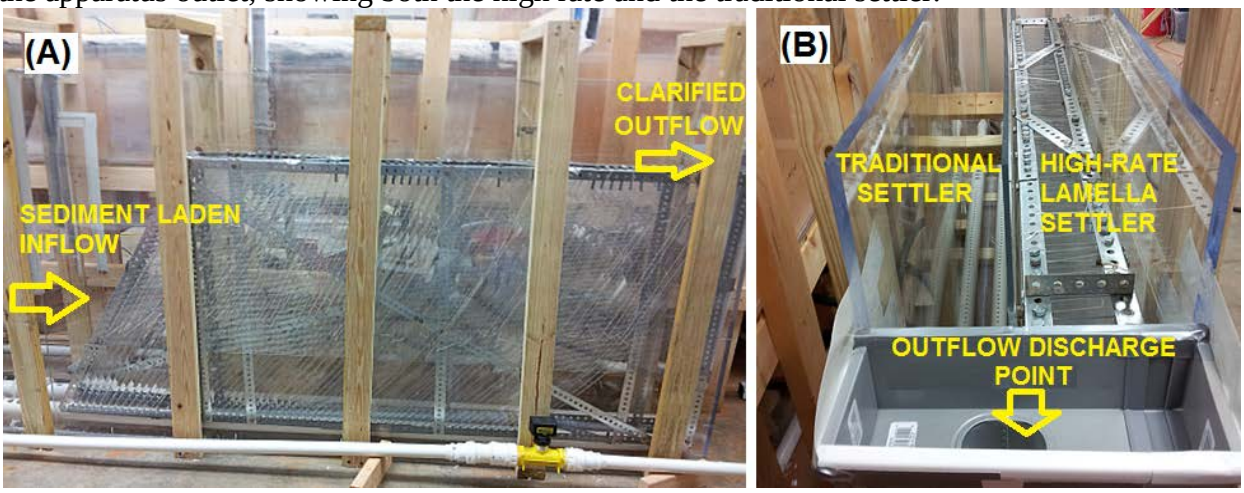

Figure 1.6: (A) View of apparatus comparing traditional and lamella settler efficiency in sediment removal; (B) View from the outlets of both settler units looking from the outlet location.

A total of 22 lb (10 kg) of fine sediment (sand sized and smaller) was steadily added in the system to maintain turbidity levels at the upstream end steady at a level of 1,000 NTUs. Samples were periodically collected at the upstream portions of the system (mixing tank, settlers' forebay and at the outlets of both control and lamella settlers. Several repetitions were performed not only to assess the comparative performance of these tanks, but also to assess the consistency of results. Figure 1.7 presents a typical comparison between the inflow turbidity (measured at the mixing tank and forebay) and the outflow turbidity (measured at lamella and control outlets). While inflow turbidity was kept at the range of 1,000 NTU, lamella outflow's turbidity never exceeded 128 NTU, and averaged 73 NTU. Meanwhile, control results from the traditional settler had much larger values, averaging a turbidity of 559 NTU for the same tested conditions. Such experimental tests were repeated 6 other times with very similar results indicating strong consistency. The average outflow turbidity of the control settler was 521% to 1,068% larger than the lamella settler average turbidity, indicating the superiority of the lamellas. Figure 1.7 also presents a picture taking during one typical experimental run comparing the appearance of the water being discharged by the control settlers with the much less turbid water discharged by the lamella settlers.

These experiments indicate that the correct deployment of lamella settlers can potentially reduce turbidity in sediment basins. There is, however, an important limitation to these findings in that the conditions that were used in the small laboratorial apparatus are not truly representative of actual sediment basins.

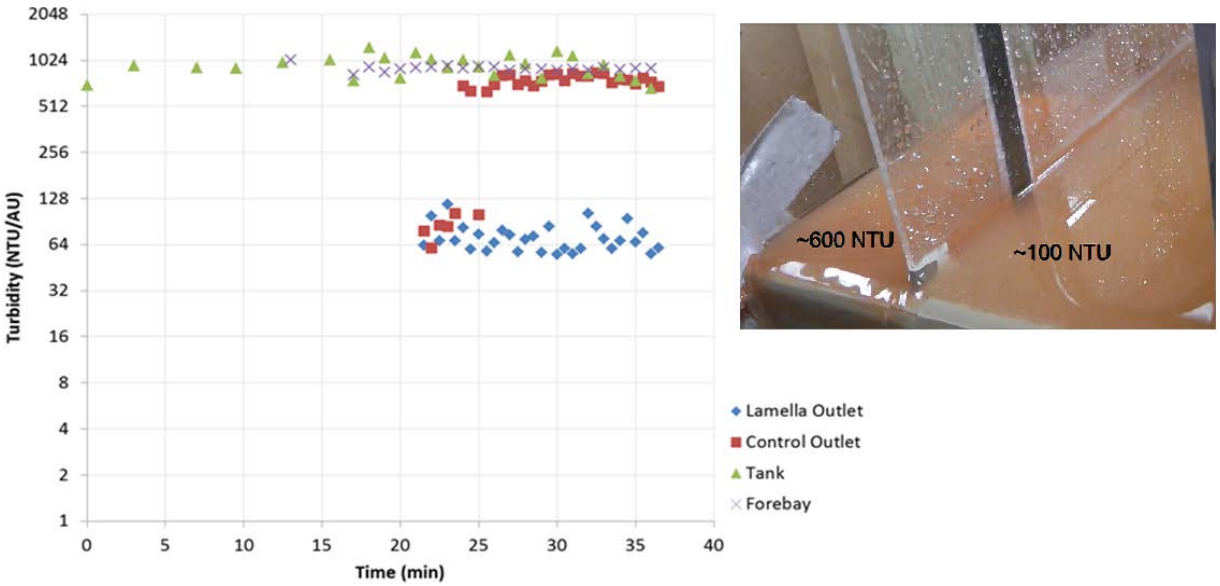

Figure 1.7: Comparison between the performance of lamella settlers and traditional (control) settlers in reducing the inflow turbidity. A photo showing the turbidity difference at the outlet is also shown.

1.2.2. Construction of a Large-scale Sediment Basin Testing System

Through a HRC funded project a large-scale sediment basin testing system was designed and constructed at Auburn University Erosion and Sediment Control Testing Facility (AU-ESCTF) (Figure 1.8), as detailed in Perez et al. (2015). The system includes an inflow channel, a sediment basin with skimmer and emergency spillway, water and sediment introduction systems. The inflow channel has a trapezoidal cross section with bottom width of 4 ft, side slope of 2 horizontal versus 1 vertical, channel depth of 2 ft (top width about 12 ft), and a longitudinal slope of 3.7%. The channel length is 96 ft and the channel is lined with Flexamat® (flexible concrete mattresses). The water introduction system is connected to three trash pumps that draw the water from the water supply reservoir, and the system can deliver a maximum flow rate of 1.45 ft^3/s (650 GPM). The flow rate from the water introduction system can be controlled by adjusting the valves and measured using a calibrated weir. The sediment introduction system uses a 6 in. diameter, 11 ft long auger that allows sediments to be introduced into the water/sediment mixing trough at a controlled rate. The sediment introduction system was calibrated by running sediment through the auger and collecting the output in a known volume container. The sediment introduction rate is currently set at 0.79 ft^3/min; if the sediment specific weight is 100 lb/ft^3, the system would introduce about 4,740 lb of sediment if the system runs for a 60-minute test. The similar system was tested for the ALDOT inlet protection project, it resulted in a turbidity about 3,000 NTU and total suspended solids (TSS) concentration about 2,000 mg/L, which are comparable to typical values observed inflow turbidity and TSS values at the sediment basin in Franklin County studied by Logan (2012). Such values are lower than the maximum turbidity and TSS values observed after severe rainfall events at that basin.

The sediment basin constructed at AU-ESCF has a total storage volume of 3,051 ft^3 including 620 ft^3 of sediment storage volume, skimmer for dewatering and emergency spillway, and is depicted in Figure 1.8. The basin geometry is as follows:

- Dimensions at the sediment basin bottom (length × width) : 44 ft × 20 ft
- Dimensions at the sediment basin top (length × width) :58 ft × 32 ft

- Maximum water depth ranging from 4.25 ft to 4.5 ft
- Longitudinal bottom slope: ~2.65%

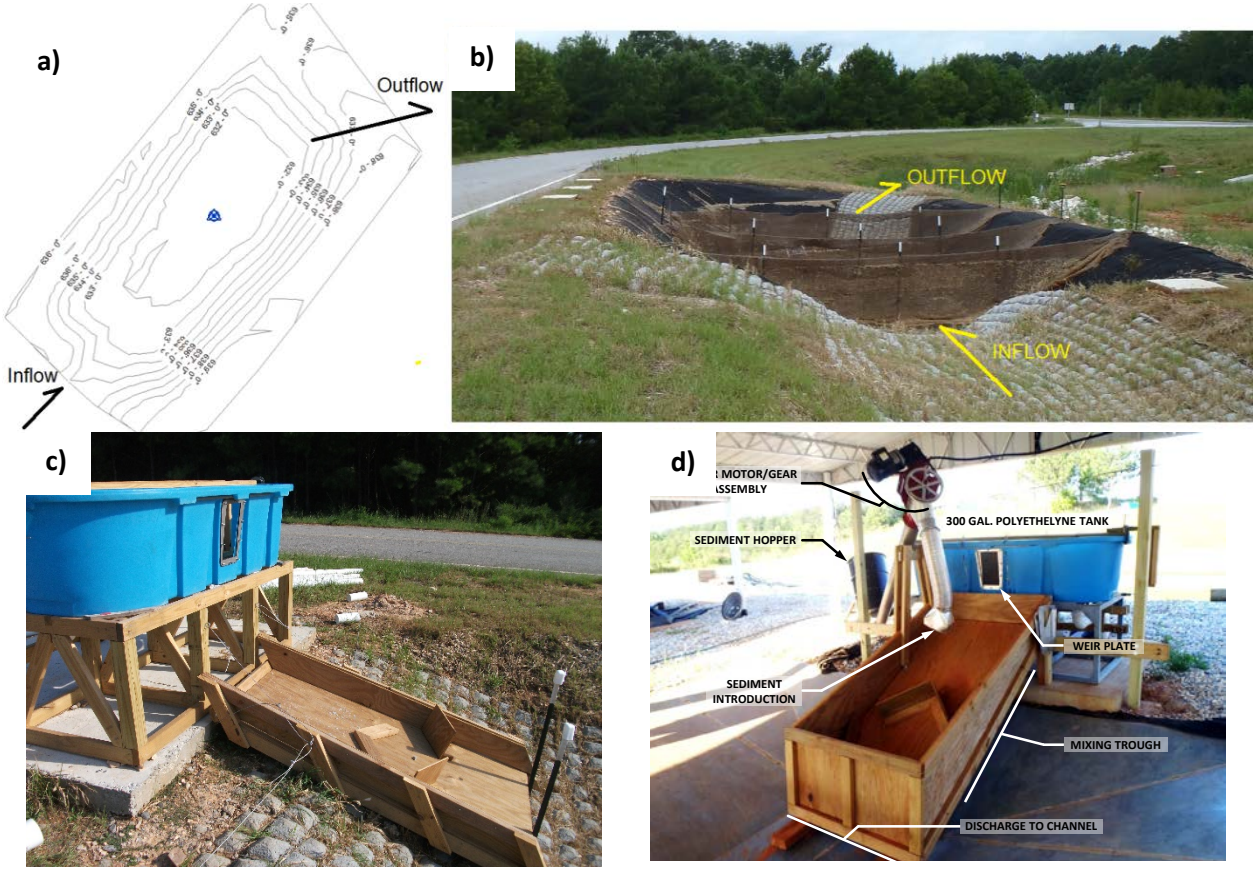

Figure 1.8: Geometry configuration and general layout of AU-ESCTF sediment basin including water and sediment introduction systems: a) contour lines and inflow and outflows points in the basin; b) picture of the basin looking toward the downstream end of the basin; c) ramp where inflows are admitted in to the channel leading to the basin; and d) sediment addition to the ramp mechanism based on an auger.

2. Research objectives and structure of the report

Building from large-scale testing involving sediment control technology, the goal of this research project was to perform large-scale evaluations of settling technologies in the sediment basin at AU-ESCTF. In particular, the goal was to assess the impacts on the sediment basin performance of:

1. Having a forebay prior to a sediment basin;
2. Changing thickness of coir fiber baffles;
3. Adding high-rate lamella settlers in the sediment basin; and
4. Adding a small-scale high-rate lamella settler to treat skimmer outflow from basins.

The assessment of the performance of the basin is mostly based on measurements performed in the sediment basin, which included total suspended solids (TSS), turbidity (with sensors and with handheld turbidimeter), mass of settled soils, and water depth in the basin. Some analyses were also obtained by means of numerical simulation of flows in the sediment basin.

The structure of this Final Research Report is as follows:

1. Chapter 3 presents the methodology for the large-scale experiments, as well as, the data collected that was used to characterize the performance of the sediment basin. It also includes the steps taken to construct the lamella settlers used in this study.
2. Chapter 4 focuses on the Research Results and is comprised by 4 sections.
    a. Section 4.1 presents the operational characteristics of the sediment basin using the current design standards adopted by ALDOT, and on proposed modification to the design that do not involve the use of lamella settlers. The characterization includes:
        i. Effects of excavated sumps upstream from the sediment basin;
        ii. Effects of changing the coir fiber baffle layer that separates the 1st and 2nd bays within the sediment basin, making it thicker, a condition referred to as *Improved Baffle*.
        iii. In all tests changes in turbidity values and on the final mass balance were evaluated, and a final most feasible and effective installation (MFE-I) configuration was determined.
    b. Section 4.2 explores the changes in the performance of the sediment basin when alternative designs using lamella settlers were used, specifically:
        i. When a lamella settler tanks are installed at the 3rd bay location, and enforces upward flows in the basin, a condition referred to as *Lamella Settlers with Upward Flow*.
        ii. When a lamella settler tanks are installed at the 3rd bay location, and enforces longitudinal flows in the basin, a condition referred to as *Lamella Settlers with Longitudinal Flow*.
        iii. When a lamella settler tank with upward flow is used to treat only the basin outflow from skimmers, with and without use of polyacrylamide (PAM) flocculant.
    c. Section 4.3 focuses on important operational aspects of the sediment basin that were observed during the completion of the proposed research plan. These operational aspects include
        i. Effects of temperature in the settling processes in the basin, and how to account for varying temperatures in evaluating the performance of sediment basins;
        ii. Relationship between turbidity and total suspended solids (TSS) parameters over the various bays in sediment basins;

iii. Characterization of the Particle Size Distribution (PSD) of suspended sediments at various points in the sediment basin;
iv. Variation of turbidity in the water column during tests, focusing on the impact of a sequence of sediment loading in the basin and changes in basin turbidity.

Section 4.4 focuses in presenting the results of numerical simulation of flow characteristics in the sediment basin using computational fluid dynamic (CFD) tools, particularly focusing on the effects of baffles in improving flow characteristics in the basin.

3. Chapter 5 summarizes the findings of this research work and present recommendations for future research on this topic.

3. Methodology

3.1. Characteristics of sediment basin, water and sediment inflows

As pointed earlier, the sediment basin was already constructed at the AU-ESCTF prior to the start of the investigation. A detailed as-built survey was conducted on June 17, 2014 using a Trimble S6 robotic total station. The survey provides existing topographical conditions of the basin. Data analyses were conducted using GIS. Figure 3.1 shows the topography in and around the surrounding area of the sediment basin. The survey was updated on December 2014 after re-grading/compacting of the basin.

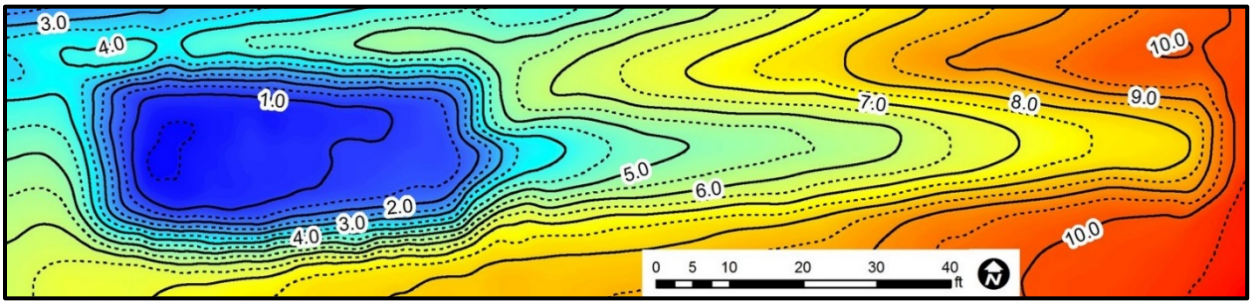

Note: dashed contour lines are ½ ft elevation increments from solid contour lines.

Figure 3.1: Sediment Basin Topography

Using the topographical survey, a general basin detail drawing was created on AutoCAD, shown in Figure 3.2(a). The constructed sediment basin measures 44 by 16 ft (13.4 by 4.9 m) along the bottom, with a total excavated footprint of 56 by 28 ft (17.1 by 8.5 m).

As an installation iteration, a forebay was constructed and prepared for testing. The forebay was designed following ALDOT standards and constructed upstream of the sediment basin along the Flexamat channel. The forebay consisted of an excavated sump positioned before a standard rip-rap ditch check with an 8 oz./yd^2 (271 g/m^2) filter fabric choker (Figure 3.2(b)). The sump measured 4 ft (1.2 m) wide, 12 ft (3.7 m) in length, and 2 ft (0.61 m) deep. The forebay was installed approximately 20 ft (6.1 m) upstream of the sediment basin entrance. This feature is intended to facilitate the capture of rapidly settable solids from sediment-laden inflow (runoff).

3.1.1. Sediment basin geometry

From a GIS analysis of the topographical survey, it was determined that the basin has a bottom elevation of 632.4 ft (193.8 m). The dead storage without outflow from skimmer is up to 0.4 ft (0.12 m) above the bottom, which is 43 ft^3 (1.2 m^3) in volume. The auxiliary spillway is situated at 635.9 ft (193.8 m) of elevation and is activated when the stage level in the basin exceeds 3.5 ft (1.07 m), slightly less than the original design depth of 4.0 ft (1.22 m). The total storage of the basin is 2,790 ft^3 (79.0 m^3). To maximize the water storage capability, no dead storage or freeboard was considered in the geometry of the basin. Volumetrically, the basin is 70% full when the stage is at 2.55 ft (0.78 m) which corresponds to a volume of 1,691 ft^3 (47.9 m^3). A detailed stage-storage relationship has been provided in Table 3.1 and a graphical representation of the live storage volume is shown in Figure 3.3.

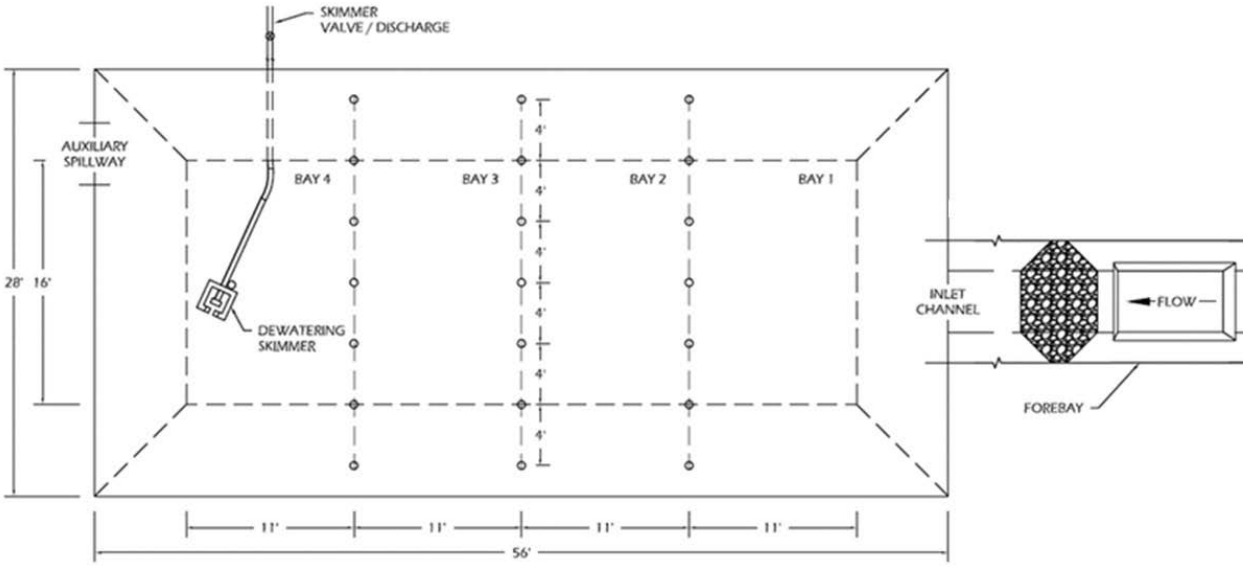

(a) sediment basin plan detail

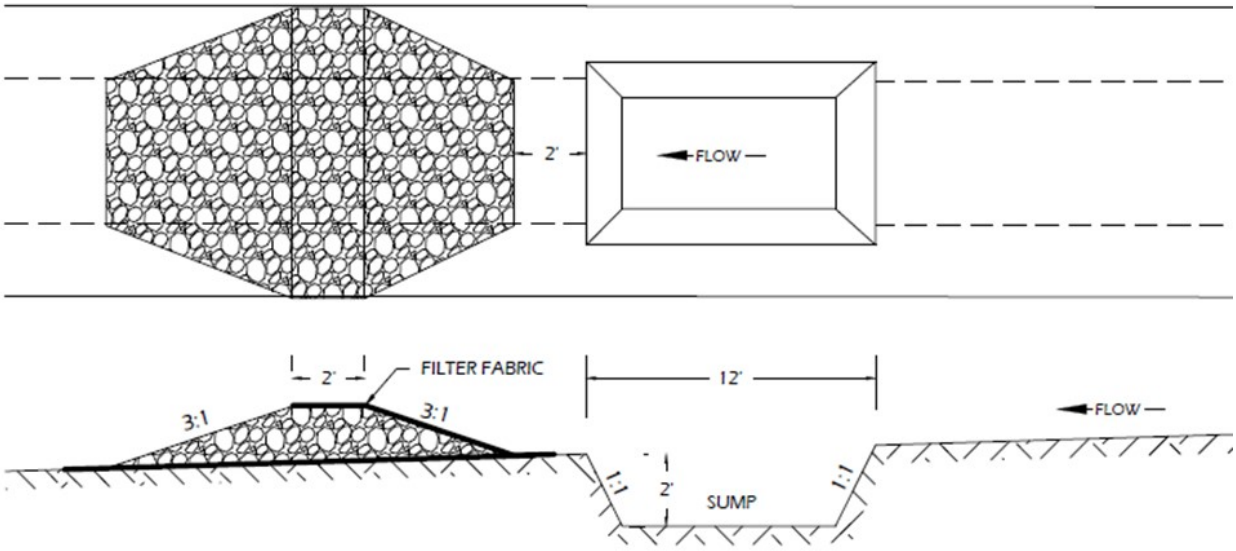

(b) forebay plan and profile details

Figure 3.2: Sediment Basin and Forebay Detail.

Table 3.1: Sediment Basin Stage-Storage Relationship

Zone	Elevation		Stage		Area		Storage	
	ft	**m**	**ft**	**m**	**ft^2**	**m^2**	**ft^3**	**m^3**
Dead Storage	632.4	192.76	0.0	0.00	0.6	0.1	0.0	0.0
43 ft^3	632.6	192.82	0.2	0.06	93.6	8.7	7.7	0.2
(1.2 m^3)	632.8	192.88	0.4	0.12	268.3	24.9	43.1	1.2
	633.0	192.94	0.6	0.18	425.1	39.5	114.5	3.2
	633.2	193.00	0.8	0.24	560.3	52.1	213.6	6.0
	633.4	193.06	1.0	0.30	667.1	62.0	337.2	9.5
	633.6	193.12	1.2	0.37	735.6	68.3	477.8	13.5
	633.8	193.18	1.4	0.43	789.9	73.4	630.5	17.9
Live Storage	634.0	193.24	1.6	0.49	838.3	77.9	793.3	22.5
2,373 ft^3	634.2	193.30	1.8	0.55	883.5	82.1	965.5	27.3
(67.2 m^3)	634.4	193.37	2.0	0.61	926.6	86.1	1146.6	32.5
	634.6	193.43	2.2	0.67	968.1	89.9	1336.1	37.8
	634.8	193.49	2.4	0.73	1010.6	93.9	1533.9	43.4
	635.0	193.55	2.6	0.79	1055.4	98.0	1740.5	49.3
	635.2	193.61	2.8	0.85	1102.3	102.4	1956.3	55.4
	635.4	193.67	3.0	0.91	1148.8	106.7	2181.4	61.8
Freeboard	635.6	193.73	3.2	0.98	1197.6	111.3	2415.9	68.4
373 ft^3	635.8	193.79	3.4	1.04	1259.5	117.0	2661.1	75.4
(10.6 m^3)	635.9 [A]	193.83	3.5	1.07	1292.9	120.1	2789.0	79.0

Notes: [A] spillway elevation`

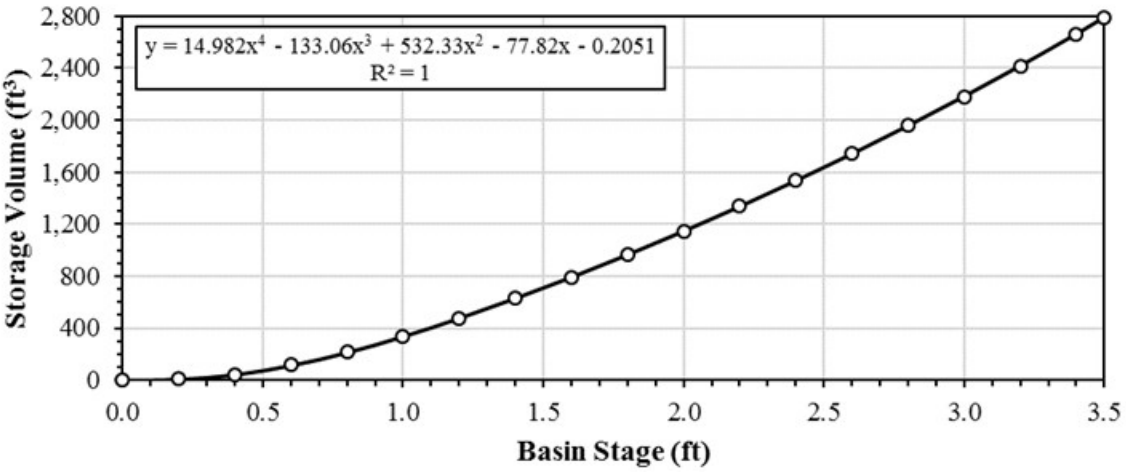

Figure 3.3: Live Storage Stage-Storage Graphical Relationship.

3.1.2. Water introduction system

The introduction of water into the basin was designed in a fashion that would allow for accurate flow rate monitoring and ease of use. To achieve the desired flow control necessary for testing, a four-stage water introduction process was developed. This setup consists of a pump system, a tank for equalizing and staging flows, shown in Figure 3.4(b) and (c), a discharge weir for controlling flow rates introduced into the channel, pictured in Figure 3.4(d), and a soil-water mixing trough for creating sediment-laden flow.

The pumping system used consisted of three semi-trash pumps. Two of these pumps were equipped with 4 in. (10.2 cm) outflow ports (NorthStar® driven with a Honda GX 270 engine, 0.86 ft^3/s [0.024 m^3/s] capacity) and the third was a 3 in. (7.62 cm) outflow port (NorthStar driven with a Honda GX160 engine, 0.59 ft^3/s [0.017 m^3/s] capacity). These pumps transported water from the AU-ESCTF upper storage supply pond into the equalizing tank located upstream the basin inflow channel. This 300 gal (1,136 L) capacity tank was customized with three inlets and four outlets. The inlets are located on the back side of the tank and are connected directly to the pumps via 3 and 4 in. (7.62 and 10.2 cm) flexible hosing and plumbing fittings. The 4 in. (10.2 cm) outlets, located directly beneath the tank, are controlled by individual gate valves, shown in Figure 3.4(a). These outlets are used to prevent overflows from the tank by returning water to the supply pond via 5 in. (12.7 cm) flexible hosing. By having all outlet valves open, the system allows for pumps to be primed and pressurized prior to commencing a test. Valves are adjusted to introduce water into the test channel at a desired flow rate by maintaining constant water level in the tank. Images of all water introduction components are shown in Figure 3.4.

(a) gate valves (b) 300-gal. equalizing tank

(c) manufactured trough baffle (d) installed weir plate

Figure 3.4: Water Introduction System.

Water flowing into the test channel was measured through a fabricated rectangular weir plate attached to an opening cut on the channel face of the equalizing tank, Figure 3.4(d). The weir was constructed to allow for different weir plates to be easily interchanged for controlling varying flow ranges. This interchangeable system allowed for any opening to be cut into an approximate 16 in. (40.6 cm) high by 10 in. (25.4 cm) blank sheet metal plate which fit into the designed opening. The weir plate was secured to the polyethylene tank by bolts and butterfly nuts to a manufactured washer plate located on the inside of the equalizing tank. Between the tank and washer plate, a rubber gasket was fitted to provide a water tight seal.

3.1.3. Sediment introduction system

The sediment introduction system (Figure 3.5) was designed using a 6 in. (15.2 cm) diameter, 16 ft (4.9 m) long auger that allows sediment to be introduced into the water/sediment mixing trough at a controlled rate. The motor, gear box, and sprocket system, were designed for the desired sediment introduction rate. A 1,740 rpm, 3.0 hp (2.2 kW) single phase motor (North American Electric, Inc.) was installed with a gear box reducer with ratio of 15:1 (WorldWide Electric Corp.). The gear box turned a 3.30 in. (8.4 cm) sprocket which was connected to a 1 in. (2.54 cm) diameter train shaft. This train shaft turned two sprockets. A 7.93 in. (20.1 cm) sprocket connected to the gearbox sprocket, and a 2.97 in. (7.54

cm) sprocket connected to the auger drive shaft. The auger drive shaft had a 7.61 in. (19.33 cm) sprocket. All sprockets were connected using a No. 40 roller chain. This gear ratio system reduced the auger drive shaft speed to approximately 18.8 rpm. The motor was equipped with a thermal protection switch and powered via single phase, 220 V electricity. To further protect the motor from overheating, 15 amp fuses were installed in the electrical circuit. A hopper was fabricated to allow the system to be loaded with sediment during an experiment. Figure 3.5(b) illustrates the complete sediment introduction assembly.

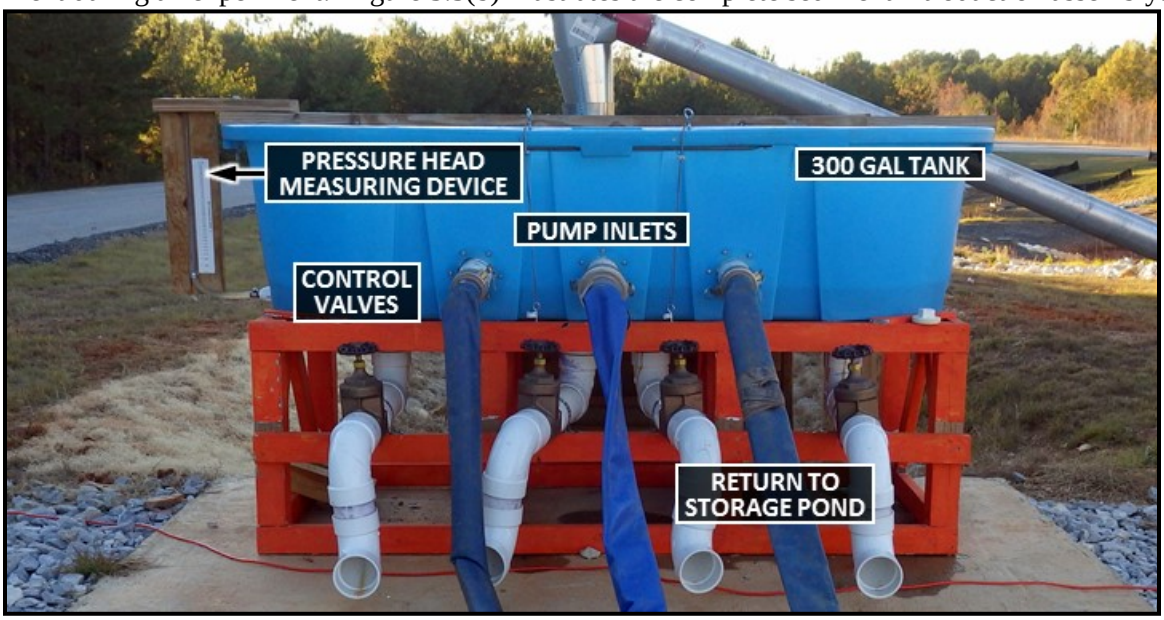

(a) flow regulation system

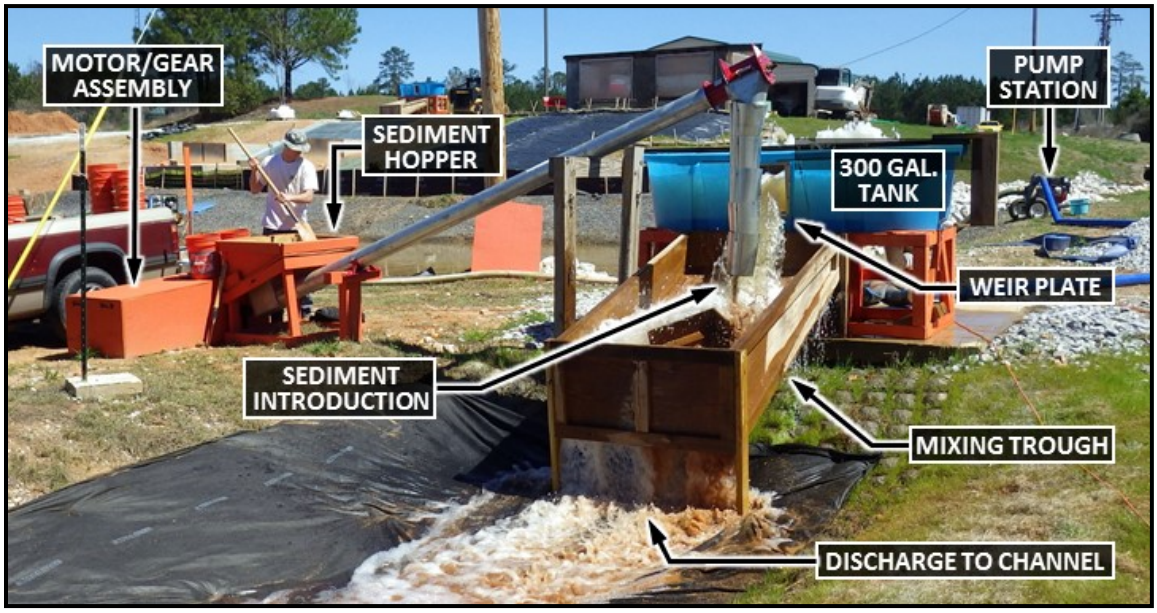

(b) sediment introduction

Figure 3.5: Water and Sediment Introduction System During Testing.

3.1.4. Sediment basin dewatering

Dewatering is achieved using 1.5 in. (3.81 cm) Faircloth Skimmer® which dewaters from the top of the water column, shown in Figure 3.6. The skimmer is connected to a 1.5 in. (3.81 cm) section of schedule 40 polyvinyl chloride (PVC) pipe and a flexible hose connection. The flexible hose connects to a 4 in. (10.2 cm) discharge PVC routed to the facility's sediment basin. A gate valve installed on the discharge line allows the flow to be shut if desired. Based on Faircloth sizing calculations, a 0.9 in. (2.29 cm) diameter orifice was cut to dewater the basin within approximately 56 hours.

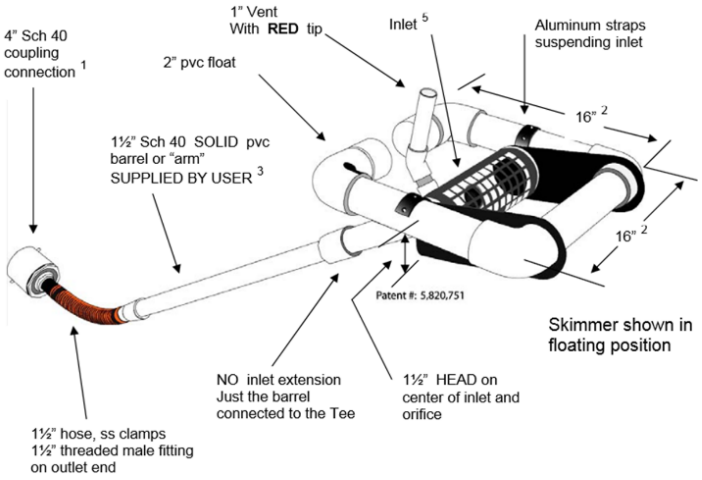

Figure 3.6: Schematic of a 1.5 in. (3.81 cm) Faircloth Skimmer (J. W. Faircloth & Son 2007)**.**

While the skimmer was the primary dewatering mechanism, infiltration and evaporation still contributed in the removal of water from the basin. An infiltration test was performed by filling the basin with water and closing the skimmer valve to evaluate the rate of water removal from the basin. Results from the first 24 hrs of the infiltration test indicated that the basin infiltrated at an average rate of 0.86 in/hr (2.2 cm/hr). Based on the stage-storage relationship of the basin, the approximate infiltration rate is 96 ft^3/hr (2.7 m^3/hr). Figure 3.7 shows the dewatering rate and stage of the basin over time during the infiltration test.

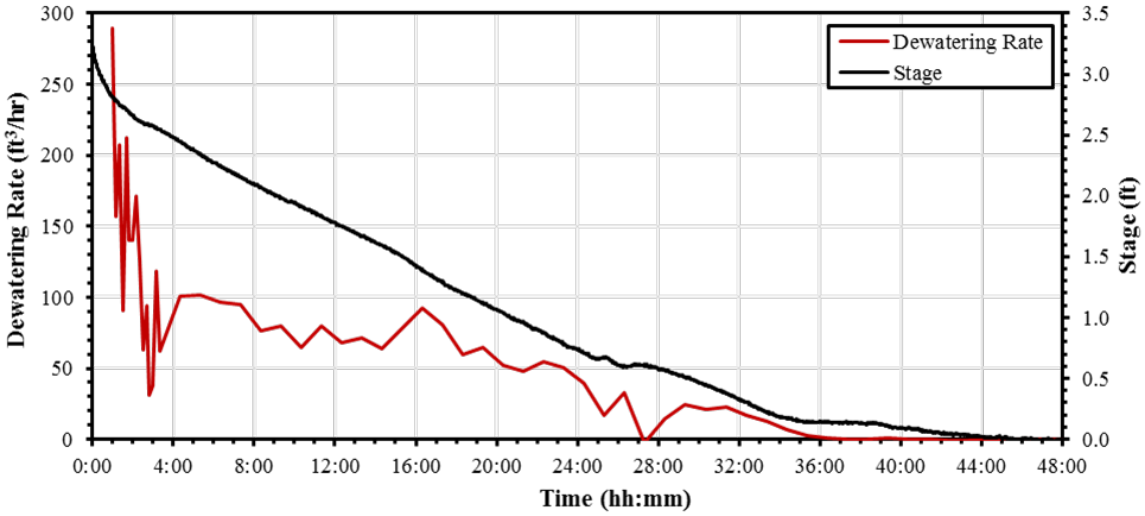

Figure 3.7: Sediment Basin Infiltration Test**.**

An auxiliary or emergency spillway (Figure 3.8) was provided to allow excessive water to overtop at a designated and protected channel. The crest of the spillway is situated 0.4 ft (0.12 m) above the live storage section of the basin. The spillway was constructed by creating a depression on the northwest corner of the basin. Breached flows are routed towards the facility's existing riprap channel and lower retention pond. The spillway is lined with Flexamat tied concrete block matting to protect from scouring during overtopping conditions. As is further elaborated ahead this spillway has an important role in the research in that there are tests that involve creation of overflowing conditions.

(a) spillway (b) spillway during flow

Figure 3.8: Auxiliary Spillway

3.2. Data collection

Data collected during testing provide comparative means of the basin's performance with the varying tested basin configurations and treatments. Water quality, flow rates, basin stage levels, sediment deposition volumes, and sediment sampling for particle characterization, were measured or collected during and after tests. Turbidity results were obtained from automated probes. Physical grab sampling was also conducted during initial tests to determine relationships between TSS and turbidity. Figure 3.9 provides an overview of the data collection instrumentation layout within the sediment basin.

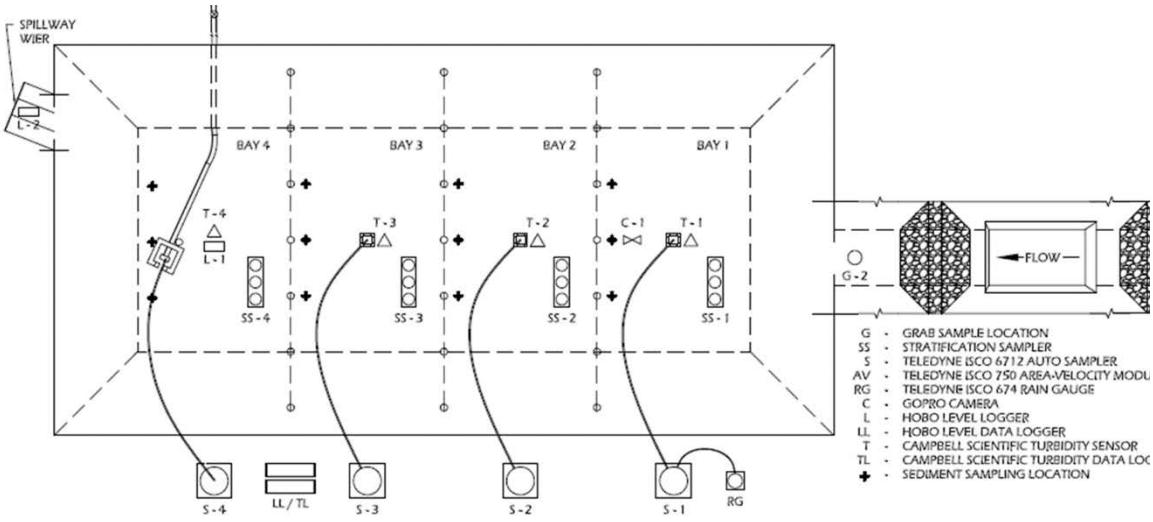

Figure 3.9: Data Collection Instrumentation Layout.

Three Campbell Scientific OBS3+ turbidity sensors with logging capabilities were used during testing. The sensors were placed Bays 1, 2, and 4. The sensors have the capability of measuring up to 4,000 NTU. A Campbell Scientific CR850 data logger was mounted near the sensors and was powered by a 12V deep cycle marine battery. Also, a SonTek Argonaut® multi-cell Doppler current profiler was installed in Bay 1 at the mouth of the sediment basin to analyze flow within the entrance of the basin. This probe monitored three-dimensional flow velocities. The sensor was powered by a 12V deep cycle marine battery. Velocity results, however, were not conclusive and are not present in this report.

Three Onset HOBO water level pressure transducers (U20-001-04) were used during testing to accurately monitor the stage of the basin throughout the duration of the experiments. Two loggers were used within Bay 4 and the third was placed in the auxiliary spillway weir box (Figure 3.10) during overflow experiments. Of the loggers placed in Bay 4, one was installed near the basin floor, and the second was installed above the high water mark, with the purpose of recording atmospheric pressure and temperature. A perforated 1.5 in. (3.8 cm) PVC tube was used as a monitoring cylinder to protect the level loggers from direct sunlight. The level loggers placed inside the basin were programed to take measurements at one minute intervals, while the level logger placed in the auxiliary spillway weir box, took readings at 10 second intervals. Figure 3.11 presents the sensors and instruments used in the investigation.

Figure 3.10: Auxiliary Spillway Weir Box.

Water sampling was only conducted during initial tests and was used to validate turbidity probe results and to determine turbidity and TSS relationships. For grab sampling, five automated Teledyne Isco 6712 full-size portable samplers were deployed, one per each of the four bays within the basin and an additional sampler near the bottom of Bay 2. Suction tubing was routed to a suction head mounted to custom built floating skimmers in the center of each of the first three bays, and on the outlet skimmer in the fourth bay. Sample collection begin once the stage in the basin reached the height of the floating skimmers.

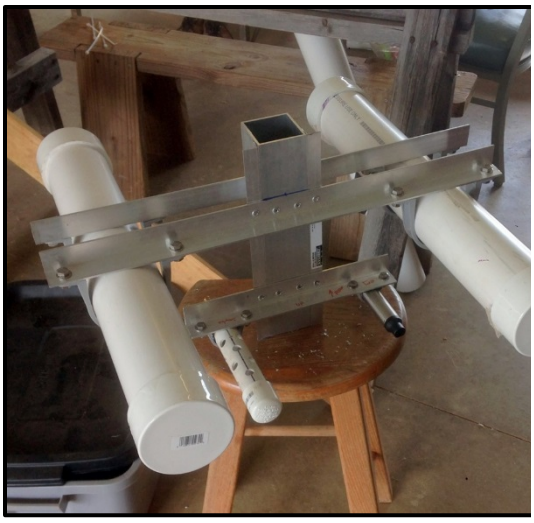

(a) floating sampling apparatus

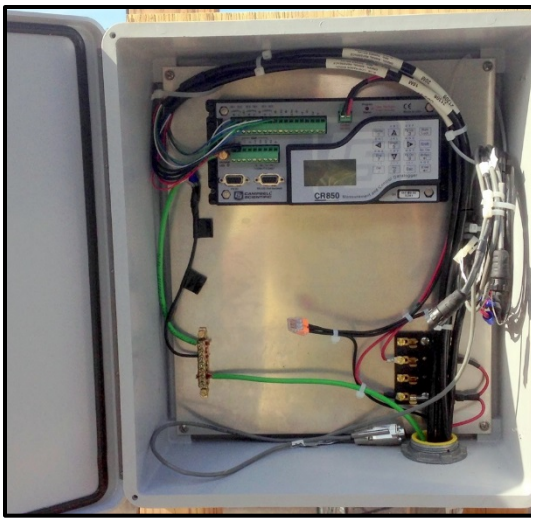

(b) turbidity data logger

(c) level logger (Onset 2016)

(d) ADV sensor (SonTek / Xylem Inc. 2016)

(e) automated sampler

(f) rain gauge (Teledyne Technologies Inc. 2013)

Figure 3.11: Data Collection Equipment.

To minimize the turbulence caused by the automated sampling, the 0.375 in. (0.953 cm) suction tubing was routed to direct purge and rinse volumes from reentering the basin. Figure 3.12 depicts the setup that used a tee connection to split sampler line to a collection point and discharge point. One-way check valves directed flows in the desired flow path. The suction line was attached to a taught steel wire angled down gradient across the basin. Since the sampler was programmed to suction the length of line between the collection point and sampler, the slope allows the drain line section between the check valve and discharge point to drain without the need of additional pumping. This setup however was abandoned after valve clogging became an issue causing air to bleed through the valves. A single purge cycle replaced the one-way valve mechanisms.

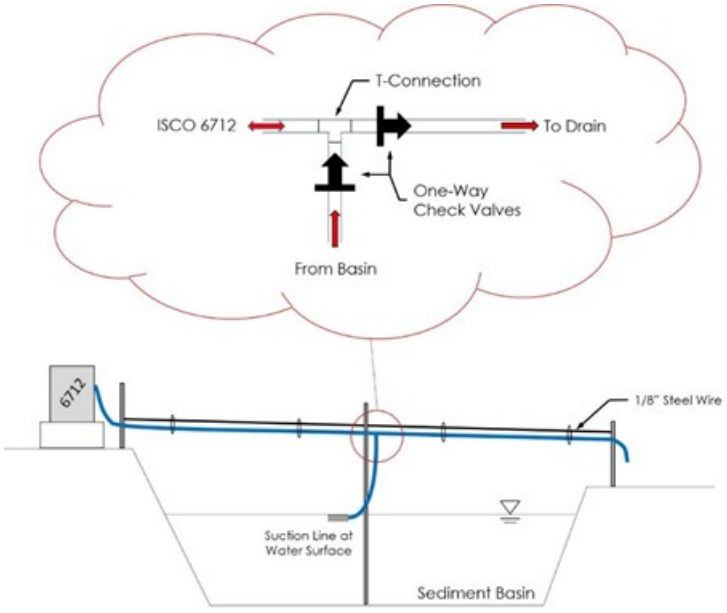

Figure 3.12: Sampler Suction and Discharge Line Routing.

Automated samplers were programed to collect 13.5 oz. (400 mL) samples through two separate collection cycles using a non-uniform time paced sampling program. The first cycle of the program collected samples every five minutes for the first 60 minutes of sampling. Thereafter, a second cycle collected one sample every 120 minutes for a period of 23 hours. A total of 24 water samples per sampler were collected, totaling approximately 96 total automated samples per test. During overtopping experiments, an additional sampler was located at the auxiliary spillway to collect samples at three minute intervals. TSS and turbidity analysis was performed using the EPA methods and testing specifications (USEPA 1999; 2003).

During the duration of the flow introduction period (30 minutes), grab samples were taken in two locations along the inflow channel. The first point was directly downstream of the mixing trough, and the second point was at the sediment basin entrance. Samples were taken at five minute intervals. All manual grab samples commenced once flows reached the sampling location and ended once all flow has subsided (i.e., reached the sediment basin). Typically, six samples were taken at the upstream point, and up to twelve samples at the downstream location due to the delayed dewatering of the forebay. Table 3.2 summarizes the water sampling regime.

Table 3.2: Water Sample Collection

Sample Type	Location	Sample Interval	Samples	Total Samples
Grab Samples	Introduction Zone	5 min.	6	18
	Basin Entrance		12	
Automated Surface Samples	Bay 1	5 min (0-60 min) / 120 min (1-24 hr)	24	96
	Bay 2		24	
	Bay 3		24	
	Bay 4		24	
Automated Bottom Sampler	Bay 2	5 min (0-60 min) / 120 min (1-24 hr)	24	24
Total Samples:				138

To account for any precipitation occurring during testing and dewatering durations, a Teledyne Isco 674 rain gauge was used with the sampler located in Bay 4. The gauge, shown in Figure 3.11(f) detailed the start time of rain events, duration, and intensity.

In addition to the data collection and instruments discussed above, another set of samples were taken to assess the change in turbidity over the depth of sediment basins during inflow stages and in the early stages of the filling. Samples were taken with small flexible 3/8-in clear tubing at three different depths (1 ft, 2 ft and 3 ft from the basin invert), and at each of the four bays in the basin. The vertical location within the bays where samples were taken corresponded to the same points that were for turbidity measurement with the turbidity probes. In total, these samples were siphoned out at twelve different locations in the basin and collected at a single point. Flow in these tubes was initiated by means of a vacuum pump once the water level was large enough in the basin to sustain the siphoning. These samples were taken approximately every 5 minutes, and stored in plastic bottles for subsequent turbidity evaluation. While TSS tests were not used in this stage, turbidity was characterized with the aid of a HACH 2100Q turbidimeter.

3.3. Lamella settler design and construction

The high-rate lamella settler was conceived, designed and constructed prior to its deployment at the AU-ESCTF. A structural analysis software was used for structural design of the lamella settler, accounting for its own weight and the soil/water weight over the plates. The settler units were developed in two part (upper/lower) as a means to reduce the weight of individual parts and the structural loading. The lamella plates were constructed with gauge 11 steel plates for a long-term settler deployment. The steel frames holding the plates were constructed in laser-cut steel beams with 2.0 in x0.5 in sections, and soldered with steel tubes 2 in × 2 in square sections, gauge 11. Construction was performed by Davis Machine Works, in Opelika, AL, and delivered to AU-ESCTF January 2015. Figure 3.13(a) presents a lower half of a lamella settler, and Figure 3.13(b) presents the entire tank assembled with the plates in it.

(a) Lower portion of a high-rate lamella settler unit

(b) Lower and upper portion of a high-rate lamella settler unit, with lamella plates installed

(c) Lamella units installed in the AU-ESCTF sediment basin.

Figure 3.13: Lamella settler unit.

3.4. Experimental procedure

To evaluate the performance of various sediment basin configurations and technology, an experimental design and testing regime was developed to mimic conditions to be expected on construction sites. Flow and sediment introduction rates were selected to mimic expected conditions from a local 2-yr, 24-hr design rainfall event. Additionally, a testing regime was designed to create a replicable experiment used to efficiently access and compare performance between various basin configurations and innovative sediment basin technology.

3.4.1. Water inflow rate selection

Sediment basins are sized based on the contributory drainage area of the site. Two sizing options for the design of a sediment basin are commonly used by ALDOT. The first method provides 3,600 ft^3 of storage per acre (250 m^3/ha) of contributory area, thereby providing storage for the first 1.0 in. (2.5 cm) of runoff. To mimic expected flow conditions based on the constructed size of the basin, back calculation procedures were performed using Bentley® PondPack® V8i hydrologic modeling software using the average 2-yr, 24-hr Type III rainfall event for the state of Alabama, of 4.43 in. (11.3 cm) (Perez et al. 2016). Using the 3,600 ft^3/ac (250 m^3/ha) design criteria, the constructed basin will provide detention for runoff emanating from a contributory drainage area of 0.775 ac (0.314 ha) since the storage of the basin is 2,790 ft^3 (78.9 m^3). Due to the small size of the drainage area, the time of concentration was set to 0.083 hrs (5 minutes). This drainage area results in a storm hydrograph volume of 8,938 ft^3 (253 m^3) with a peak flow rate of 2.47 ft^3/s (0.070 m^3/s).

The second sizing method considers the complete detention of runoff volume generated from a 2-yr, 24-hr event over the contributory area (ALDOT 2010). Following TR-55 methodology, a curve number (CN) of 88.5 was applied to the entire contributory area (Perez et al. 2014). It was also assumed that the time of concentration for the event would be 0.083 hour (5 min.). Using these parameters, an iterative hydrologic analysis was performed using a 2-yr, 24-hr soil conservation service (SCS) Type III rainfall distribution with a state-wide rainfall of 4.43 in. (11.3 cm), which resulted in a contributory area of 0.242 ac (0.098 ha) (USDA 1986). The resulting stormwater runoff volume was 2,790 ft^3 (79.0 m^3) with a peak flow rate of 0.77 ft^3/s (0.022 m^3) occurring at 12.1 hours.

The intent of flow introduction was to provide the sediment basin with the total volume of runoff produced by a 2-yr, 24-hr rainfall event over the course of 30 minutes, while also mimicking the expected peak flow rate. Information obtained from hydrographs for the 2-yr, 24-hr design storm events are summarized in Table 3.3 for both the 0.775 ac (0.314 ha) and 0.242 ac (0.098 ha) hypothetical drainage areas derived from the two sizing methods. Figure 3.14 is a plot showing the hydrographs for the two drainage areas from the 2-yr, 24-hr rainfall event (4.43 in.).

To investigate various contributory drainage areas, corresponding stormwater volumes, and peak flow rates for the SCS Type III local 2-yr, 24-hr storm event, several iterations were analyzed. Based on the basin sizing analysis and preliminary sediment basin filling test runs, the targeted flow introduction rate of 1.50 ft^3/s (0.042 m^3/s) for a 30-minute water introduction duration was selected. This rate maximizes the storage capability of the basin, filling the entire volume during a 30-minute test. This targeted test flow rate produces 2,700 ft^3 (76.5 m^3), and is nearly double the peak flow rate (0.77 ft^3/s) of the selected design rainfall event, exceeding the peak by 0.73 ft^3/s (0.021 m^3/s) for 0.242 ac (0.098 ha) drainage area.

Table 3.3: Sediment basin storage parameters

Sizing Parameter	Contributory Area [A]		Storm Volume [B], ft^3 (m^3)	Peak Flow, ft^3/s (m^3/s)	Avg. Testing Flow Rate [C], ft^3/s (m^3/s)		
	ac (ha)	ft^2 (m^2)			30 min	45 min	60 min
1,800 ft^3/ac (125 m^3/ha)	1.549 (0.627)	67,474 (6,268)	17,864 (505.9)	4.93 (0.140)	9.92 (0.281)	6.62 (0.187)	4.96 (0.140)
3,600 ft^3/ac (250 m^3/ha)	0.775 (0.314)	33,747 (3,135)	8,938 (253.1)	2.47 (0.070)	4.97 (0.141)	3.31 (0.094)	2.48 (0.070)
2-yr, 24-hr event	0.242 (0.098)	10,541 (979.3)	2,793 (79.1)	0.77 (0.022)	1.55 (0.044)	1.03 (0.029)	0.78 (0.022)

Notes: [A] Based on design or sizing parameter
[B] Simulated runoff volume for SCS Type III 2-yr, 24 hr rainfall event (4.43 in), and available storage in AU-ESCTF sediment basin is 2,790 ft^3 (79.0 m^3)
[C] Calculated using the basin storage 2,790 ft^3 (79.0 m^3) divided by the flow introduction periods (30, 45, and 60 min), and not derived from hydrographs in Figure 3.14.

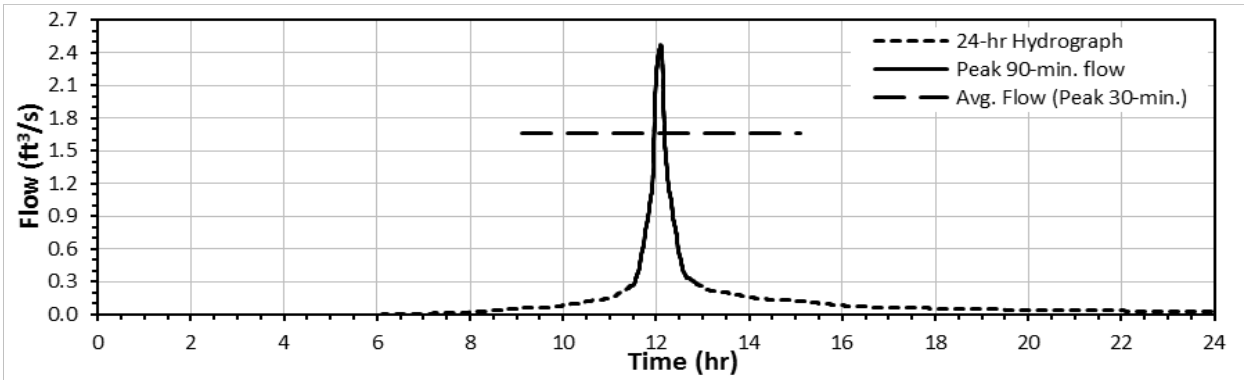

(a) 0.775 acre basin

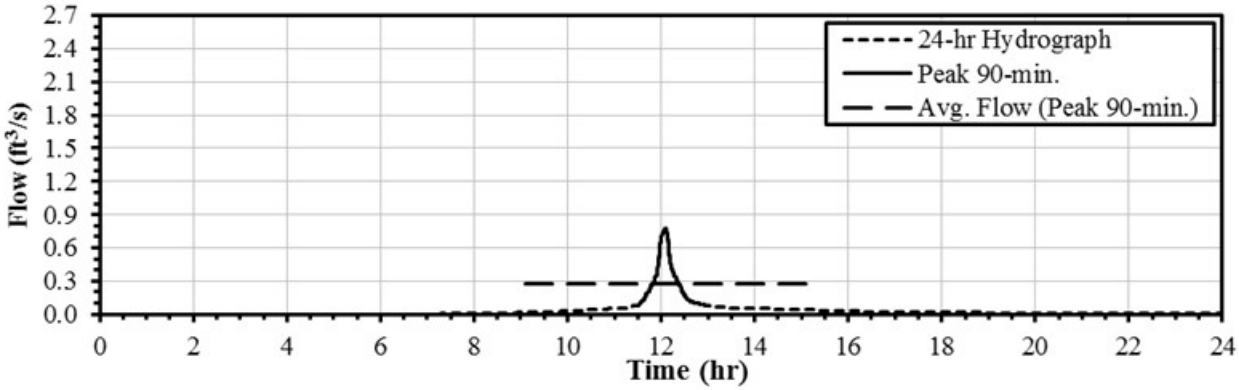

(b) 0.242 acre basin

Figure 3.14: Representation of 2-yr, 24-hr rainfall event hydrographs.

The selected flow introduction rate of 1.50 ft^3/s (0.042 m^3/s) is also representative to the average flow rate over the peak 30 minutes (1.66 ft^3/s [0.047 m^3/s], Figure 3.14(a)) for 0.775 ac (0.314 ha) drainage area, which is designed under the 3,600 ft^3/ac (250 m^3/ha) criteria.

3.4.2. Sediment introduction rate selection and soil characteristics

To mimic expected sediment transport, the sediment introduction rate was computed using the modified universal soil loss equation (MUSLE), which estimates sediment yields based on individual storm events (Williams 1975). MUSLE uses runoff variables to estimate soil loss on the basis that runoff is a better indicator of sediment yield rather than rainfall amount. The MUSLE is given by the equation: $S = 95(Qp_p)^{0.56}KLSCP$, where: S is sediment yield (tons), Q is the 2-yr, 24-hr storm runoff volume (acre-ft), p_p is the event peak discharge (ft^3/s), and K, LS, C, P are MUSLE parameters.

Based upon experimental flow calculations conducted for the state of Alabama, the MUSLE equation was applied to the peak 30 minutes of the design storm, which produces of 935 ft^3 (26.5 m^3) with a peak discharge of 0.77 ft^3/s (0.022 m^3/s). A soil erodibility factor (K) of 0.085 was selected and a slope-length and steepness factor (LS) was determined to be 0.83, representative of 16% slopes at 20 ft (6.1 m) lengths for conditions of high rill to interrill erosion ratios (Pitt et al. 2007). Although erosion control practices (i.e., mulching, temporary seeding, etc.) would be implemented alongside sediment controls, the worst-case design scenario for a vegetative cover practice factor (*C*) of 1.0 was chosen for bare soil conditions. Similarly, the ponding or erosion control practice factor (*P*) was selected to be 1.0. This situation may be encountered where sediment basins are constructed prior to final site grading and the installation of erosion controls and/or vegetative establishment. Using the aforementioned variables, total sediment yield was computed for an output of 1,348 lbs (611 kg). The sediment load targeted metering rate is 44.9 lbs/min (20.4 kg/min) over the 30-minute test duration. Calibration of the sediment introduction system revealed a soil introduction rate of 45.2 lb/min (20.5 kg/min). Based upon this rate, the sediment introduction concentration is 8,044 mg/L (1,356 lbs / 2,700 ft^3) if all introduced sediment would flow into the basin. However a certain amount of large-size sediments is deposited in the inflow channel.

For sediment-laden tests to be replicable, a stockpile of soil, native to the state of Alabama, was used for all tests. The soil used for sediment introduction was acquired from a source local to Opelika, AL. The soil stock was sieved through a 0.5 in. (1.3 cm) screen to remove large aggregate and organic debris prior to use in the testing apparatus. A particle size analysis as well as a compaction test was conducted in the geotechnical laboratory to characterize the soil properties. The average particle size distribution of the three analysis performed is shown in Figure 3.15.

Table 3.4 summarizes results of the sieve analysis of the soil performed under ASTM Standard D422-63(07) 2007. Under the Unified Soil Classification System (USCS), the soil is categorized as a poorly graded sand with silt (ASTM Standard D2487-11 2011).

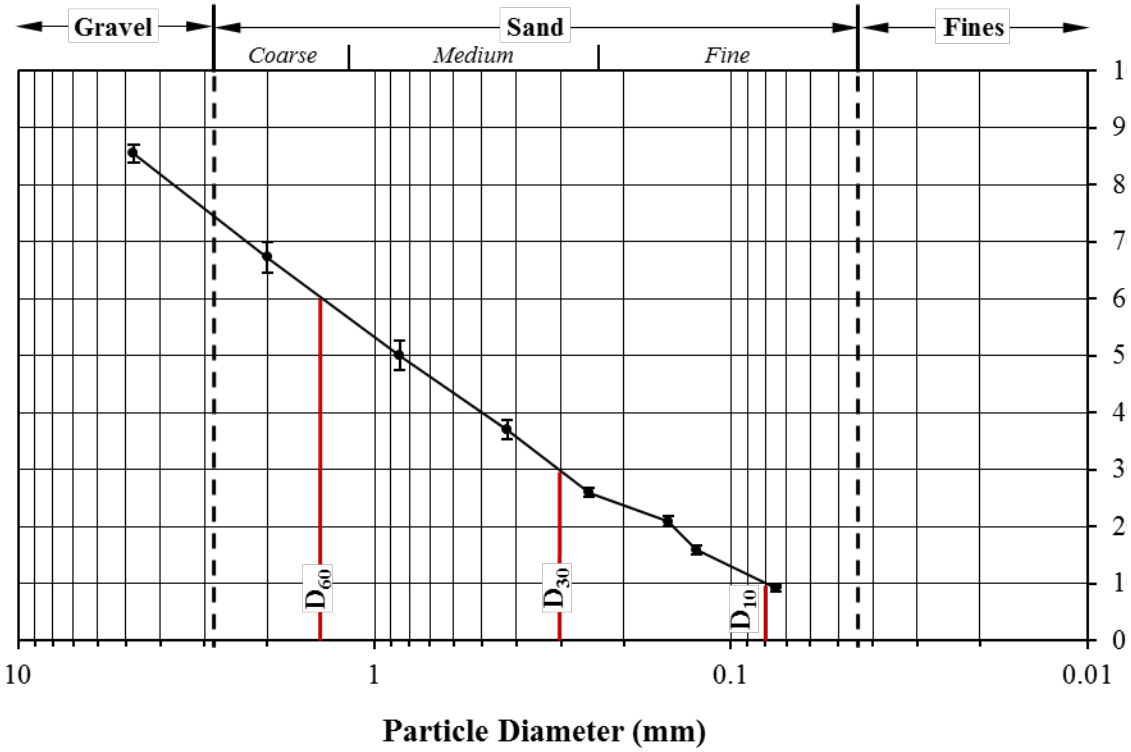

Figure 3.15: Particle size Distribution for sediment.

Table 3.4: Sieve Analysis of Sediment

Sieve	Apparent Opening Size (mm)	Percent Finer (%)				
		Sample No. 1	Sample No. 2	Sample No. 3	Avg.	Std. Dev.
#4	4.750	89.4%	87.6%	87.6%	87.5%	1.6%
#10	2.000	73.9%	69.5%	69.5%	70.2%	2.8%
#20	0.850	56.0%	51.3%	51.3%	52.4%	2.6%
#40	0.425	40.5%	37.0%	37.0%	38.1%	1.7%
#60	0.250	26.6%	24.7%	24.7%	25.8%	0.8%
#100	0.150	21.3%	19.3%	19.3%	20.5%	0.9%
#120	0.125	14.7%	13.8%	13.8%	14.8%	0.9%
#200	0.075	8.4%	8.0%	8.0%	8.5%	0.5%
Pan	0.000	0.0%	0.0%	0.0%	0.0%	0.0%
D_{60} = 0.055 in. (1.40 mm)			D_{30} = 0.008 in. (0.20mm)		D_{10} = 0.003 in. (0.08 mm)	
C_u = 17.7			C_c = 0.81		% Gravel = 12.5	
USCS classification: SP-SM, poorly graded sand with silt						

Notes:
USCS: Unified Soil Classification System
D_{60}, D_{30}, D_{10} = soil particle diameter at which 60%, 30%, or 10% of the mass of a soil sample is finer
C_u = coefficient of uniformity
C_c = coefficient of curvature

The soil was also analyzed for the maximum practically achievable density. A standard proctor test (ASTM Standard D698-12 2012) was performed on the soil to determine the maximum dry density (ρ_{dmax}) and the optimum moisture content (OMC) for the soil. The ρ_{dmax} was determined to be 108.1 lbs/ft^3 (1,732 kg/m^3) at an OMC of 15.5%. The developed proctor curve is shown in Figure 3.16.

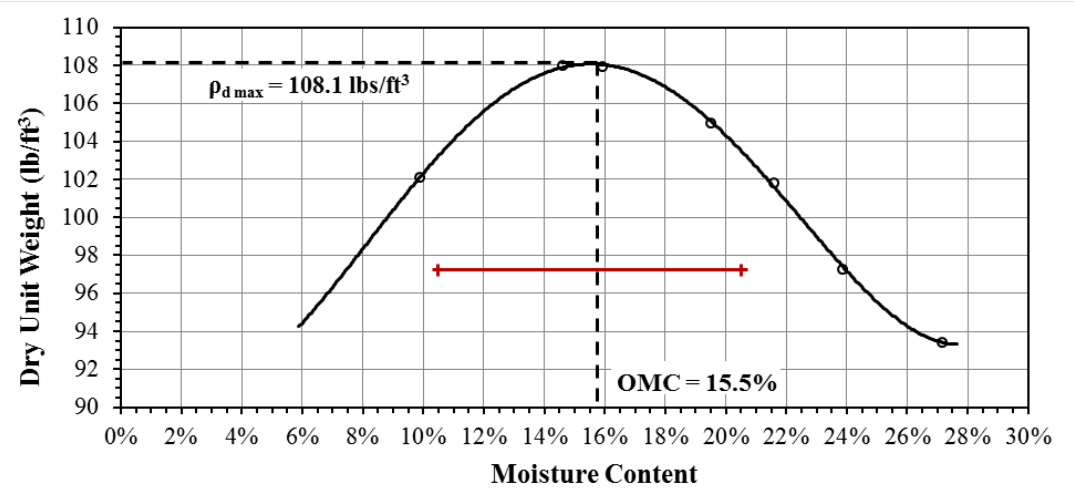

Figure 3.16: Soil geotechnical report.

As indicated in Figure 3.16 with a red solid line, the dry unit weight for 90% compaction was calculated to be 97.3 lbs/ft^3 (1,559 kg/m^3) with a moisture content ranging between 10.5 to 20.5%. Also, In addition to analysis performed in the geotechnical laboratory, a soil sample was submitted for testing to the Auburn University Soil Testing Laboratory which returned a report indicating the sample composition was of 46.9% sand, 28.1% silt, and 25% clay. This analysis corresponds to a loam soil type on the USDA soil texture triangle (USDA 1987).

3.4.3. Description of the sediment basin testing regime

To assess the performance of the sediment basin under various configurations and with the use of lamella settling technology, a staged experimental testing regime was developed. As data were analyzed following initial tests, modifications to the regime were made throughout testing to provide the most effective means of evaluating treatments. The developed regime, shown in Figure 3.17, is comprised of seven series of evaluations (S1 through S7) with a total of 27 tests. The first test within each series, L1, started with a clean and empty basin, free of sediment. Subsequent tests (i.e., L2 and L3) were conducted once the basin had completely dewatered, however sediment contained from preceding tests was not removed from the basin. Performance was evaluated based upon the exposure of the three tests, which mimics the installation of a new sediment basin at a construction site that is not maintained (i.e., dredged of sediment) between subsequent storm events. To gain a better understanding of basin performance under the condition where a storm event occurs while the basin is partially full from a preceding event, overtopping tests were incorporated into the testing regime. These overtopping tests (i.e., S4-S7), were comprised of a set of three replicate fill, partially empty, and overtop cycles (L1-A through L3-B), totaling six tests per evaluation. Part A of each of these evaluations filled the basin completely without overtopping. Part B began once 30% of the volume within the basin had dewatered, resulting in 70% of the test inflow passing through the auxiliary spillway. Volumetrically, the basin is 70% full when the stage is at 2.55 ft (0.77 m), which corresponds to a volume of 1,691 ft^3 (47.9 m^3). All tests, regardless of series type, were conducted with a 1.50 ft^3/s (0.042 m^3/s) flow rate and 45.2 lb/min (20.5 kg/min) sediment introduction rate for a 30-minute duration.

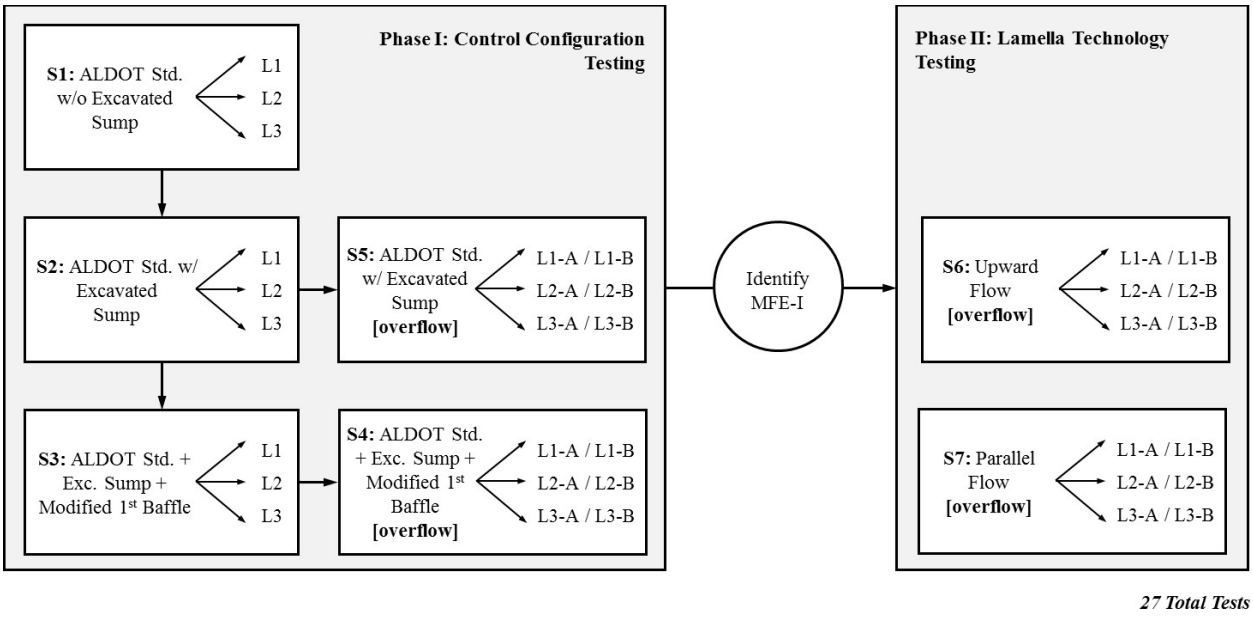

(a) testing regime

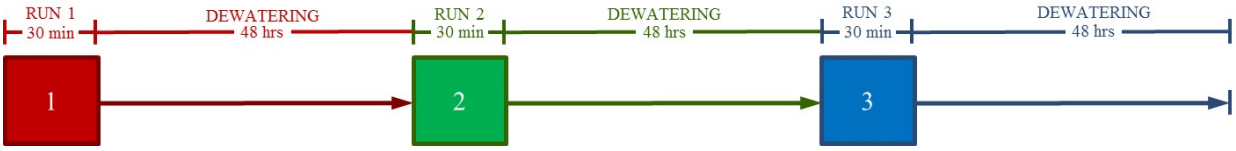

(b) empty condition test series sequence

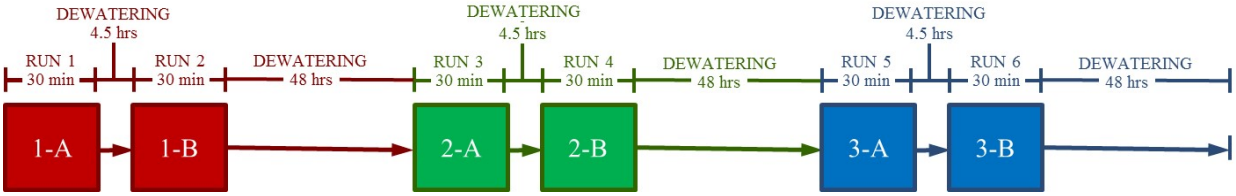

(c) overflow condition test series sequence

Figure 3.17: Developed sediment basin testing regime and test series sequence.

Test series S1 and S2 were conducted to provide sediment basin performance comparisons when an excavated sump was included in the forebay or not. The inclusion of the sump in subsequent testing (S3 through S7) was determined from performance data comparisons. Once the use of an excavated sump was assessed, the next series of tests (S3) evaluated a modified first baffle system installed between the first and second bay. Both the treatments with the excavated sump and modified first baffle were then evaluated under the overtopping testing condition (S4 and S5). Between the treatments using a sump and modified first baffle, the most feasible and effective installation (MFE-I) was selected to proceed with further testing. The MFE-I was then evaluated under the overtopping test condition (S4).

The second phase of testing focused on deploying high-rate lamella settling technology within the third and fourth bays of the basin. Two separate configurations of the technology were tested within the basin (i.e., upward and parallel flow geometry) and each will be evaluated under an overtopping series of tests (S6 and S7). The designed testing regime allowed for direct comparisons between the MFE-I and the use of the high-rate settlers in both tested configurations.

3.5. Numerical simulation of sediment basin filling using CFD tools

Another task that was included in this research was the numerical simulation of the filling process of the sediment basin. The goal of this simulation was to obtain more insights on the magnitude of flow velocities and flow circulation in the basin during the process of filling. This is relevant because sediment particles can stay in suspension and create higher turbidity values for higher flow velocities. Numerical simulation can indicate what conditions are associated with higher velocities. Also, it is useful in determining the impact of porous baffles in flow circulation.

The CFD basin model constructed in this research introduced a few simplifications on the basin geometry such as assuming an axis of symmetry and a short inlet channel to reduce the mesh size and speed up simulations. The specific model setup and dimensions are presented in Figure 3.18. The basin has been separated into four bays with three layers of porous baffles, though simulations with no baffles were also performed. The CFD simulation strategy was based on using the open-source multiphase flow solver interFOAM (Openfoam.org, 2016) to resolve the flows with free surfaces. In this way, the Navier-Stokes equations are solved along with the volume of fraction (VOF) algorithm (Hirt and Nichols 1981), as presented in equations 3.1-3.3 below:

$$\frac{\partial \rho}{\partial t} + \nabla \cdot (\rho \vec{U}) = 0 \qquad 3.1$$

$$\frac{\partial (\rho \vec{U})}{\partial t} + \nabla \cdot (\rho \vec{U} \vec{U}) - \nabla \cdot (\mu \nabla \vec{U}) - \rho g = -\nabla p - F_S \qquad 3.2$$

$$\rho = \alpha \rho_w + (1 - \alpha) \rho_a \qquad 3.3$$

Where ρ_a and ρ_w correspond to the water and air density, respectively, $\vec{U}$ is the velocity vector, p is the pressure, g is the gravity acceleration, μ is the dynamic viscosity, F_S is the interface forces and α is the water fraction (from 0 to 1) in the fluid mixture. When a computational cell is completely occupied by water, α is equal to 0; any cell at the air and water interface (water surface) has α less than 1; when a cell is completely above the water surface, α is equal to 0. The turbulence modeling was achieved with the SST k-omega model (Menter, 1993), not detailed here.

In in the CFD simulation the coir baffles are simulated as porous media. In this context, porous media is defined as a flow region that creates head loss governed by Ergun Equation (Ergun, 1952), which refers the pressure head loss Δp and is caused by simultaneous kinetic and viscous energy losses associated with an average velocity U:

$$\Delta p = -(D\mu U + 0.5 I \rho U^2) L \qquad 3.4$$

$$D = 150(1 - e)^2/(\varphi^2 D_p^2 e^3) \qquad 3.5$$

$$I = 3.50(1 - e)/(\varphi D_p e^3) \qquad 3.6$$

Where D is the Darcy coefficient or viscous resistance, I is inertial coefficient or inertial resistance, L is the porous media length, e is the sphericity of particles, ϕ is the porosity of the medium, Dp is the diameter of particles comprising the porous media.

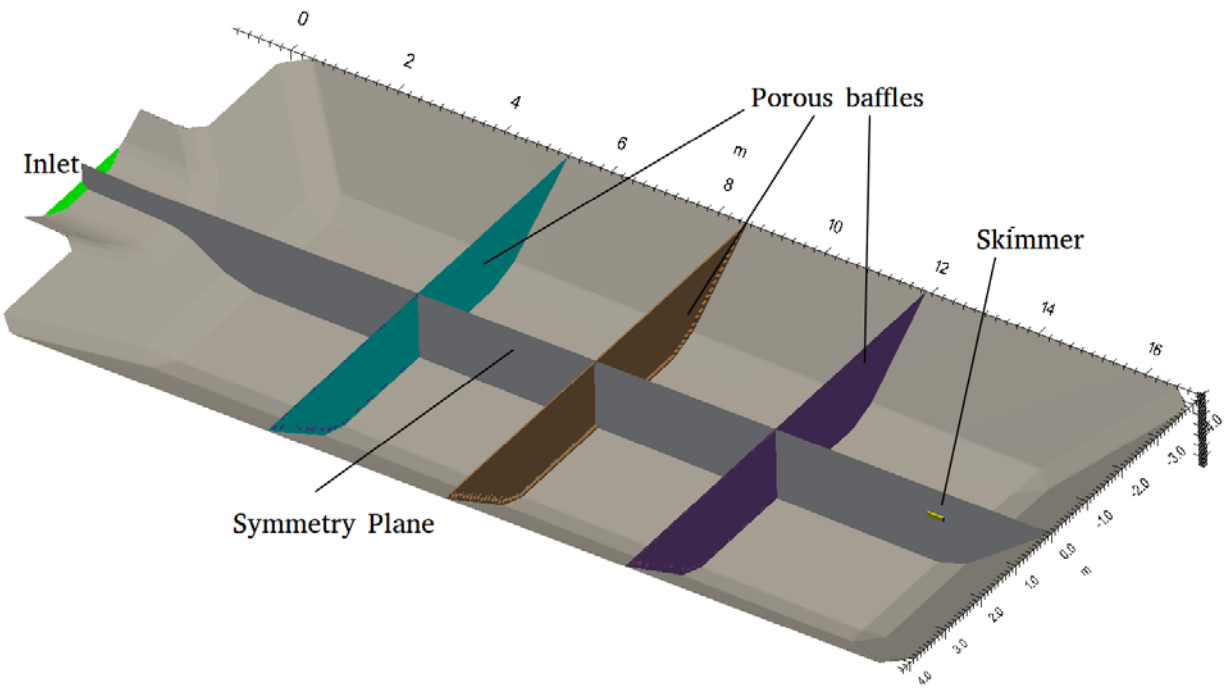

Figure 3.18: Schematic of the sediment basin used in this study.

4. Research results and discussion

The present chapter presents results from all field measurements along with discussion of the observations. The chapter is structures in four mains sections

- Section 4.1: Control configuration (Figure 3.17) testing results. These experiments did not involve the use of high-rate settlers.
- Section 4.2: Lamella settler technology testing,
- Section 4.3: Discussion of temperature effects on turbidity, relationship between Total Suspended Soils and
- Section 4.3: Numerical modeling simulation results of flow conditions of the sediment basin undergoing filling.

4.1. Control configuration testing results

This section describes the data and results collected and analyzed for the control treatments tested in the sediment basin to determine the MFE-I. The evaluated treatments included:
S1: ALDOT standard configuration,
S2: ALDOT standard configuration with excavated sump in forebay + standard first baffle,
S3: ALDOT standard configuration with excavated sump + modified first baffle,
S4: ALDOT standard configuration with excavated sump + standard first baffle (overflow),
S5: ALDOT standard configuration with excavated sump + modified first baffle (overflow).

4.1.1. ALDOT Standard Configuration

The first series of tests (S1) conducted in the sediment basin was the ALDOT standard configuration without the inclusion of an excavated sump in the inflow channel. The configuration was evaluated under a series of three tests. Overflow evaluations were not performed on this configuration. The average turbidity results of the three runs (i.e. S1-L1, S1-L2, S1-L3) were obtained from the probes used in bays 1, 2, and 4 and are plotted on Figure 4.1. These results, and all other results corresponding to turbidity time series, correspond the average between the three repetitions performed for the treatment.

From the plot, there are three evident trends discernable from the slope of the turbidity. The first 30 minutes is referred to as the filling period where turbidity is consistent with an average of 767 NTU in Bay 1. Initial turbidity in Bay 2 and Bay 4 are as high as in Bay 1, however sharply decrease to 314 and 306 NTU, respectively at the conclusion of the filling period. This indicates that the baffle between Bay 1 and Bay 2 is effective in isolating the highly turbid inflow into Bay 1. After the filling period concludes, there is a sharp decrease in turbidity values as the water in the basin is stilled, allowing for particles to settle without any turbulence. The rapid settling period is approximately the duration extending from 45 to 60 min. During this time frame turbidity values decrease to 243, 217, and 268 NTU in Bay 1, Bay 2, and Bay 3, respectively. The sharp decrease in turbidity within Bay 1 indicates that the turbulent inflow is the predominant factor resulting in elevated turbidity levels during the first 30 min of the test duration when water is being introduced. Beyond the 1 hr period, turbidity values continue to decay at a very slow rate. This period is referred to as the polishing period. At the 12 hr time frame, turbidity values are essentially identical within the three measured bays with an average value of 113 NTU.

Interestingly, there is little difference in turbidity between the three bays after the filling period. Bay 2 also had the lowest turbidity values after the rapid settling period. This may indicate that the baffles may only be critical in reducing turbidity during the time where stormwater is entering or moving through the basin.

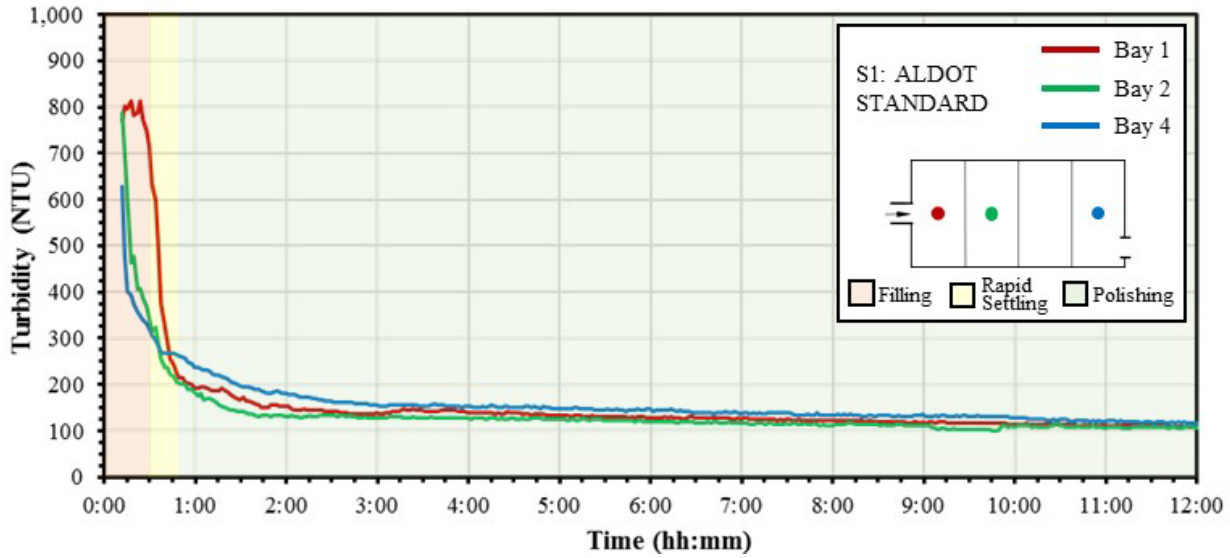

Figure 4.1: Turbidity time series for S1 ALDOT standard configuration.

4.1.2. Excavated Sump

The second treatment tested was the addition of an excavated sump in the forebay of the inflow channel (S2). Turbidity as function of time is plotted in Figure 4.2. The turbidity variations are similar to that of the ALDOT standard configuration (S1), with the same filling, rapid settling, and polishing periods discernable. The initial turbidity in Bay 1 was slightly lower than in S1, averaging 698 NTU during the 30-min. filling period. After 12 hrs of settling, the average turbidity in the basin was 137 NTU across the three bays, slightly higher than values seen in S1

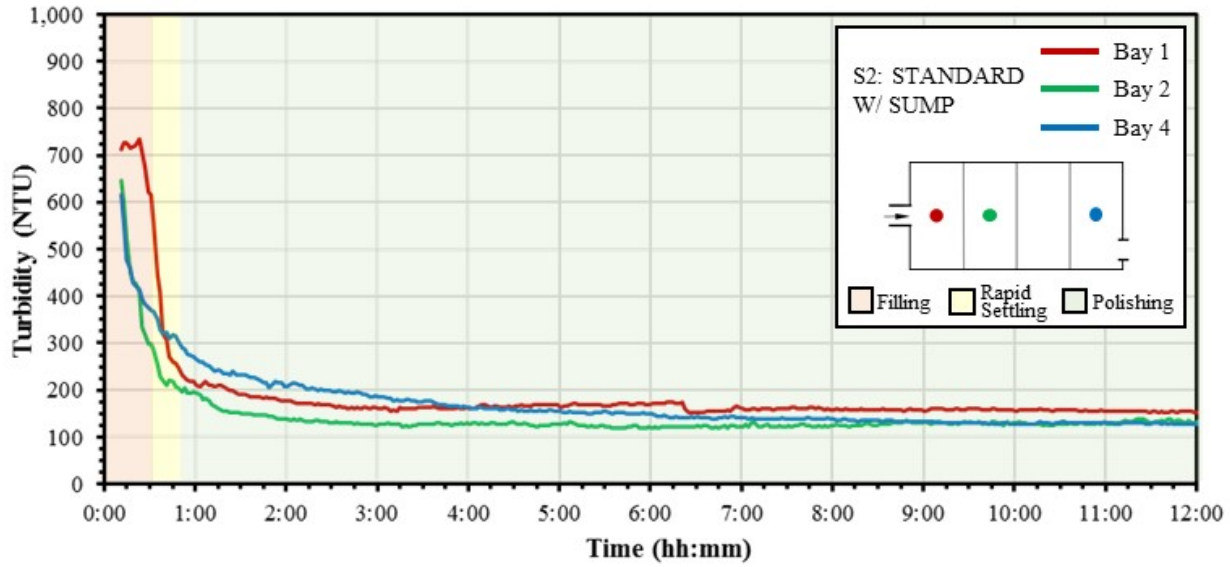

Figure 4.2: Turbidity time series for S2 ALDOT standard with excavated sump.

Figure 4.3(a) and (b) show the comparison of sediment deposition along the forebay section of the channel. As can be seen in the photographs, a significant amount of sediment was captured for both treatments. Sediment containment for the excavated sump treatment (S2) extended beyond the sump as a significant amount of deposition occurred at the hydraulic jump, or transition between supercritical and subcritical flow in the channel.

A comparison of the differences within the first 90 min. of testing between S1 and S2 treatments is shown in Figure 4.3(c). From the plot, it is evident that the S2 treatment had slightly lower turbidity in Bay 1 during the filling period, however turbidity in Bay 4 during the same period was slightly higher than it was during the treatment without the excavated sump, S1. After the filling period, the turbidity for both treatments acts similarly.

(a) inflow channel without excavated sump (S1) (b) inflow channel with excavated sump (S2)

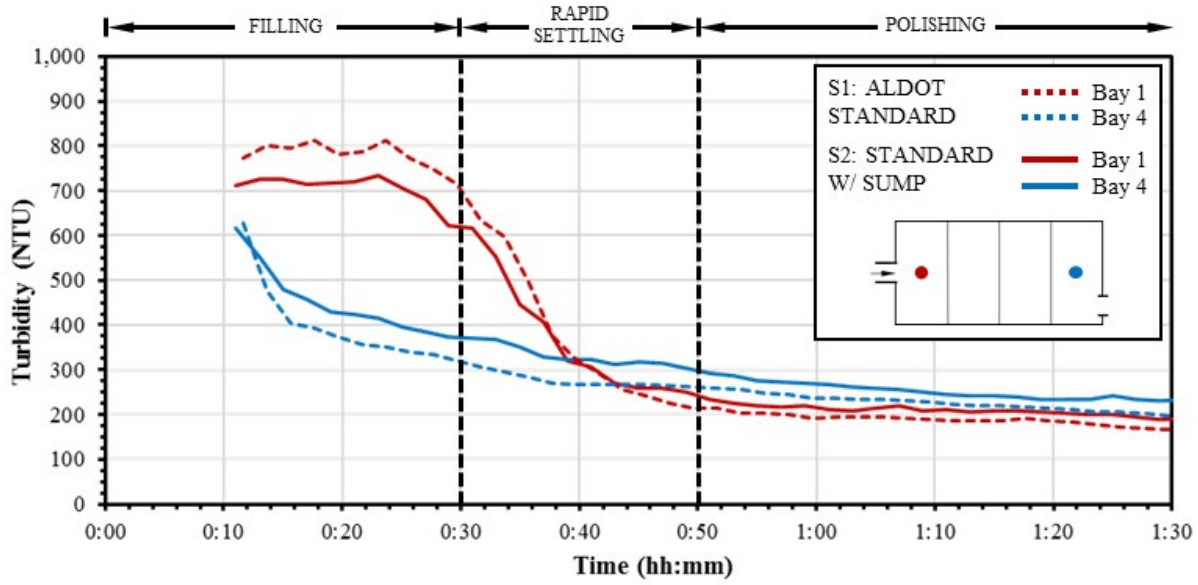

(c) turbidity comparison

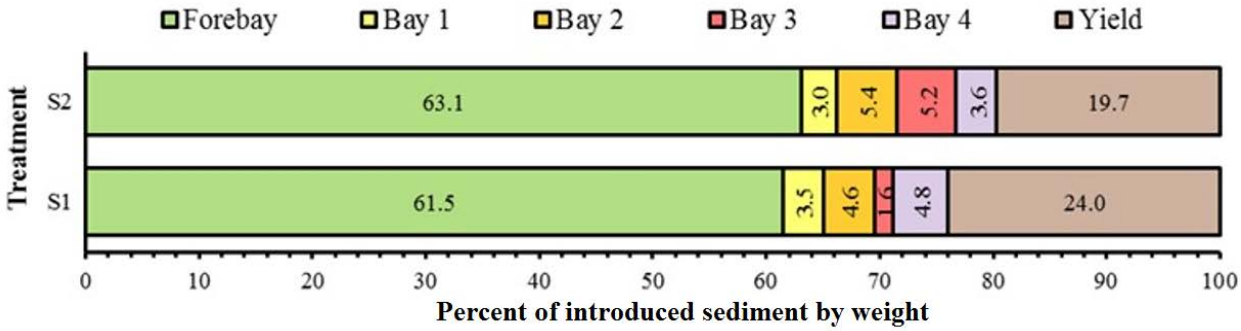

(d) sediment retention across entire system as percent of introduced sediment by weight.

Figure 4.3: Comparison of S2 and S1 treatments.

A comparison of the sediment captured in the basin is provided in Figure 4.3(d). It is noticed that the S2 excavated sump treatment captured approximately 1.6% more sediment than the S1 standard configuration. Furthermore, an additional 3.3% of sediment was captured within Bays 1 through 4. These small difference in capture effectiveness, would be difficult to correlate to the addition of the sump without additional replicate tests for statistical comparison.

The inclusion of the excavated sump was observed to have no significant difference in the performance of the sediment basin from a water quality and sediment retention standpoint. Therefore, the excavated sump was left in place for subsequent tests. It was observed that sediment captured within the forebay became resuspended during subsequent tests.

4.1.3. Modified First Baffle

The third series of testing was the treatment with the modified first baffle. The treatment was subjected to three back-to-back 30-minute events. Results from the modified baffle treatment (S3) were compared to the standard baffle treatment (S2). Both treatments were performed with the excavated sump in the forebay. Turbidity results from the modified first baffle treatment are shown in Figures 4.4 and 4.5.

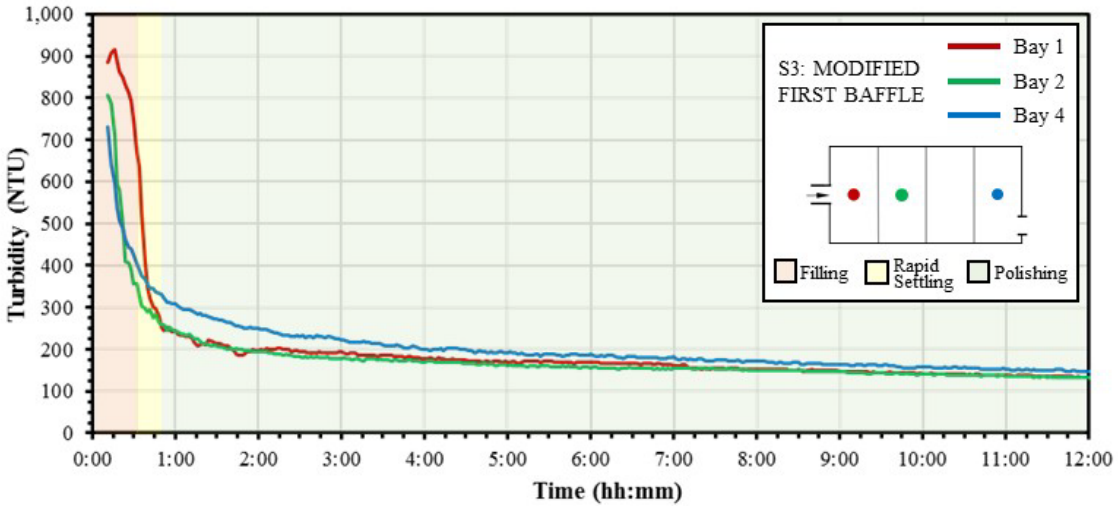

(a) turbidity (0 to 12 hrs.)

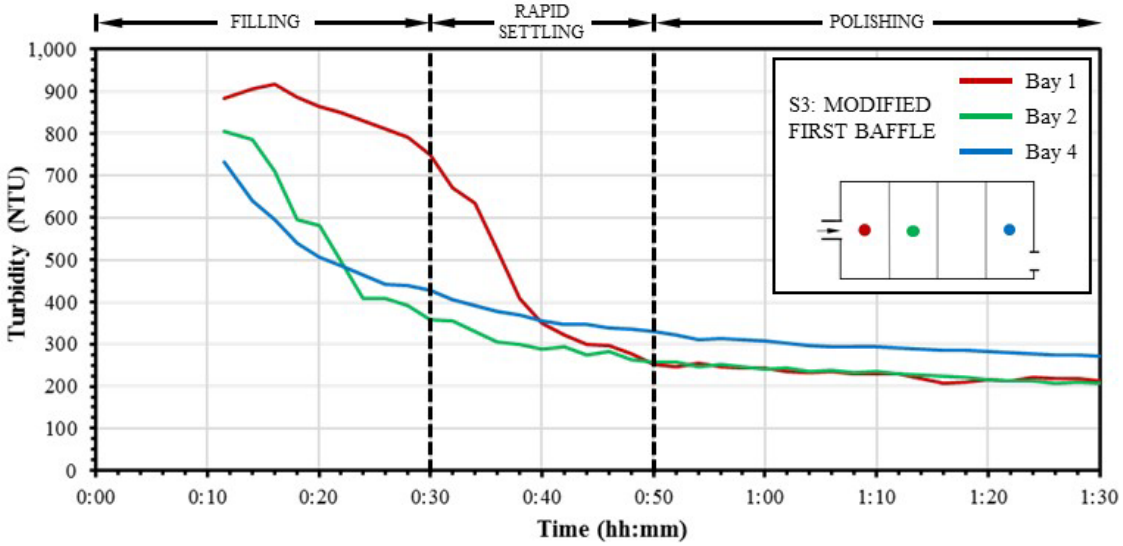

(b) turbidity (0 to 1.5 hrs.)

Figure 4.4: Turbidity time series for S3 modified first baffle treatment.

Visual observations during testing indicated that use of the modified first baffle resulted in less turbulence in Bay 2 and Bay 3 when compared to treatments using the standard first baffle. Turbidity results obtained from the probes were compared between Bay 1 and Bay 2, and is presented in Figure 4.5(a), is at odds with these visual observations. These results indicate that turbidity during the modified baffle treatment (S3) was slightly higher (approximately 100 NTU) in both Bay 1 and Bay 2 during the filling and rapid settling period than the treatment with the standard baffle (S2). The results also show that during the polishing period, the turbidity was relatively unchanged between Bay 1 and Bay 2, which was a different behavior than what was observed with the standard baffle treatment (S2).

To further compare turbidity results, Bay 2 turbidity was divided by Bay 1 turbidity for each sample, to determine the efficiency in turbidity reduction between the two bays. Figure 4.5(b) shows a plot of this efficiency comparison. Points below 1.0 (shaded in green) indicate that there was a reduction in turbidity between the two bays, while points above 1.0 (shaded in orange) indicate there was an increase in turbidity between the bays. Results from this comparison show that the treatment with standard first baffle (S2) outperformed the modified first baffle treatment (S3).

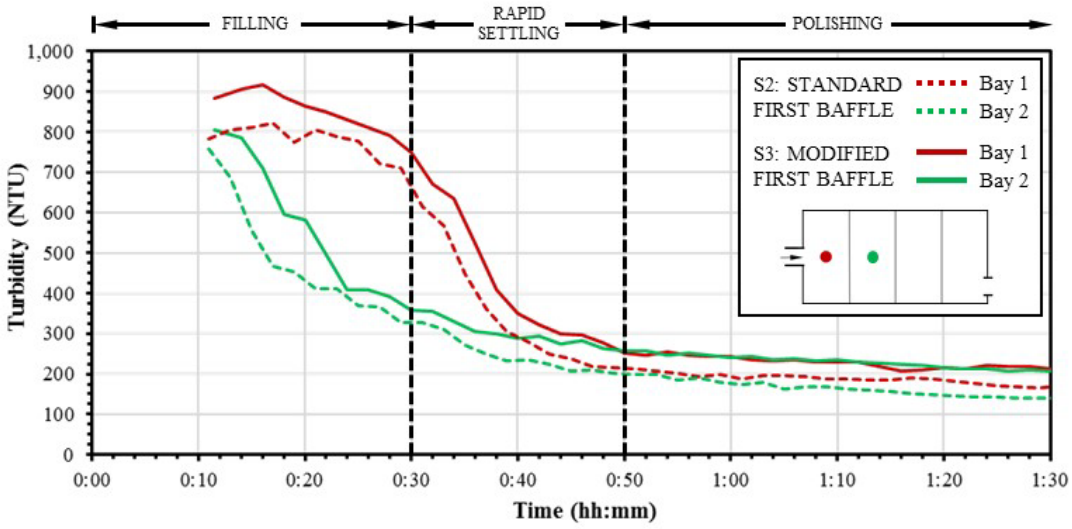

(a) turbidity comparison

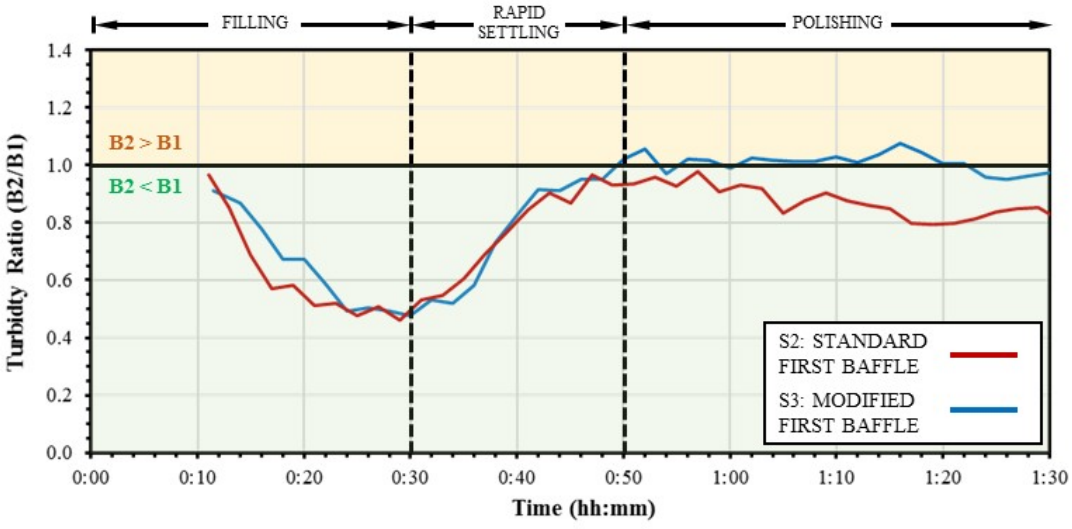

(b) treatment efficiency

Figure 4.5: Comparison between turbidity time series for S3 and S2 treatments.

Sediment retained in each bay was compared to the standard baffle (S2) treatment, Figure 4.6(a). Figure 4.6(b) shows the sediment retention effectiveness within the four bays of the basin. Comparing the two treatments, there was 4.5% more sediment captured in Bay 1 during the modified first baffle treatment (S3) than sediment captured in Bay 1 during the standard first baffle treatment when comparing with the total sediment captured within the four bays of the basin.

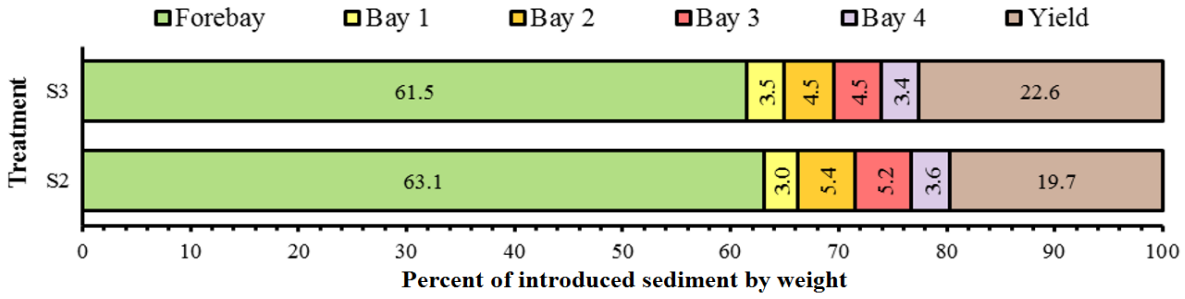

(a) sediment retention across entire system as percent of introduced sediment by weight

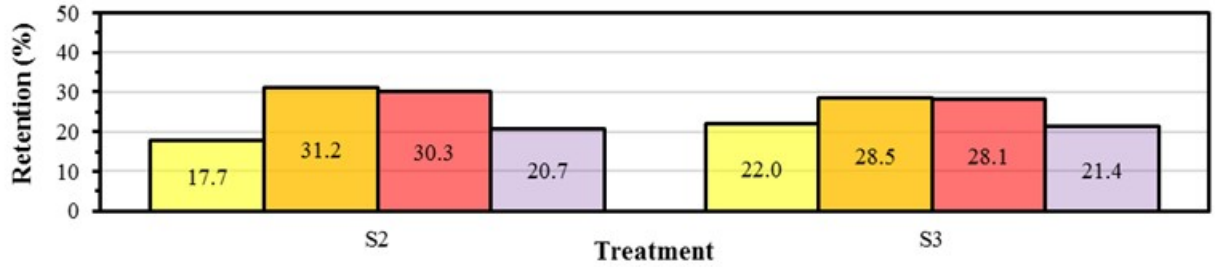

(b) percent retention within bays 1 through 4

Figure 4.6: Sediment Retention Comparison of S3 and S2 Treatments.

While sediment retention was slightly improved using modified first baffle treatment (S3), the turbidity results from this comparison indicated that the modified first baffle was not advantageous.

4.1.4. Overflow Tests – S4 and S5 treatments

Tests leading to the overflow of the sediment basin, or Overflow Tests, were conducted on both the standard first baffle (S5) and modified first baffle (S4) installation configurations. The purpose of these tests was to evaluate how the baffles influenced the performance of the basin during conditions that force water to flow through the auxiliary spillway. Turbidity data for the two treatments are shown in Figure 4.7. The data follow the same pattern that was observed in the single test series (S2 and S3), where the turbidity between Bay 1 and Bay 2 is relatively unchanged for the modified first baffle treatment (S4). In contrast, there is a discernable difference between turbidity in Bay 1 and Bay 4 with the standard first baffle treatment (S5). During the second fill cycle (i.e., 5:00 to 5:30), the turbidity in Bay 1 increases dramatically. However, turbidity in Bay 2 and Bay 4 only experiences a gradual increase in turbidity rather than the spike that is observed in Bay 1. This indicates that Bay 1 has the most influence in absorbing the turbidity impact from a subsequent runoff event when the basin is partial filled with water or not empty. This further illustrates how the first baffle system is the most important in retaining turbidity in Bay 1.

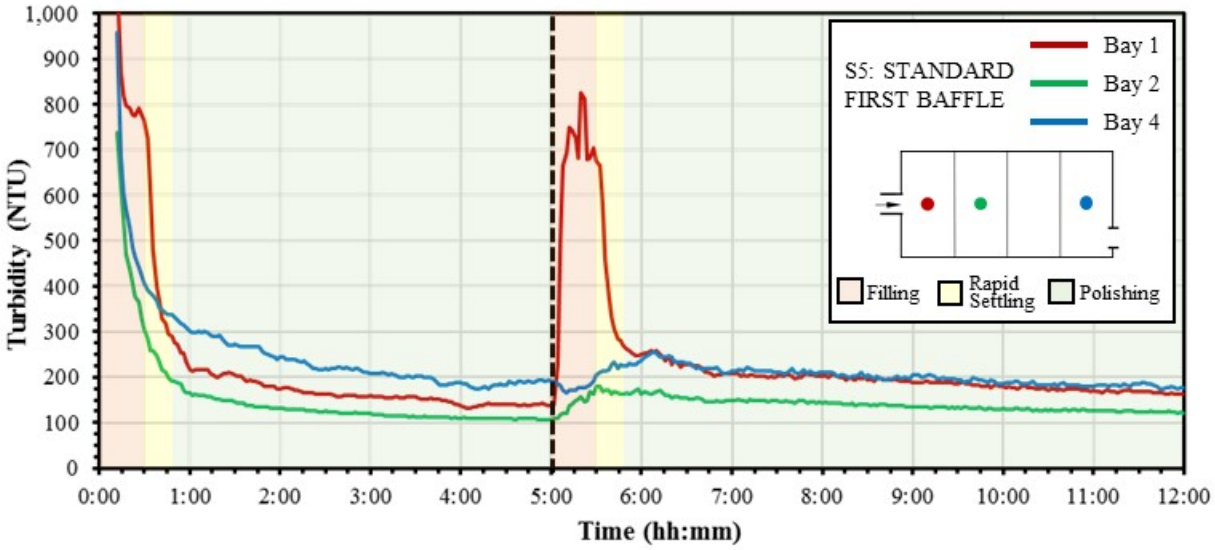

(a) standard first baffle, S5, turbidity

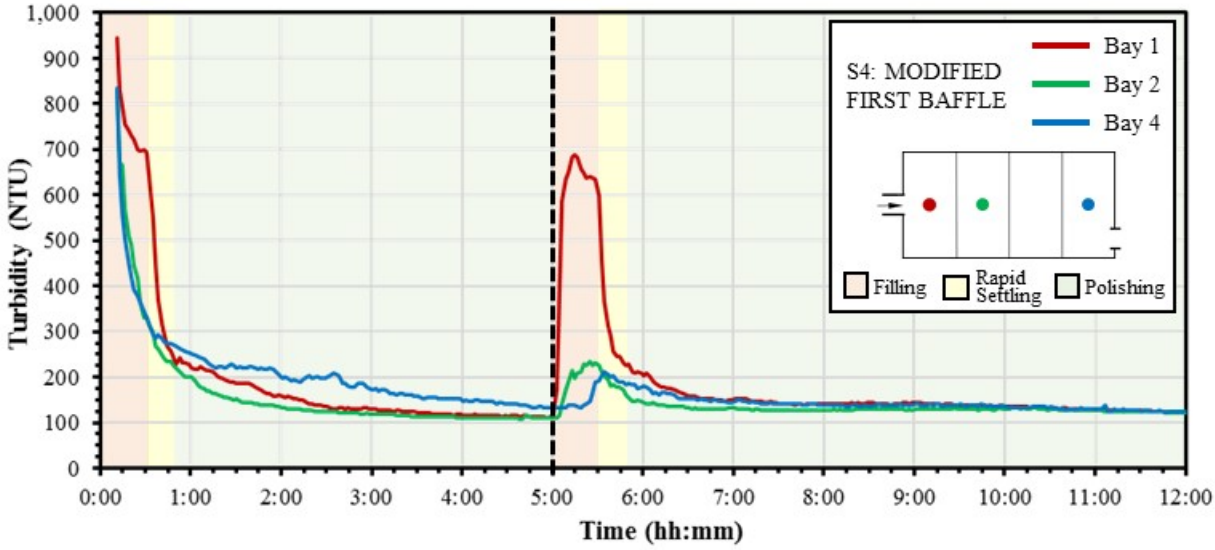

(b) modified first baffle, S4, turbidity

Figure 4.7: Comparison between turbidity time series for S5 and S4 Treatments.

The ratio between Bay 2 and Bay 1 turbidity was compared for the two treatments, each normalized by dividing by Bay 1 turbidity, Figure 4.8. Results from the comparison show that the standard first baffle treatment (S5) outperformed the modified first baffle treatment (S4), further validating results from the single fill experiments, S2 and S3. During the filling period (i.e. 00:00 to 00:30 and 5:00 to 5:30) and the polishing periods (i.e., 00:50 to 5:00 and 5:50 to 12:00), the average performance difference between the treatments show that the standard first baffle is 26.5% and 19.5% more effective at reducing turbidity between Bay 1 and Bay 2, respectively. These results corroborate past research studies (Thaxton et al. 2004; Thaxton and McLaughlin 2004) that have identified diminishing returns with smaller percent opening size.

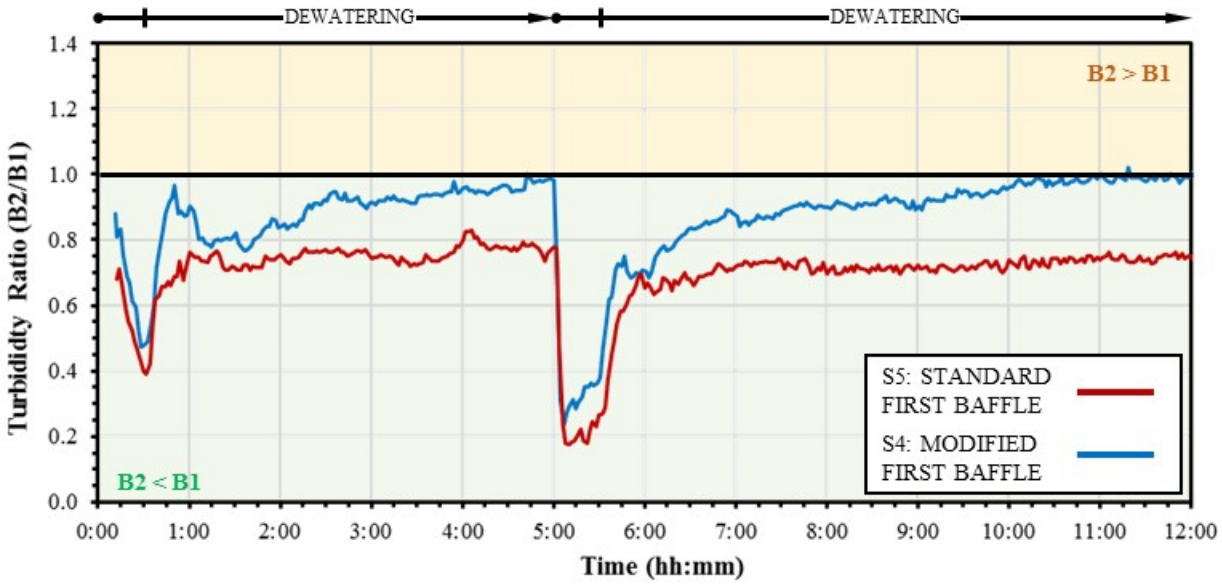

Figure 4.8: Comparison between turbidity time series for S5 and S4 Treatments.

4.2. Lamella Technology Testing Results

4.2.1. Lamella Settlers positioned at Bay 3

Due to the results from the control configuration testing (Phase 1), it was determined that the ALDOT standard sediment basin configuration with the excavated sump in the forebay was the MFE-I. This configuration was used for testing the lamella settlers in the two configuration (i.e. upward flow and parallel flow). The lamella settler was installed in such way that inflows would be admitted at the bottom of the basin and escape toward the laterals, which corresponded to treatment S6. It was not possible to direct the flows to the top of the lamella settler units because the depth of the sediment basin was too shallow. Wing walls built in wood were fitted in the sides of the settler to prevent short circuiting of flows. Later, the lamella settlers were re-arranged in the sediment basin to allow for flows to pass through the lamella plates in a longitudinal fashion. This treatment condition was referred to as S7, and also required slight adjustments to the wing walls next to the basin to prevent significant short circuiting.

Furthermore, it was determined that the data obtained from the overflow configuration tests provided more comparative data than did the tests performed with the single fill condition. Therefore, only overflow type tests were performed for Phase II tests. A series of overtopping tests were run on the lamella system installed in the upward and parallel flow configurations. Figure 4.9 shows the turbidity plots for the two installation treatments.

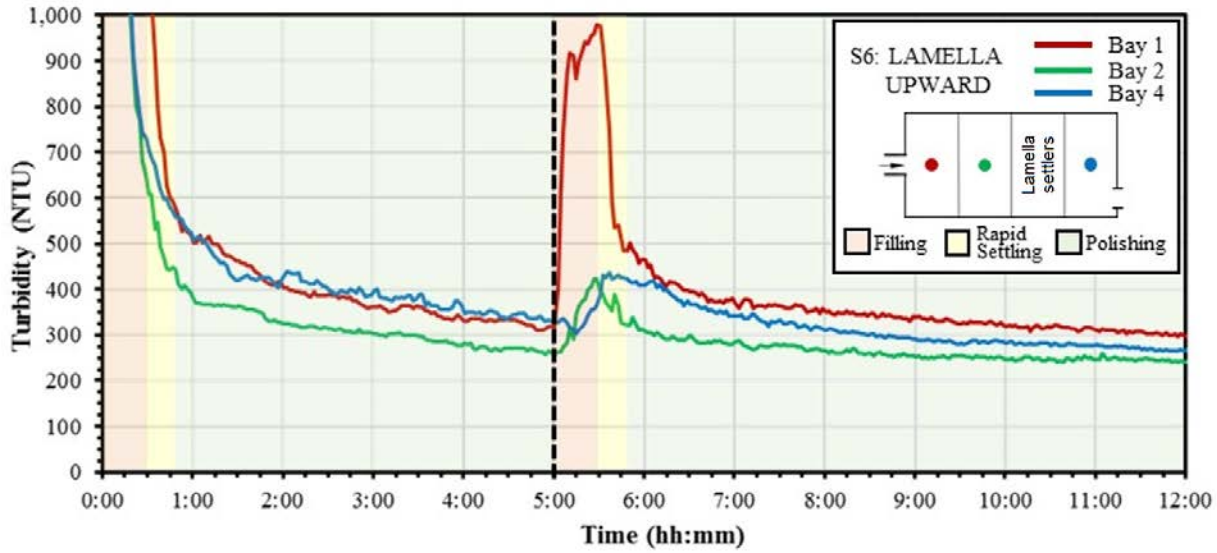

(b) lamella settlers in upward flow configuration

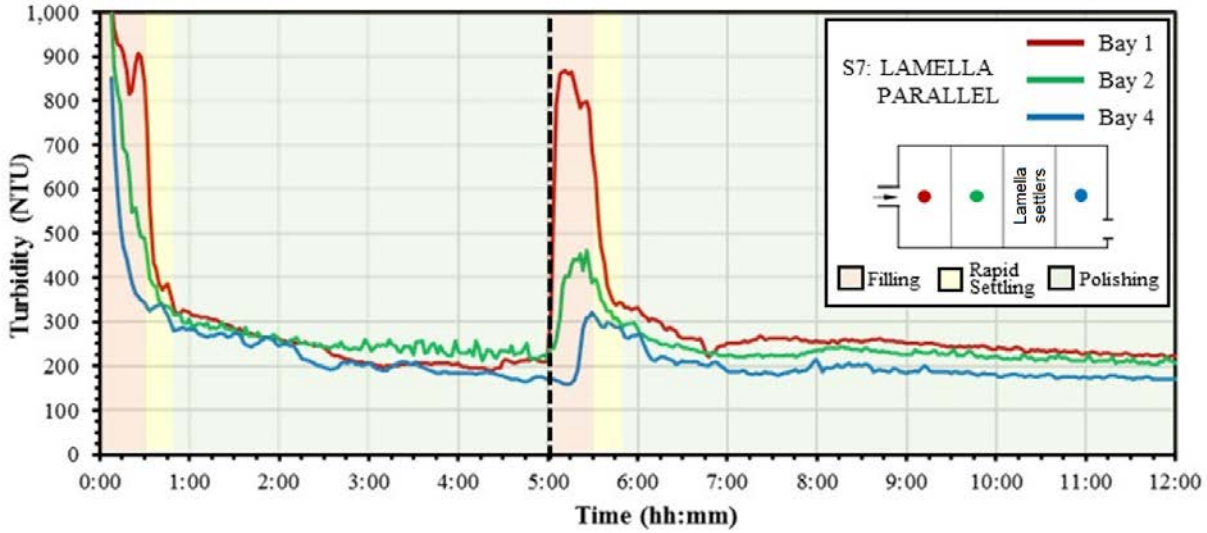

(c) lamella settlers in parallel flow configuration

Figure 4.9: Comparison between turbidity time series for S6 and S7 Treatments.

The lamella system had clear positive on the water quality behavior of the sediment basin in either configuration. Interestingly, the turbidity for both configurations was significantly higher than turbidity observed in Phase I testing. This difference was attributed to temperature influences that are described further in the next section, but also higher turbidity in the inflows that were received in bay 1, as is shown in subsection 4.3.4. To evaluate the efficiency of the system in reducing turbidity across the basin, a ratio of Bay 4 turbidity to Bay 1 turbidity is plotted in Figure 4.10 for the MFE-I (S5) and the two lamella treatments (S6 and S7).

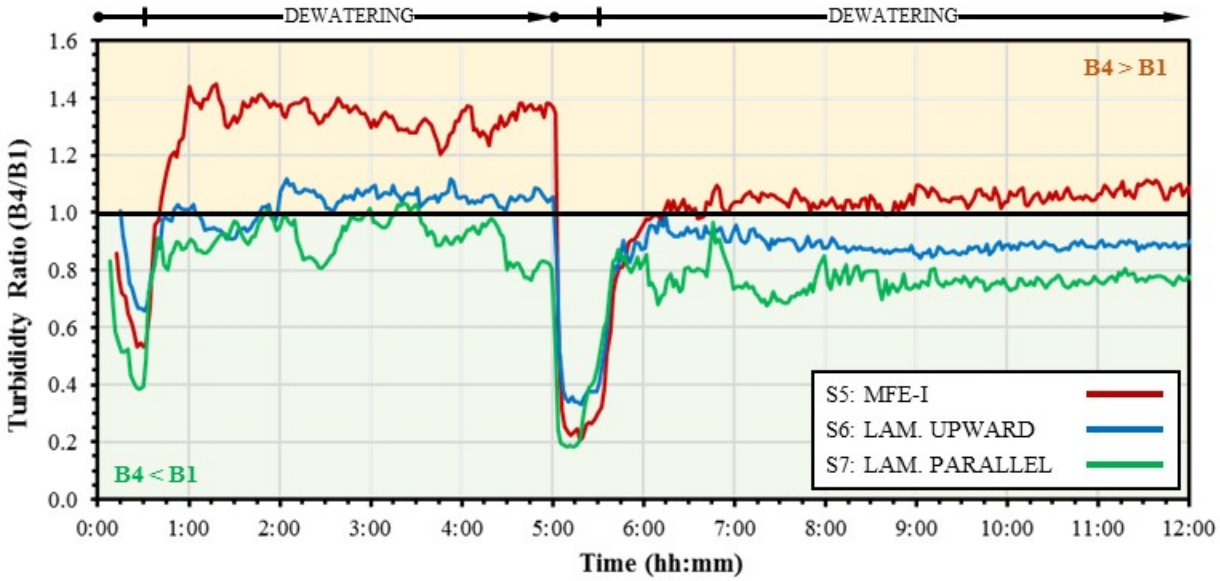

Figure 4.10: Comparison between turbidity time series for S5, S6, and S7 Treatments.

When comparing turbidity ratios between Bay 1 and Bay 4, it is evident that the lamella parallel flow configuration outperformed the lamella upward flow configuration and the MFE-I treatment. The lamella upward treatment performed better than the MFE-I only during dewatering periods (i.e. 00:30 to 5:00 and 5:30 to 12:00). Turbidity in Bay 4 was actually higher throughout the dewatering periods for the MFE-I configuration and reduction between Bay 4 and Bay 1 was only observed during the dewatering period of treatments using lamella settlers. During the filling periods (i.e. 00:00 to 00:30 and 5:00 to 5:30), the lamella system in upward flow configuration (S6) compared to the MFE-I (S5) had a decrease in performance of 36.6%. During the polishing periods (i.e. 00:50 to 05:00 and 05:50 to 12:00), the lamella system in upward flow configuration (S6) outperformed the MFE-I (S5) by 18.2%. The average increase in performance for the lamella system in parallel flow configuration (S7) compared to the MFE-I (S5) was 6.5% during the filling periods (i.e. 00:00 to 00:30 and 5:00 to 5:30) and 29.0% during the polishing periods (i.e. 00:50 to 05:00 and 05:50 to 12:00).

However a noticeable difference, these results are not as dramatic as the differences in the turbidity obtained during the controlled tests performed in the laboratory. One possible cause could be the scale of the experimental apparatus, which was much smaller than the sediment basin used in this investigation. A second possible cause was the conditions of sediment inflows and the usage of bays in the sediment basin, which were absent in the lab phase. Finally, all laboratory experiments led to overflow conditions which could have enhanced sediment resuspension in the scenario without lamella plates.

While there is a clear drop in the turbidity values from Bay 1 to Bay 4 using the lamella settler in parallel flow condition (S7), the drop is not as dramatic as it was observed in the laboratory studies by our research team. It was decided then to evaluate the efficiency of the lamella settler units in two different configurations involving the treatment only of the water leaving the basin through the skimmers. The next subsection presents these field test results.

4.2.2. Lamella Settlers treating skimmer discharge

An additional task added to the scope of this research was to test the performance of the small-scale lamella settler (SSLS, Figure 4.11) to treat skimmer flow discharge. The overarching goal of the approach is to assess the benefits of using of a high-rate settler to treat the effluent of a sediment basin

discharged by the skimmer after it passed through the sediment basin in condition S7 when the high rate lamella settlers (HRS, Figure 3.13). The finalized high-rate settler box is presented in Figure 4.11, whereas the typical turbidity results obtained with this approach are presented in Figure 4.12.

Results indicated that the use of a SSLS has eliminated completely “spikes” in turbidity in the discharge. Such spikes were noticeable in during the 2nd stage of the inflow admission, which generated overflows. By having the SSLS treating the skimmer outflow, there was no sign of any turbidity increase, indicating that “first flush” conditions have been eliminated and that the turbidity levels are more predictable as they exiting the system. In absolute terms, however, there were no significant changes in the turbidity observed in Bay 4 (downstream from the lamella settlers within the sediment basin) and the turbidity discharged from the smaller settler unit. This may indicate a limit has been achieved for the particles that can be removed by physical processes within the sediment basin.

Figure 4.11: Completed small-scale lamella settler (SSLS) tank and unit in operation

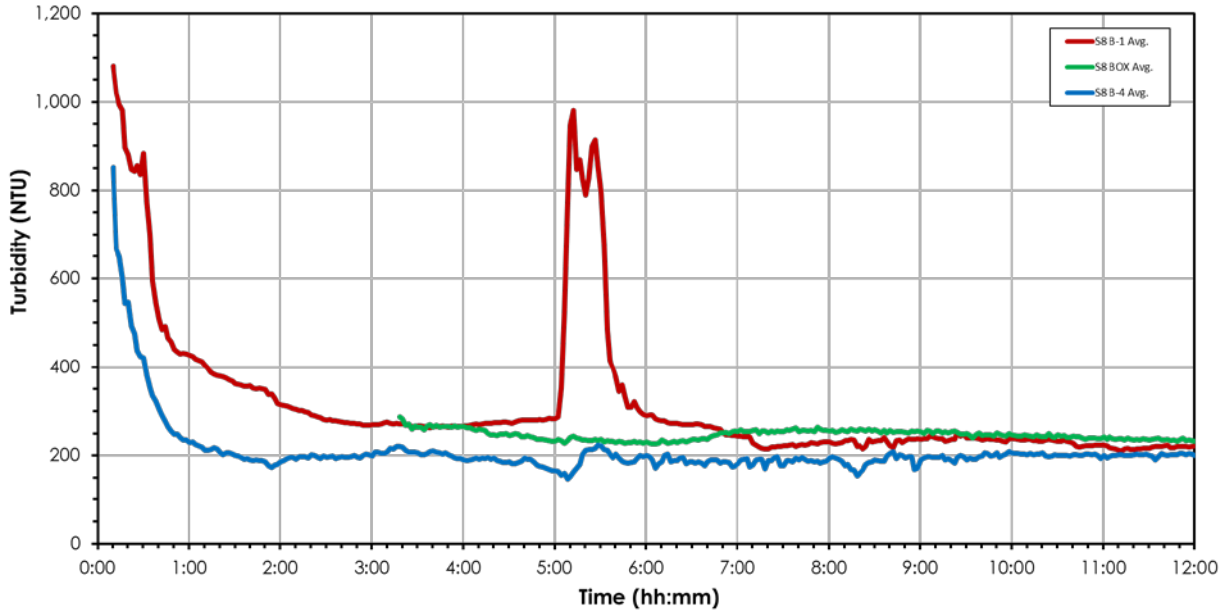

Figure 4.12: Performance of the sediment basin based on turbidity logger results measured at the entrance of the sediment basin (red), after the in-basin high-rate settler (blue), and after the small-scale lamella settler that treated skimmer effluent (green).

This physical limit can be explained by the size of the sediment particles in suspension, which are generally too small to be removed even by means of the SSLS with upward flow configuration. However, the effectiveness of this last treatment step can be improved by means of flocculants, such as polyacrylamide (PAM). One key difference of the proposed approach is to apply PAM only to the basin outflow. This provides an opportunity for physical sediment settling to occur first, and then use PAM only to promote settling to very fine sediments. The rationale is to decrease the PAM dosage in sediment basins, decreasing the potential of environmental discharge of these flocculants. The retaining of these flocculants that would prevent the discharge would be promoted within the actual SSLS unit.

To test the effectiveness of PAM combined with the SSLS, a mixing unit presented in Figure 4.13 was constructed. The mixing unit has dimensions of 4 ft by 8 ft, and has shallow (4-in height) walls. It is designed to allow for residence time of water in the range of 50 to 80 seconds, depending on the flow rate and slopes, and discharge water with flocculants in the SSLS unit. Small PAM blocks were cut into pieces and these were installed in the contraction flow zones of the mixing unit, where velocity and turbulence is higher. This allows for improved mixing of PAM and the sediment-laden flows.

Figure 4.13: Mixing tank unit constructed for the addition and mixing of flocculant in inflows reaching the small-scale lamella settler (SSLS) unit.

Figure 4.14 presents the PAM mixing unit installation. The size of the mixing unit matches the plan area of the lamella settler, so the unit was installed on the top of the SSLS unit itself. The pipe outlet that received the skimmer discharged was extended to the opposite side of the mixing unit. The mixing unit was sloped so that the discharge would reach the entry

As is also shown in Figure 4.14, the pieces of PAM were cut and placed on the corners of the mixing unit, where flow velocity was at the largest value. During tests, it was noticed the formation of flocs within the mixing unit, and even some floc settling there even before flows reached the SSLS unit. Samples were taken for turbidity measurements using a HACH 2100Q turbidimeter at various locations within the mixing tank and the small lamella settler unit. Turbidity results measured at the inlet of the system – the skimmer outlet pipe – and the outlet of the HRS tank are presented in Figure 4.15. The results correspond to three experimental repetitions in sequence (Runs 1 to 3) in which the lamella settlers were present in the sediment basin. The conditions mimic runs performed earlier in this research, with the only difference that the outflow from the skimmer passes through the mixing tank and the SSLS unit.

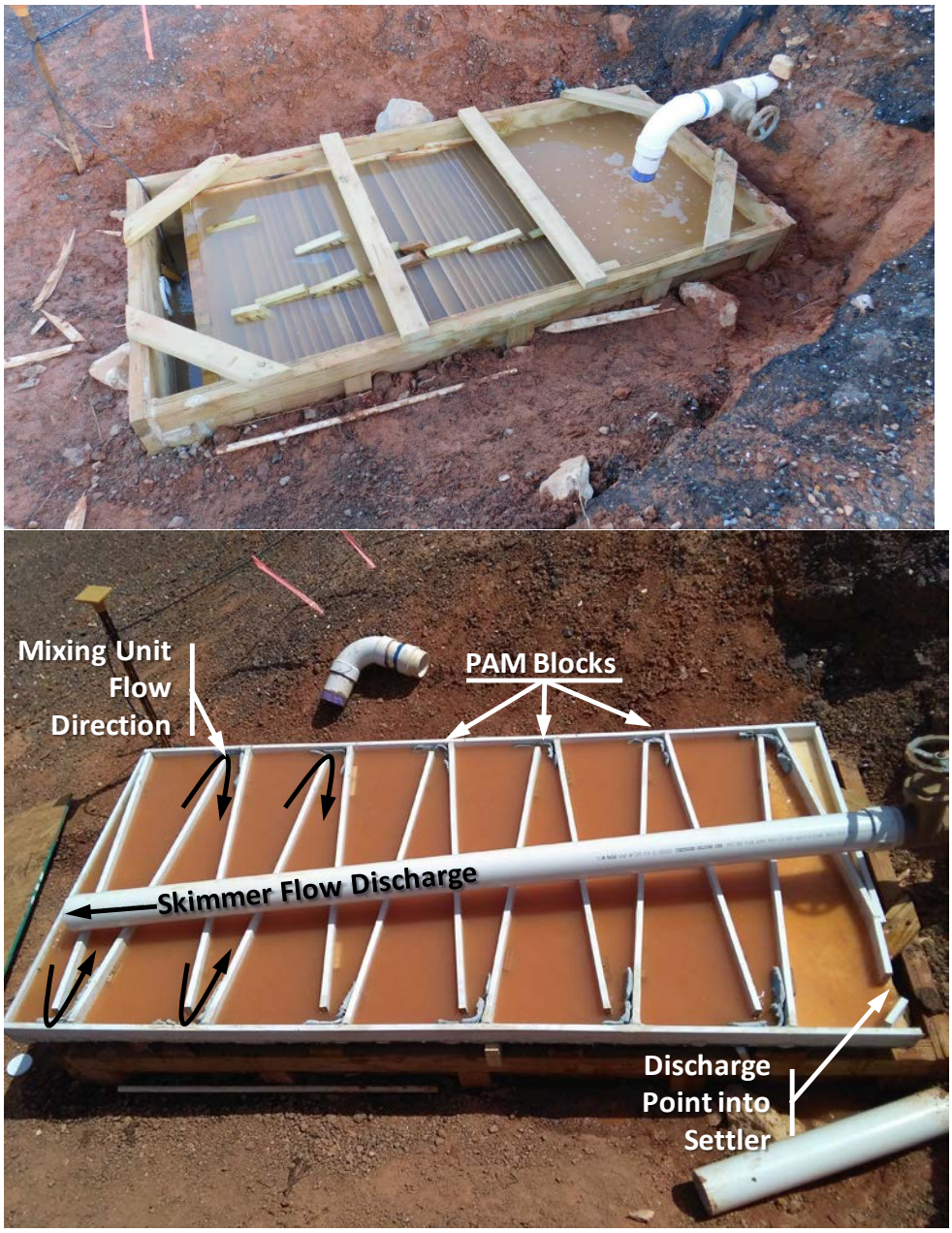

Figure 4.14: SSLS tank originally and after the PAM mixing unit was installed on the top.

As it may be noticed from the turbidity results Figure 4.15, turbidity results presented a significant drop between the inlet and outlet of the mixing unit and small lamella settler unit. The range of turbidity drop between these two points was between 46%, observed in the initial tests, and 88% which was observed in the third run, with a very significant average turbidity reduction of 75%.

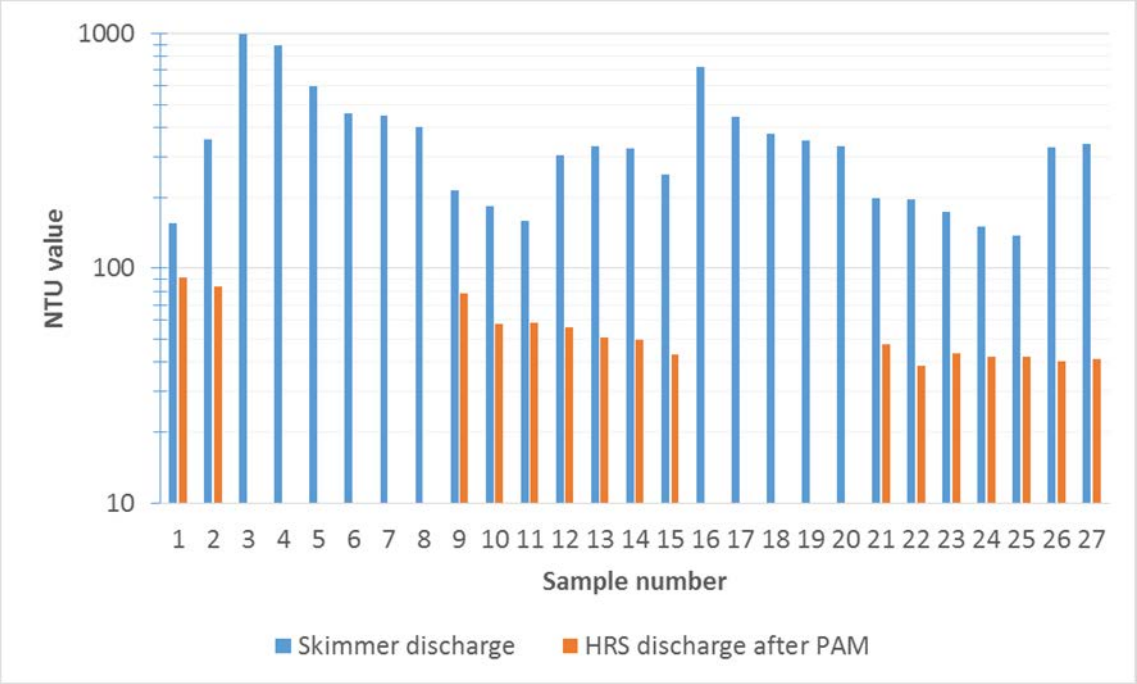

Figure 4.15: Turbidity results from samples collected at the inlet of the mixing tank (blue bars) and the outlet of the HRS with the use of PAM (orange bars). Orange bar results were only obtained when the water within small lamella settler reached its discharge level.

While the mechanisms for PAM addition, as well the corresponding dosage, still need to be fine-tuned, these results indicate great potential of this combination. This can potentially avoid the use of active treatment processes, such as water recirculation via pumps within sediment basins, reducing costs and increasing the effectiveness of sediment control. Also of significance, the use of this alternative may result in decreased use of PAM, as these would be added to skimmer flows carrying the smallest particles that were not removed in the sediment basin, instead of adding flocculant to sediment basin inflows that carry large fractions of sediment particles that do not need PAM for improving settling. One limitation of the use of SSLS with PAM is that it will not prevent the discharge of turbid water in case there is basin overflow. Such situation would be possible in sediment basins that have small storage volumes due to limiting factors such as limited available surface areas. In such conditions, a possible alternative would be the combination of high rate lamella settlers within the sediment basin with the use of PAM. Such conditions, however, were not tested in our research project.

4.3. Discussion of field measurements

The following section provides discussion on temperature variability and TSS analysis performed during the sediment basin experiments.

4.3.1. Temperature influence

Water quality results showed significant discrepancies between turbidity levels throughout the duration of the experiments. This is exemplified by Figure 4.16 where the turbidity in Bay 1 and Bay 4 is plotted for the MFE-I (S5) treatment and the lamella in upward flow configuration (S6).

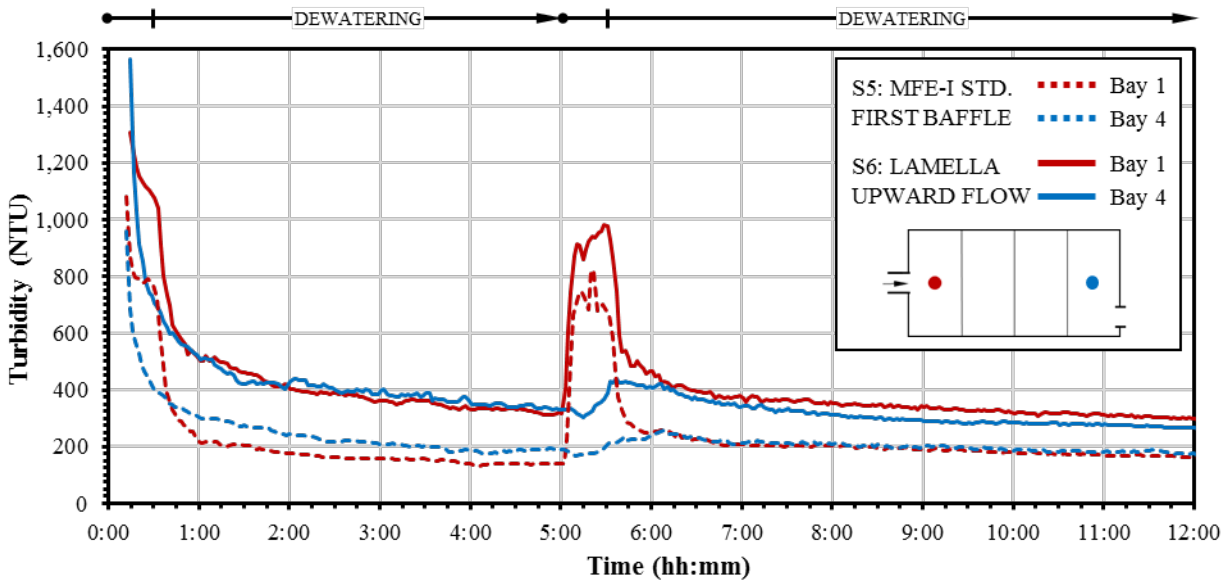

Figure 4.16: Turbidity Discrepancy Between Treatments

The testing methodology developed for these experiments ensured variables remained consistent from test to test. The only variables that were not controllable were those attributed to weather. Testing was not conducted during rainfall events, and wind likely had no noticeable effect on mixing within the basin. Temperature however did fluctuate throughout the year and was the likely culprit in these observed turbidity differences. Figure 4.17 shows a plot of the average water temperature of the tests performed and the plot of the average daily temperature for the weather station located at the Auburn University Regional Airport (KAUO) (Weather Underground 2016).Table 4.1 shows a summary of all tests performed in the sediment basin and the corresponding average water temperature for the tests. Temperatures were obtained from the level loggers used to monitor water depth over the course of tests. Water temperatures ranged between 54.0 to 88.3 ºF (12.2 to 31.2 ºC).

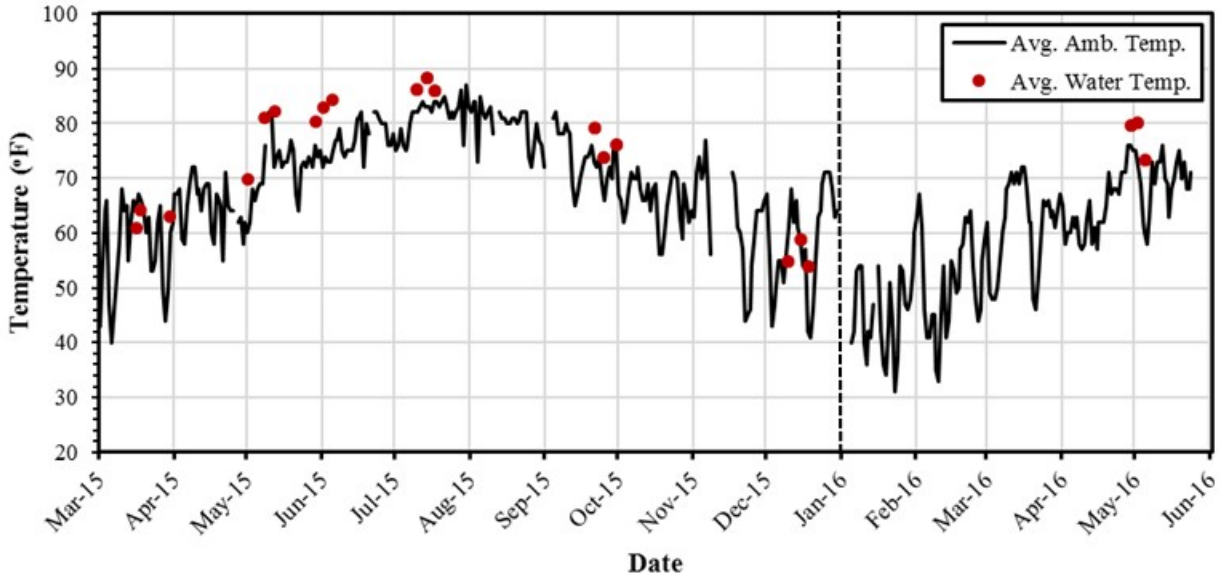

Figure 4.17: Temperatures for Tests Performed in Sediment Basin.

Table 4.1: Average water temperature for tests performed in sediment basin.

Treatment	Segment	Date	Avg. Water Temp., ºF (ºC)
S1: ALDOT Standard w/o Excavated Sump	L-1	3/16/2015	61.0 (16.1)
	L-2	3/18/2015	64.3 (17.9)
	L-3	3/30/2015	62.9 (17.2)
S2: ALDOT Standard + Excavated Sump	L-1	5/1/2015	69.7 (20.9)
	L-2	5/8/2015	80.9 (27.2)
	L-3	5/12/2015	82.1 (27.8)
S3: ALDOT Standard + Excavated Sump + Modified First Baffle	L-1	5/29/2015	80.4 (26.9)
	L-2	6/1/2015	83.0 (28.3)
	L-3	6/5/2015	84.4 (29.1)
S4: ALDOT Standard + Excavated Sump + Modified First Baffle [overflow]	L-1	7/10/2015	86.2 (30.1)
	L-2	7/14/2015	88.3 (31.2)
	L-3	7/17/2015	86.0 (30.0)
S5: ALDOT Standard + Excavated Sump [overflow]	L-1	9/21/2015	79.2 (26.2)
	L-2	9/25/2015	73.8 (23.2)
	L-3	9/30/2015	76.1 (24.5)
S6: Lamella Upward Flow [overflow]	L-1	12/10/2015	54.9 (12.7)
	L-2	12/15/2015	58.7 (14.8)
	L-3	12/18/2015	54.0 (12.2)
S7: Lamella Parallel Flow [overflow]	L-1	4/29/2016	79.7 (26.5)
	L-2	5/2/2016	80.0 (26.7)
	L-3	5/5/2016	73.4 (23.0)

Through Stokes law, settling velocity is dependent on acceleration due to gravity, specific gravity of a suspended particle, diameter of spherical particle, and the kinematic viscosity of the fluid. The only variable that changes between tests is the kinematic viscosity which is a direct function of water temperature. Viscosity and settling velocity are inversely proportional, as the viscosity increases, the settling velocity decreases. The kinematic viscosity of water is directly proportional to water temperature, as temperature increases, water viscosity decreases. Therefore, the settling velocity of a spherical particle under Stokes law increases as the temperature of water increases.

To determine the effect of temperature on the tests conducted, a plot was created to develop a ratio of settling velocities at varying temperatures. Kinematic viscosity was plotted against temperature for 47 known temperature points. This data set was fitted to a polynomial regression curve to develop a relationship for the points, Figure 4.18(a). The settling velocity for a theoretical particle of $3.9x10^{-4}$ in. (0.01 mm) was then calculated for 37 data points (i.e. 32 to 96.8 ºF [0 to 36 ºC]) using Stokes law and the developed regression equation for viscosity. The settling velocity for those points was divided by the settling velocity at 65 ºF (18.3ºC), which corresponds to the average annual water temperature in the state

of Alabama. This allowed the development of a settling velocity ratio, Figure 4.18(b). With the range of water temperatures experienced during testing, the settling velocity can vary as much as 200%.

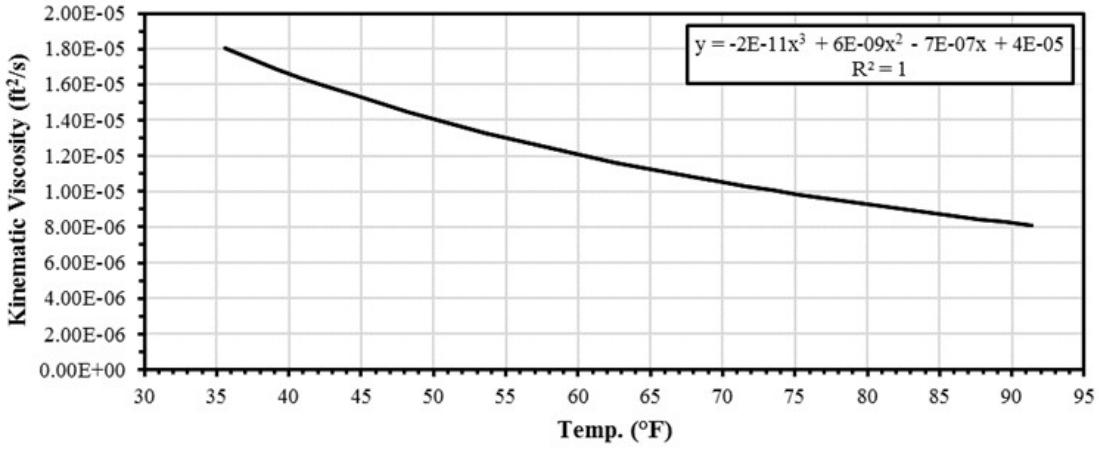

(a) temperature and kinematic viscosity relationship

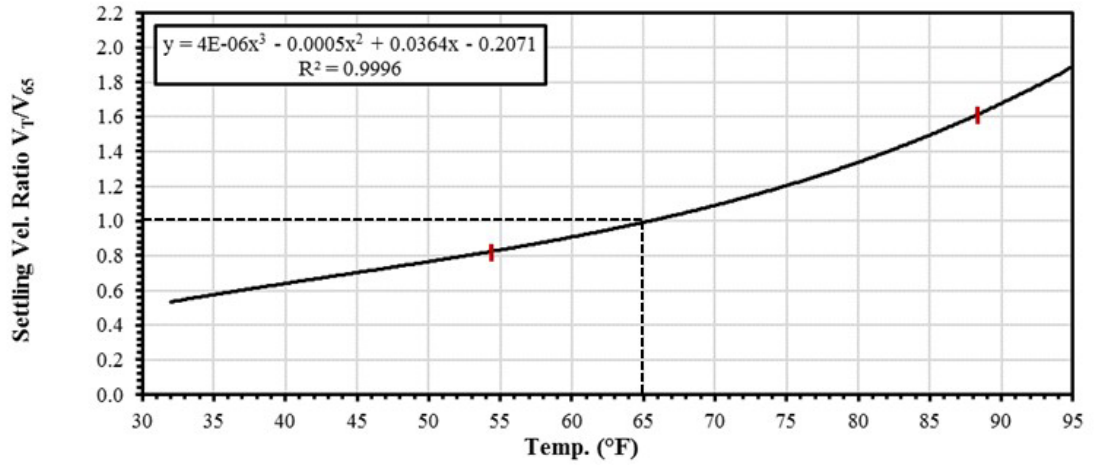

(b) developed settling velocity ratio

Figure 4.18: Temperature Effect on Settling Velocity.

While there are no existing studies correlating turbidity to viscosity or settling velocity, this settling velocity ratio relationship was developed to transform turbidity curves to a baseline temperature, 65 ºF (18.3ºC). By applying this correction, turbidity curves for tests performed at temperatures above the baseline are shifted down, while data for tests performed at temperatures lower than the baseline are shifted up. Applying this technique provided a normalization to the data that is shown in Figure 4.19.

An empirical approach was conducted in a Nor-lake, Inc.® Enviro-Line walk-in environmental chamber under controlled conditions to provide testing data to the developed temperature normalization approach, as shown in Figure 4.20. Experiments were conducted in a plastic tank filled with 15 gallons (56.7 L) of tap water. Approximately 7.1 oz. (200 g) of soil sieved to the No. 200 (0.074 mm) sieve was added to the tank and agitated with a power drill paint mixer. The three Campbell Scientific OBS3+ turbidity probes were installed at the surface of the tank and continuously monitored water quality over the duration of the experiment. Ambient temperatures in the chamber were increased at 10 ºF (5.5 ºC) intervals ranging from target temperatures of 45 to 95 ºF (7.2 to 35 ºC), Figure 4.21(a). Temperatures in the chamber and tank were monitored using a standard alcohol thermometer and two Hobo level loggers. Once

equilibrium conditions were reached in the tank, mixing was conducted to resuspend sediment in the water. The tank was then allowed to sit undisturbed to allow for settling to occur.

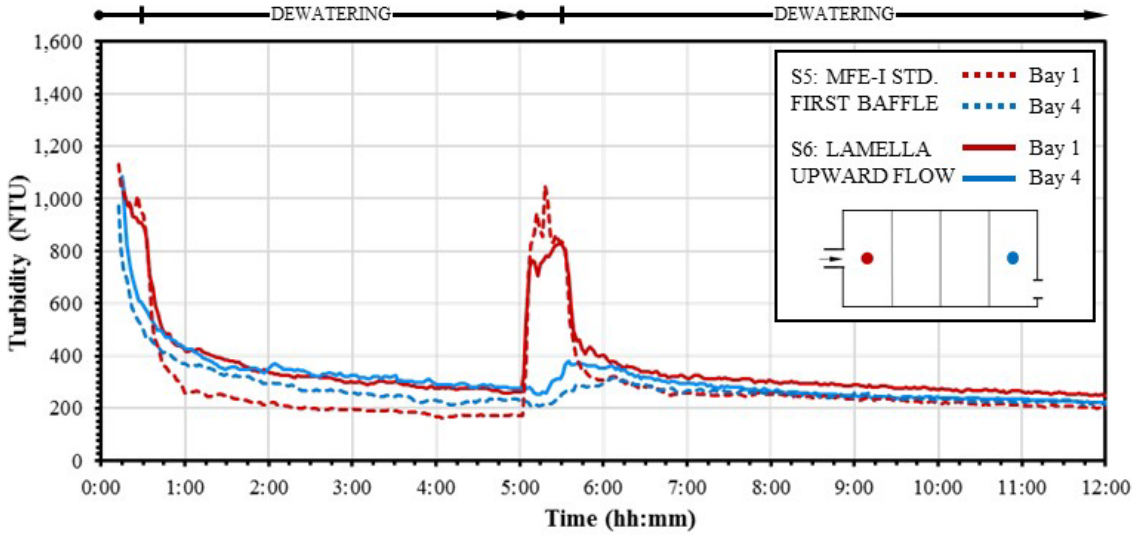

Figure 4.19: Temperature Normalization for S5 and S6 Turbidity Data.

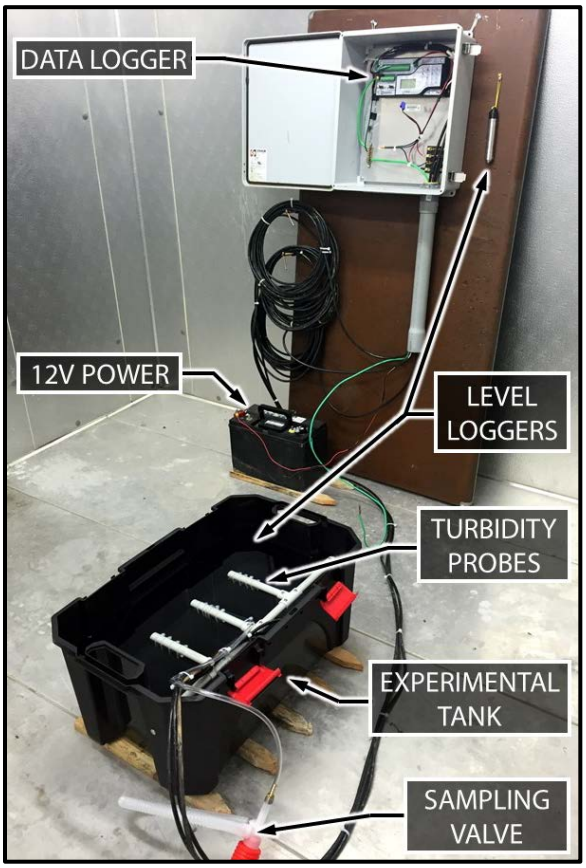

(a) apparatus in environmental chamber

(b) installed probes in clean water

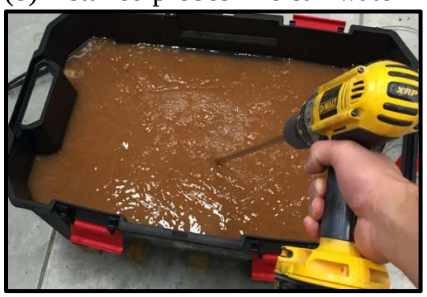

(c) mixing sediment and water

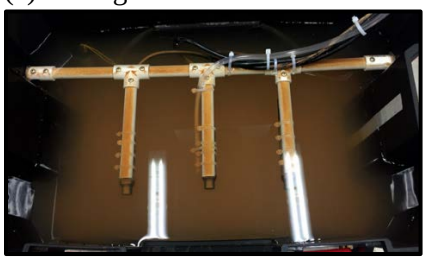

(d) tank after settling period

Figure 4.20: Environmental Chamber Temperature Adjustment Testing.

Differences in the turbidity decay rate were observed through the turbidity probes and are plotted in Figure 4.21(b). Of the six temperature ranges tested, three followed the trend of increasing turbidity decay rate with increased temperature: 47 ºF, 64 ºF, and 73 ºF (8.3 ºC, 17.8 ºC, and 22.8 ºC). The turbidity standard deviation between these three temperatures averaged 23.3 NTU throughout the first six hours of the experiment. The temperature adjustment factor was applied to these three temperature experiments to normalize the data to 65 ºF (18.3ºC). This adjustment is shown in Figure 4.21(c). The adjusted turbidity standard deviation between these three temperatures averaged 4.8 NTU throughout the first six hours of the experiment. The applied adjustment increased the correlation of the three data series by a factor of 4.9.

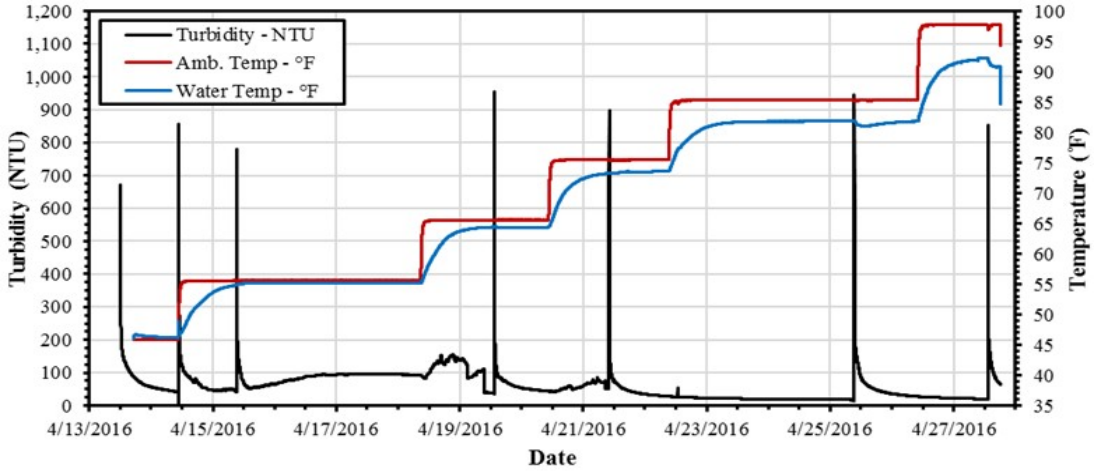

(a) turbidity and temperature data summary for all experiments

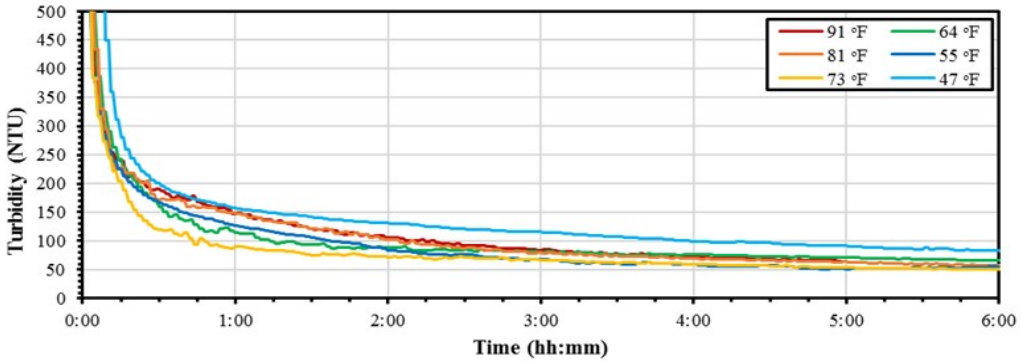

(b) turbidity results for tested temperatures

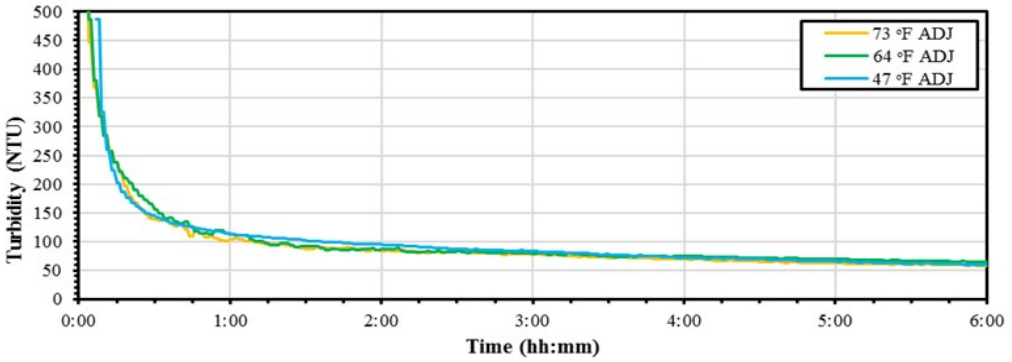

(c) adjusted turbidity based on temperature for select experiments

Figure 4.21: Temperature Adjustment Experimental Results.

While further replications would be required to verify this proposed temperature adjustment factor, preliminary data supports the hypothesis that the decay rate of turbidity follows the same pattern as the ratio of settling velocity at different temperatures.

4.3.2. TSS Relationship

The primary means of evaluating the performance of the treatments tested in the sediment basin was through the turbidity data that was read by the probes installed in Bays 1, 2, and 4. However, grab samples were also obtained from initial tests (i.e. S1 and S2) using automated samplers in Bay 1, Bay 2, Bay 2 bottom, Bay 3, and Bay 4. These samples were analyzed for turbidity and TSS using laboratory methods. The purpose of these samples was to determine the relationship between turbidity and TSS to correlate measurements taken by the probes. The TSS vs. turbidity results were separated by bay and plotted to determine the best fit polynomial relationship as shown in Figure 4.22. The plotted relationships show a relatively strong relationship between TSS and turbidity with R^2 values ranging between 0.75 and 0.93. The TSS – Turbidity results analysis also indicate that:

- TSS and turbidity results are positively related, as expected. Also as expected, the range of maximum TSS and turbidity decay across the sediment basin bays. However, the drop in peak TSS is about 8-fold, whereas the drop in peak turbidity is about 2-fold. This confirms that the bulk of TSS in the beginning of the sediment basin is created by larger sediment particles (e.g. sands), whereas at the downstream end, even with significantly smaller TSS values finer particles still create very large turbidity values. This is confirmed by the particle size distribution (PSD) results that are presented in this report in the next section.
- The TSS-Turbidity correlation is more complex (e.g. high non-linearity) and poorer (lower R^2) in the samples taken in the Inflow channel, Bays 1 and 2 during the Filling stages of the flow. This correlation tends to improve in the Settling stage in all these locations once inflows stop. An exception is Bay 2, top layer, TSS values where still large up to 11 minutes after inflow stopped, possibly due to still lingering currents and turbulence in the flow.
- Samples taken at Bay 3 and 4 showed strong correlation between TSS and turbidity both during inflow and settling stages. It is speculated that the other two coir baffles indeed help to decrease further effects of turbulence created at the inflow region of the basin. In other words, while the baffles seem to have limited impact to decrease overall turbidity, they seem to present a more significant role in helping to decrease TSS values across the bays of sediment basins.

These results confirm that the presence of the baffles calming flow conditions have an important effect in preventing large increases of TSS in Bay 4, where the discharge takes place, particularly in the early stages of the sediment basin filling, when the levels of TSS and Turbidity are larger.

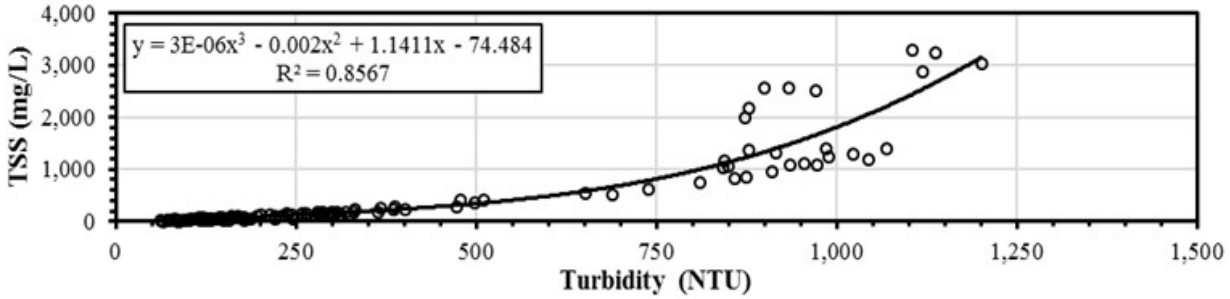

(a) Bay 1

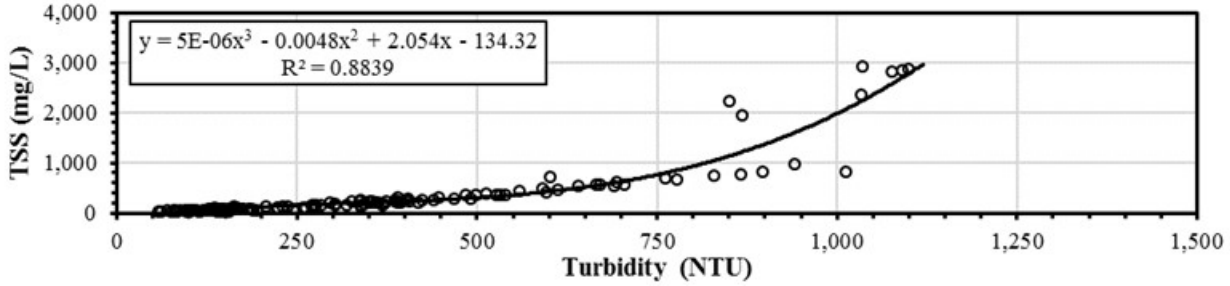

(b) Bay 2

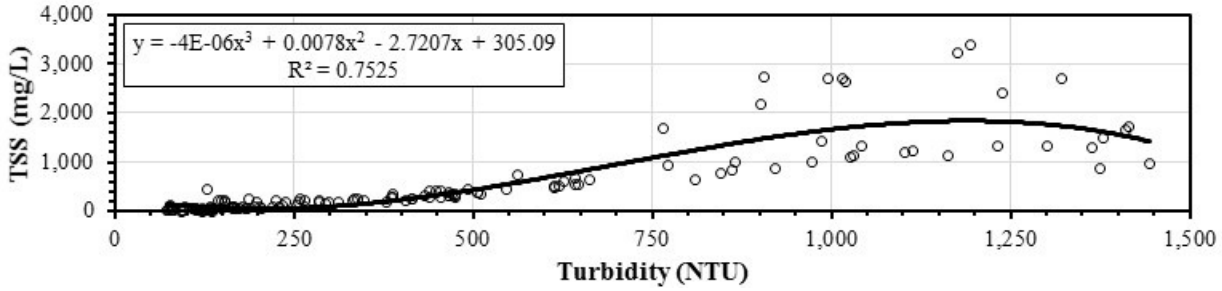

(c) Bay 2 Bottom

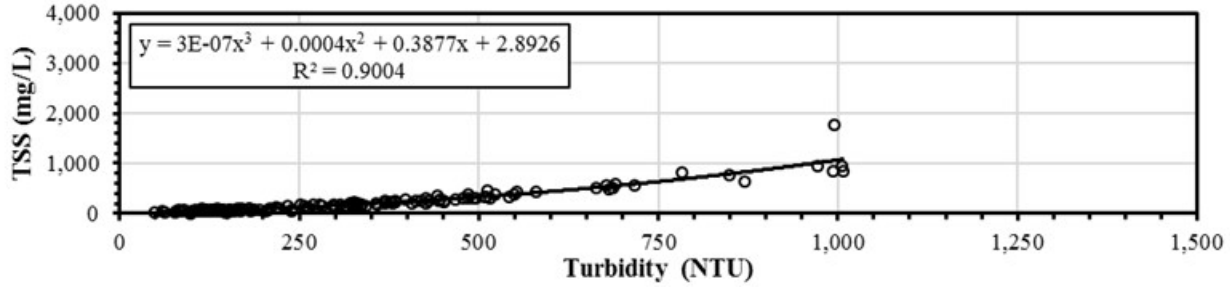

(d) Bay 3

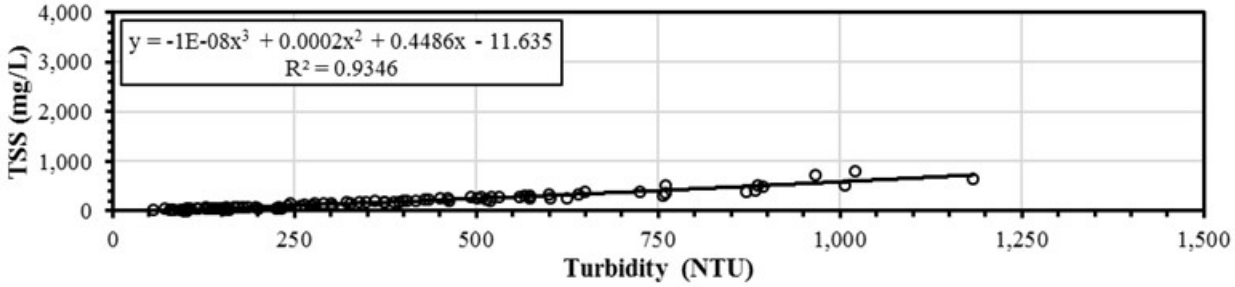

(e) Bay 4

Figure 4.22: TSS vs. Turbidity Relationship in the various bays of the sediment basin.

4.3.3. Particle size distribution results

As it was pointed earlier, a PSD study was performed with samples were taken for a condition S5 (specifically from Test 1-A). The goal was to evaluate eventual differences in the characteristics of soils present in the water-sediment suspensions that are created in sediment basin tests. It was hypothesized that during the different stages of the sediment-laden flow in the basin characteristics of the sediment sizes would differ, with coarser fractions being less abundant as inflows advanced toward the sediment basin outlet at Bay 4.

Indeed, as is shown in Figure 4.23, the original soil contain much higher percentage of particle with sizes ranging from 0.1 mm to 1.0 mm than the samples collected upstream from the excavated sump (UP sump) and at the sump. However, it is noticeable the difference in the soil particles present in the sample taken from Bay 2, which had a greater fraction of fines and a statistical mode (i.e. peak percentage) of 7 μm. Samples taken downstream from the lamella settler units within the sediment basin (labelled HRS) and at Bay 4 are similar and present statistical mode also of 7 μm, however the fraction of fines is even higher. Comparing PSD results from Bay 2 and Bay 4, it can be noticed a reduction in the concentration of soil sizes between 12 μm and 100 μm mm. This indicates that this is the particle size range in which the physical settling within the lamella settlers takes place.

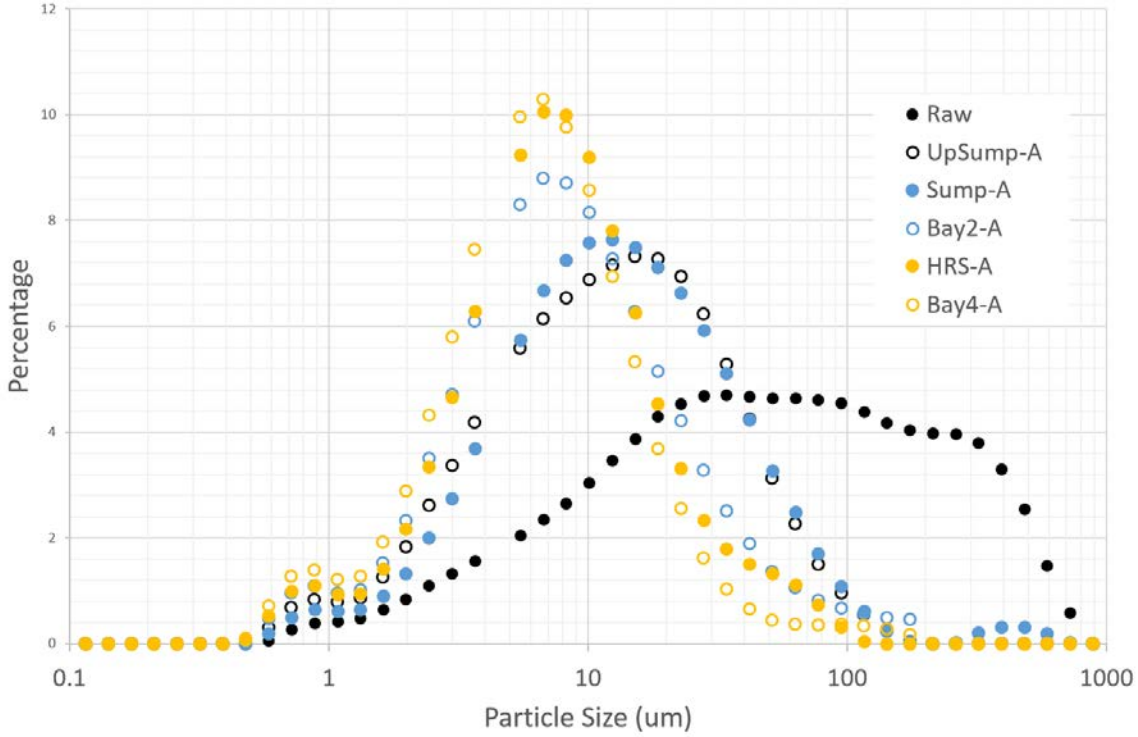

Figure 4.23: PSD results of sediments in water samples at different basin regions collected from condition S5, Test 1-A.

4.3.4. Turbidity variation with depth over the experimental repetitions

The present subsection presents measured results of turbidity distribution during the basin filling and dewatering processes for each of the configurations presented in the previous section. Figure 4.24 presents the turbidity at each of the three monitored depths in the basin for the first and last bays in the sediment basin for Configuration 1 (ALDOT standard design). The turbidity results are averaged over the three repetitions for this test configurations, and time zero corresponds to the flow admission in the basin.

The average turbidity for Tests 1-A, 2-A and 3-A (initial filling cases) are reported for each depth as soon as the water depth reached the elevation of the sampling device. This corresponded in average to 15 minutes for the 1-ft elevation station, 24 minutes for the 2-ft elevation station and close to 29 minutes for the 3-ft elevation station. As for the average results for tests 1-B, 2-B and 3-B (second filling), samples were collected in the 1-ft and 2-ft elevation stations as soon as 5 minutes into the test. Within 10 minutes, water depth increased to a point where samples could also be collected by the 3-ft elevation station.

For Test 1-A, 2-A and 3-A results, as it would be anticipated, turbidity values were at the highest levels during flow admission stages. Turbidity declined immediately after inflow admission stopped, and the rate of drop was more pronounced in the Bay 1. Turbidity values were in general higher at the Bay 4 than Bay 1 within the sediment basin during filling stages, particularly for the second and third filling cycles (L2 and L3). Also, turbidity levels increased from the surface toward the bottom of the basin. This points to potential changes in the geometry changes of the sediment basin inverts, ensuring a small slope that keeps a smaller flow depth at bay 4.

For Test 1-B, 2-B and 3-B results, it was noticed a fast growth of the turbidity in Bay 1 triggered by the second inflow admission in the basin. Turbidity levels of samples collected at the three elevations are consistent, with smallest turbidity values reported at the 3-ft elevation station. As inflows stop, turbidity values begin to drop in the Bay 1 immediately. Results on the Bay 4 are not as straightforward. The growth in turbidity in the last bay is delayed by 15-20 minutes after flow starts, and is first noticed in samples collected at the 3-ft elevation station. Turbidity in samples from the 3-ft elevation station are the maximum one for about 15 minutes into the test, when then the turbidity begins to grow in the lower layers. This seems to indicate that a plume of fine soils is advected in the upper layer of the flow within the basin.

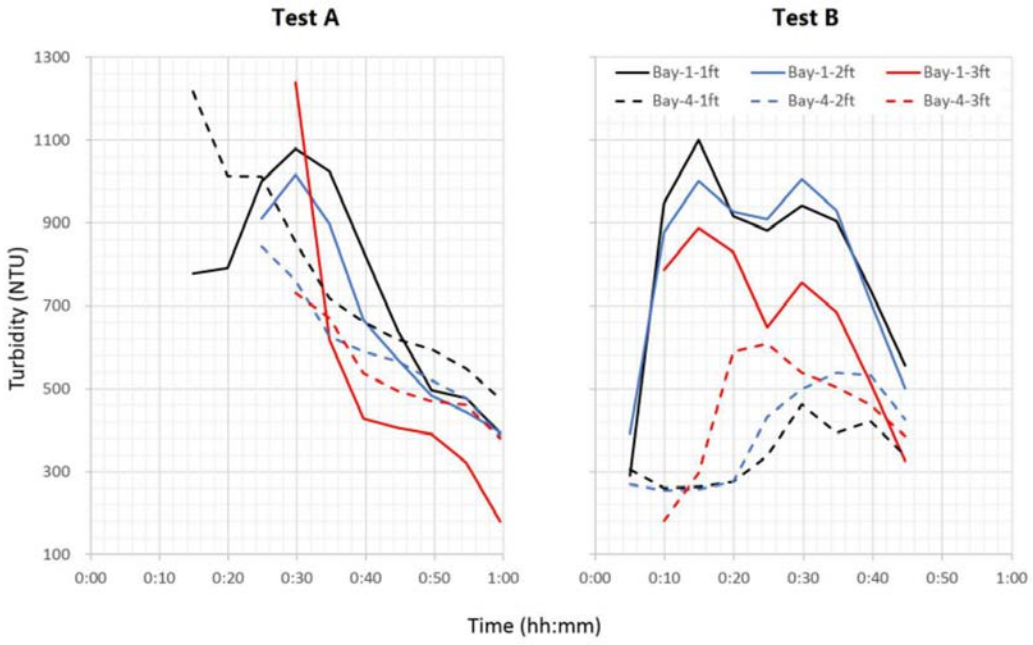

Figure 4.24: Average turbidity over time at different depths within Bay 1 and 4 with Configuration S5 during initial filling (Test A, corresponding to 1-A, 2-A and 3-A), and second filling that led to overflows (Test B, corresponding to 1-B, 2-B and 3-B).

As it was noticed, the turbidity values of samples collected in all bays and depths vary considerably over the duration of a given test. It was also noticed that, in general, turbidity values increased during the

second and third runs of a given configuration. To quantify this process, it was decided to calculate the average turbidity during the filling process and the early dewatering stages, which ranged from 45 to 60 minutes. This calculation was performed for treatments S4 to S7, and for each configuration averages were computed for Test A (initial filling) and Test B (second filling leading to overflow). Results from these calculations are presented in Figure 4.25. In this Figure, four flow regimes are consistent with the terminology presents in Figure 3.17.

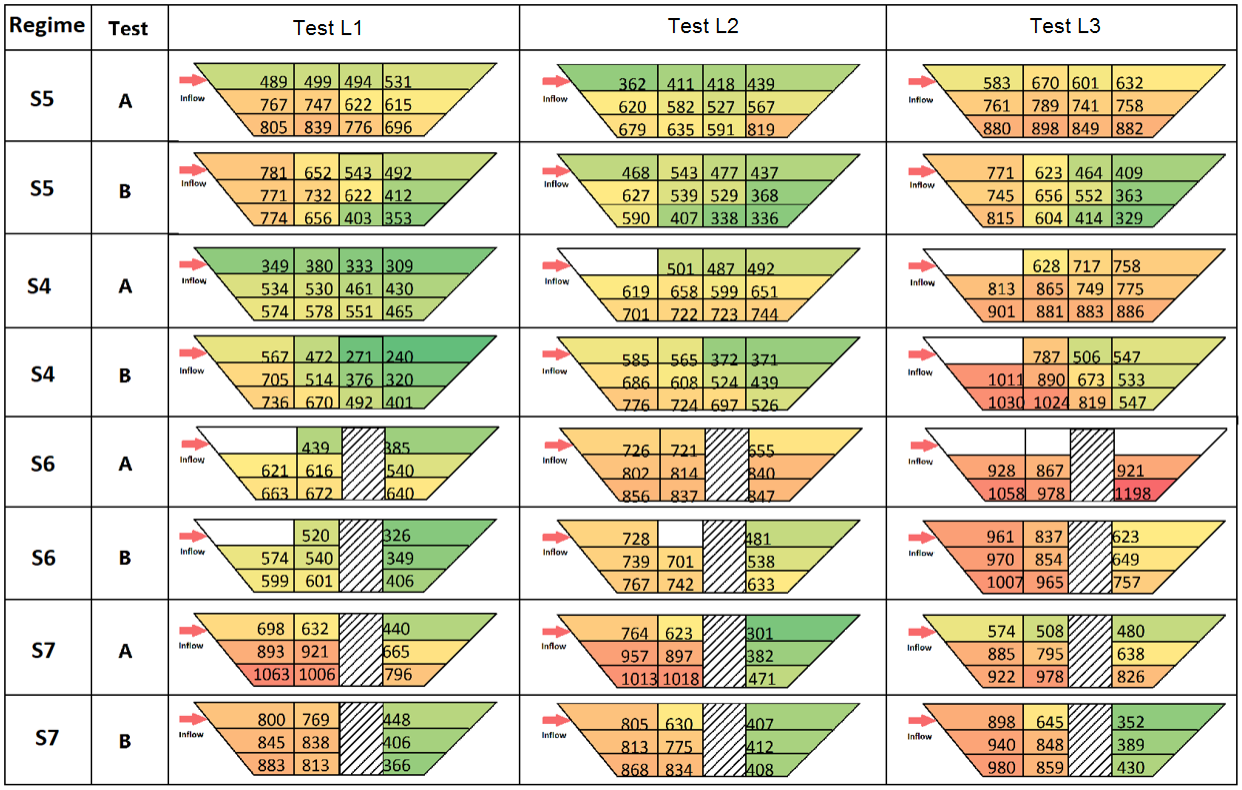

Figure 4.25: Average turbidity calculated for each run at different depths and bays grouped by each tested case. The hatched area in bay 3 for configurations 3 and 4 correspond to the location of the HRS

As is noticed, despite of the efforts in execute the runs adhering to the experimental protocol, there are differences in the turbidity values that are admitted to Bay 1. Highest inflow turbidities were observed for regime S7 (lamella settler with parallel flow) tests, and smallest inflow turbidity values were for regime S4, tests with improved baffle. One interesting observation is the difference in Tests A and B results. For Test A results, turbidity in general increase between Tests L1 and L3 for all bays and depths. For these tests, the average turbidity at Bay 4 is comparable with the other bays, indicating that the degree of turbidity of the basin undergoing initial filling becomes uniform and large. This is an important outcome, as it shows a loss in performance of basins after various inflows as the basins initiate the dewatering process.

On the other hand, Test B results with inflows occurring with higher basin initial water level showed in general a decreasing turbidity gradient as flows moved from Bay 1 toward Bay 4 and the basin spillway. These tests were less impacted by the effect of the repetitions, and indicate that the basin is more effective in decreasing the turbidity across the bays when it is initially partially filled. From all the tested configurations, the HRS parallel was the most effective in decreasing turbidity across the basin. Overall, between tests A and B, the average drop in turbidity in the top layer of the basin for condition S7 was 352 NTU (from 757 NTU to 405 NTU). This corresponds to 47% in the average turbidity measured in the top of Bay 1, which in turn is representative of the turbidity of inflows arriving at the sediment basin.

4.4. CFD modeling results of flows in the sediment basin

This subsection presents CFD results representing the process of basin filling with the use of interFOAM, focusing on determining the effects of porous baffles to the flow characteristics. The simulations were performed with a mesh size of 371 thousand cells, with higher discretization present near the boundaries of the basin. Simulation results include velocity, vorticity, turbulent kinetic energy, etc. within various locations in the basin, but the focus of the research was placed on flow velocity since this variable is fundamentally important to the processes of settling and resuspension in sediment basins. The rationale of the present section is to evaluate what are the benefits of installing porous baffles in sediment basins in terms of flow velocities. It is important to reiterate that the measurement of velocity in various points of the basin is not practical, and CFD tools can be useful in determining such flow characteristics.

Averages of velocity magnitudes in each bay over time with and without baffles were calculated and are presented in Figure 4.26. Simulation results indicate that during the initial minutes the averaged flow velocity is very high due to the small depth across the basin. The average velocity at Bay 1 with and without baffles are relatively similar, however significant differences in the average velocity at Bays 2 to 4 are noticed when baffles were considered. Porous baffles, as it would be anticipated, created a strong drop in velocities in all bays. Within 2 minutes of the simulation there is a significant drop in the flow velocity in Bay 1, due to depth build-up created by the filling. At about 3-4 minutes the average velocity values across the basin are comparable, but results with baffles are consistently smaller. Over time, however, the difference between average velocity results with and without porous baffles decreases.

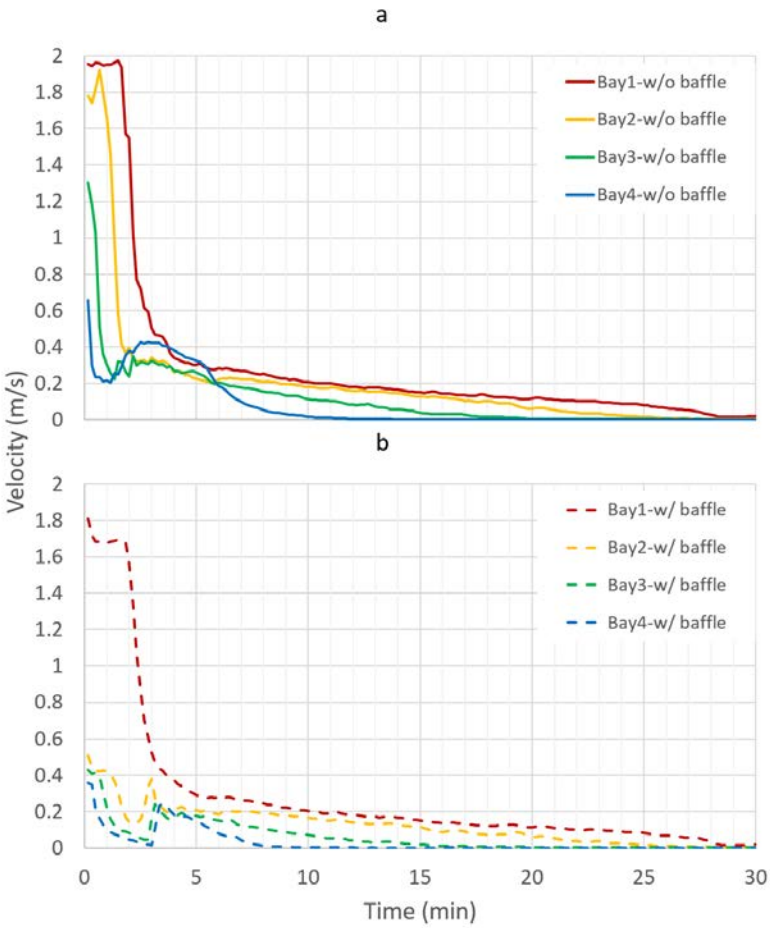

Figure 4.26: Averaged water phase velocity in the sediment basin undergoing filling process for the simulations without and with porous baffles.

The presence of baffles also influences the water circulation patterns in the sediment basin, particularly in the early stages of the flow, as it is shown in Figure 4.27. Velocity magnitudes and streamlines are shown at 3 minutes following the flow admission. While flow pattern is not that different in the region of Bay 1, it may be noticed that the absence of baffles created a zone of strong recirculation near Bay 4, right about where the skimmer was installed. On the other hand, results with porous baffles indicates smaller velocities and more circulation of flow between Bays 2 and 3.

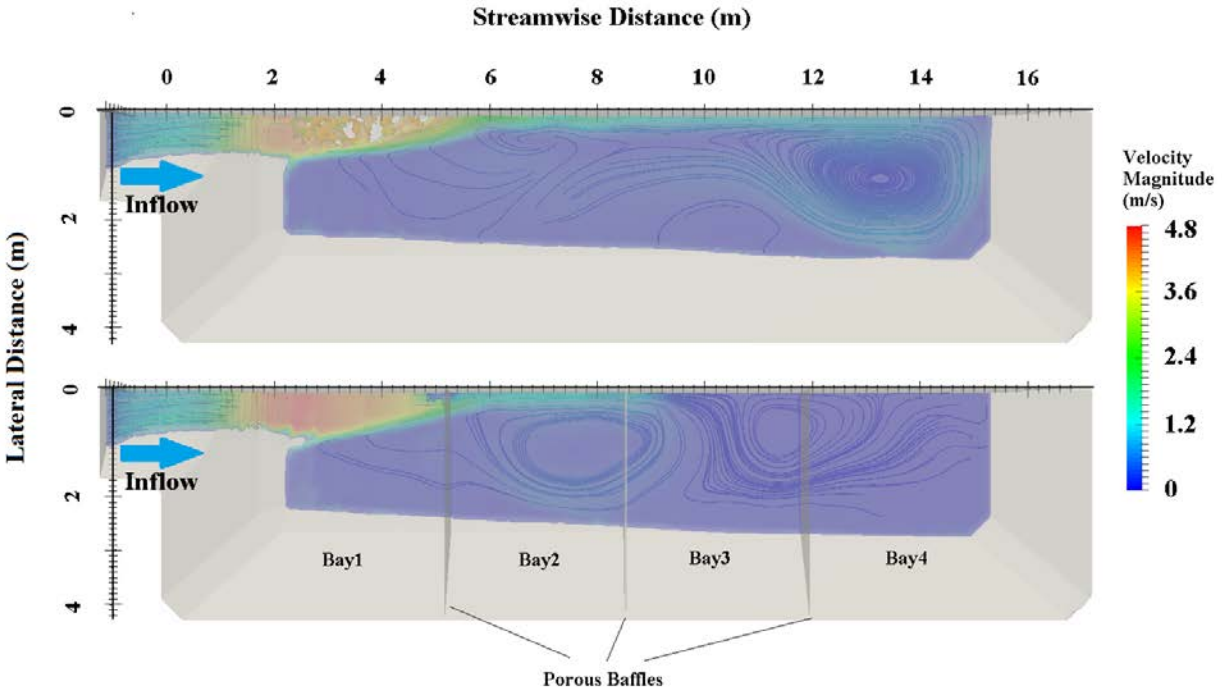

Figure 4.27: Plan view of flow velocity distribution in the sediment basin for the treatment without (upper) and with (lower) porous baffles (t=3min). Results are presented for ½ of the sediment basin assuming a longitudinal symmetry axis.

5. Conclusions and recommendations for future studies

This investigation provided important insights and demonstrated the relevance of large-scale, reproducible sediment basin testing techniques to improve current practices and to achieve greater in-field performance. The made use of a large-scale sediment basin at the AU-ESCTF intended to test several sediment basin design configurations. The investigation involved several types of performance measurements of the current standard design and evaluated alternatives aimed at the improvement of sediment basin performance.

One of the great aspects of the AU-ESCTF apparatus is to control testing conditions, enabling measurements to be taken without unpredictable runoff and erosion contributions on active construction sites. This sediment basin testing apparatus enables a method to test systematically basin configurations and treatment technologies in controlled scenarios. These scenarios, while replicating field conditions, enable repetitions of tests, which in turn provides a higher degree of certainty that the measurements and results are consistent. Results of these tests will lead to improved design guidance that practitioners can refer to when incorporating sediment basins as an element of the stormwater pollution prevention plan for construction sites.

The constructed sediment basin has a total storage of 2,790 ft^3 (79.0 m^3). The metered water and sediment introduction apparatus were developed to allow researchers to control the inflow of material into the basin. Hydrological analyses were used to determine applicable flow and sediment rates for testing, which lends to a uniformed testing procedure that can be applied in various geographical areas based on local rainfall and soil hydrology characteristics. A phased testing regime allowed for evaluating sumps, modified baffles, and high-rate lamella settling technology. The basin was subjected to a number of tests in eight series to evaluate treatments under replicated events and overtopping conditions. Data collection included: water quality parameters (TSS, turbidity, and temperature), inflow rates, basin stage levels, sediment deposition volumes, and sediment sampling for particle characterization. Such measurements were used to evaluate the performance of various tested practices in the basin.

The developed methodology allowed AU-ESCTF researchers to provide testing guidance for the evaluation of sediment basin technology. The following are the conclusions of this research project:

- Observed results showed that the use of an excavated sump in the forebay had no significant effect on water quality treatment in the basin in terms of turbidity. In terms of sediment weight, the alternative with an excavated sump increased in 1.6% the sediment capture in the forebay region. The sediment weight was also increased by 3.3% within Bays 1 through Bay 4. While these changes are too significant, the presence of an excavated sump increase the capture of larger sediment particles outside the sediment basin, resulting in easier maintenance for the basin.
- The use of a modified coir first baffle with 10.9% percent open area was shown to be less effective in treating turbidity than the standard ALDOT baffle configuration.
- The MFE-I was determined to be the ALDOT standard configuration with excavated sump in the forebay. The MFE-I was used for Phase II testing of the high-rate lamella settlers in the upward and parallel flow configurations.
- Both lamella settler configurations treated stormwater more effectively than the MFE-I system without the settlers, and the most effective was the alternative with parallel flows (S7 treatment). The drop in turbidity between Bay 1 and Bay 4 for S7 treatment was more significant than the corresponding one for S6 treatment (lamella settlers with upward flow) by 18.2%. When comparing this drop between S7 and S5 treatment (MFE-I), the difference is 29.0%.
- During all overflow tests performed, the sediment basin had a higher efficiency during the overtopping event then did during the empty fill condition. This indicates that having dead storage

in the basin is important to provide dilution to highly turbid receiving flows, and to dissipate the energy, reducing resuspension of settled particles. Future studies should focus on other scenarios with the sediment basin partially filled, for instance 10% or 30% filled prior to the second inflow admission.

- Cold water temperatures have an effect in decreasing sediment basin effectiveness. With lower temperatures and higher water viscosity it has been noticed that the turbidity decay over time is less pronounced than conditions at higher temperature. However, further investigations on the effects of temperature are still necessary to assess the effects of temperature to settling in sediment basins in a more comprehensive way.
- The TSS-Turbidity relationships derived in this study varied according to the location in the sediment basin and according to the turbulence in the basin. During inflow conditions, the levels of TSS were much larger in Bays 1 and 2 than the values measured in Bays 3 and 4. When inflows stopped, the TSS-Turbidity correlation improved significantly, which indicates that turbulence in the earlier stages of the filling can result in resuspension of larger sediment particles, which in turn impact TSS. Finally, the drop in TSS across the four bays was much more pronounced than the drop in turbidity, which points to the usefulness of dividing the sediment basin with porous baffles.
- Measurements of turbidity at various depths and locations in the basin pointed to the loss of performance of the sediment basin over the three test repetitions, particularly in the case when the basin is initially empty. From all tested treatments, the lamella settler with parallel flows (S7 treatment) was the one with best performance in preventing large increase in turbidity levels in the basin over the three test repetitions.
- Particle size distribution (PSD) results obtained with laser diffraction technology indicated that the fraction of larger suspended sediment present in the approach channel and Bay 1 inflow is much higher than in the rest of the sediment basin. Also, a comparison between the PSD results upstream and downstream from the lamella settler indicated a measurable drop in the number of particles in the size range of 12 μm to 100 μm, which indicates that this is the range of sediment sizes that these plate settlers are more effective in capturing.
- The last experimental conditions tested, which were added to the initial scope of work to the project, evaluated the alternative use of a small lamella settler unit to decrease the turbidity of the sediment basin effluent, and discharged by the skimmer. The smaller storage provided by the small lamella settler did not impact the turbidity, but created a buffer than prevented any turbidity spike at Bay 4 to be discharged. However, when flocculant was mixed and added to the inflows in the small settler unit, there was a significant drop in turbidity from the skimmer discharge and the settler discharge. The levels of turbidity were consistently under 100 NTU, and the average settler discharge turbidity was four times smaller than the skimmer inflow.
- Numerical modeling results obtained with CFD flow simulations of the basin filling process demonstrated that the porous baffles have a large impact in dropping the average velocity at the bottom of the basin during early stages of the filling process. Over time, the positive impacts of porous baffles decrease since the overall velocities in the basin decrease with the gradual volume accumulation.

Future research efforts should result from this project, allowing for further improvements to enhance the performance of sediment basins used in the field while also lending to educational outreach that will continue to increase the general knowledge in the ESC industry. The recommended topics for the continuation of this research are the following:

1. Flow characterization in sediment basins undergoing filling and dewatering processes are still largely unknown and most design recommendations are based on empirical evaluations.

2. Continuation and expansion of research in the temperature impacts in sediment basins, eventually enabling methods improve the performance of sediment basins operating with low temperature runoffs.
3. Evaluate more extensively the use of lamella settler tanks to treat skimmer discharges using flocculant, rather than apply these at the entrance of the sediment basins. The rationale is that a wide range of sediment particles entering sediment basins can be removed by settling process. With a more parsimonious use of flocculants only to treat the finest fractions that are discharged by skimmers it is expected that the discharge of these chemicals in the environment can be reduced, along with the overall consumption of flocculants in construction sites.
4. More extensive application of flow simulation may provide further insights on the processes, geometry characteristics of basins and result in some design recommendations. Such design recommendations will point to more effective basin geometries and construction details.

References

Alabama Department of Environmental Management (2013). "Water Division - Water Quality Program: Division 335-6."Montgomery, AL.

Alabama Department of Transportation (2010). "ALDOT Sedimentation Basin Recommendations."Montgomery, AL.

Alabama Department of Transportation (ALDOT) (2015). Standard Best Management Practices. Montgomery, AL.

Alabama Soil and Water Conservation Committee (2009). "Alabama Handbook for Erosion Control, Sediment Control and Stormwater Management on Construction Sites and Urban Areas."Montgomery, AL.

ASTM Standard D698-12 (2012). "Standard Test Methods for Laboratory Compaction Characteristics of Soil Using Standard Effort." ASTM International, West Conshohocken, PA.

ASTM Standard D2487-11 (2011). "Standard Practice for Classification of Soils for Engineering Purposes (Unified Soil Classification System)." ASTM International, West Conshohocken, PA.

Christopher, S. T., Joseph, C., and Richard, A. M. (2003). "Hydrodynamic Assessment of Various Types of Baffles in a Sediment Detention Pond." Proc., Total Maximum Daily Load (TMDL) Environmental Regulations–II, 557-557.

Clark, W., Beard, T., Mims, D., Pickett, J., Richards, C., and Bowman, A. (2012). "Hold the Dirt: Sedimentation and Urban Growth in an Alabama Watershed." Retrived from https://earthzine.org/, Nov. 2012.

Ergun, S. (1952). Fluid flow through packed columns. Chemical Engineering Progress. 48: 89-94, 1952.

Haan, C.B., Barield, B.J., and Hayes, J.C., (1994). Design Hydrology and Sedimentology for Small Catchments. San Diego, California: Academic Press, Inc.

Hach (2015). "Products." <http://www.hach.com/>. (Aug. 1, 2016).

Hirt, C.W. and Nichols, B.D. (1981). Volume of fluid (VOF) method for the dynamics of free boundaries. J. Comput. Phys. 39(1): 201-225, 1981.

J. W. Faircloth & Son, Inc., (2007). "1.5" Faircloth Skimmer Cut Sheet." <fairclothskimmer.com>. (July 10, 2014).

Logan, C. P. (2012). "Assessing Performance Characteristics of Sediment Basins Constructed in Franklin County, Alabama." Master of Science, Auburn University, Auburn, AL.

McLaughlin R. A. and Jarrett, A.R. (2008) SoilFacts: Surface Outlets for Sediment Basins. N.C. State University Extension SoilFacts Publication AG-439-65W

McLaughlin, R.A., and McCaleb, M.M. "Passive treatment to meet the EPA turbidity limit." American Society of Agricultural and Biological Engineering Presentation Paper 711P0710cd (2010).

Menter, F. R. (1993) "Zonal two equation k-w turbulence models for aerodynamic flows" 23rd Fluid Dynamics, Plasmadynamics, and Lasers Conference Orlando,FL.

Read More: https://arc.aiaa.org/doi/abs/10.2514/6.1993-2906

Montgomery, J. M. (1985). Water Treatment Principles and Design, John Wiley & Sons Inc., New York, NY.

Onset (2016). "Products." <http://www.onsetcomp.com/>. (September 20, 2016).

Perez, M.; Fang. X; Zech, W.C. and Vasconcelos, J.G. (2015) "Design and construction of a large-scale sediment basin and preliminary testing results". Auburn University Highway Research Center Report.

Perez, M. (2016). Improvements in the Design and Application of Erosion and Sediment Control Technologies for the Construction Industry. PhD Dissertation, Auburn University, 2016.

Perez, M. A., Zech, W. C., Donald, W. N., and Fang, X. (2014). "Methodology for Evaluating Inlet Protection Practices Using Large-Scale Testing Techniques." ASCE Journal of Hydrologic Engineering, 20(4).

Pitt, R., Clark, S. E., and Lake, D. W. (2007). Construction Site Erosion and Sediment Controls: Planning, Design and Performance, DEStech Publications, Lancaster, Pa.

SonTek / Xylem Inc. (2016). "Products." <http://www.sontek.com/>. (September 20, 2016).

Teledyne Technologies Inc. (2013). "Products." <http://www.isco.com/>.

Thaxton, C. S., Calantoni, J., and McLaughlin, R. A. (2004). "Hydrodynamic Assessment of Various Types of Baffles in a Sediment Retention Pond." Transactions of the American Society of Agricultural Engineers, 47(Compendex), 741-749.

Thaxton, C. S., and McLaughlin, R. A. (2004). "Hydrodynamic and Sediment Capture Assessment of Various Baffles in a Sediment Retention Pond." 2004 ASAE/CSAE Annual International MeetingOttawa, Ontario, Canada.

United States Department of Agriculture (1986). "Technical Release 55: Urban Hydrology for Small Watersheds." Natural Resources Conservation Service, Washington, DC.

United States Department of Agriculture (1987). "Soil Mechanics Level I: Module 3 - USDA Textural Classification."Washington, D.C.

United States Environmental Protection Agency (1999). "EPA Method 160: Total Suspended Solids (TSS) ", United States Environmental Protection Agency, (USEPA).

United States Environmental Protection Agency (2003). "Standard Method 2130: Analystical Method for Turbidity Measurement." United States Environmental Protection Agency, (USEPA).

United States Environmental Protection Agency (2006) *Stormwater Menu of BMPs – Sediment Traps* EPA Office of Water, Washington DC, November 2009. Online access in 8/21/2013 at http://cfpub.epa.gov/npdes/stormwater/menuofbmps/index.cfm?action=browse&Rbutton=detail&bmp=59&minmeasure=4

United States Environmental Protection Agency (2009). "Effluent Limitations Guidelines and Standards for the Construction and Development Point Source Category." EPA Federal Register, Washington, DC, 62995-63058.

United States Environmental Protection Agency (2012). "National Pollutant Discharge Elimination System General Permit for Discharges from Construction Activities." Office of Water, Washington, DC.

Weather Underground, I. (2016). "Weather History for KAUO." <https://www.wunderground.com/>. (August 30, 2016).

Williams, J. R. (1975). "Sediment-Yield Prediction with Universal Equation using Runoff Energy Factor." U.S. Dept. of Agriculture, Agricultural Research Service, Southern Region, New Orleans, LA, 244-252.